Risk of radiation-induced cancers in patients treated with contemporary radiation therapy for early-stage lung cancer

Bhupesh Parashar

Submitted in partial fulfillment of the requirements for the Degree of Doctor of Public Health in

Mailman School of Public Health

COLUMBIA UNIVERSITY

2021

ABSTRACT

Risk of radiation-induced cancers in patients treated with contemporary radiation therapy for early-stage lung cancer

Bhupesh Parashar

Purpose: In the contemporary management of early-stage lung cancer with Radiation Therapy (RT), there is increased imaging utilization for the diagnosis and treatment and follow-up after completion of treatment. We evaluated whether this increased radiation exposure to patients with early-stage lung cancer that receive stereotactic body radiotherapy (SBRT) significantly increases the risk of radiation-induced carcinogenesis (RIC). Methods: Following IRB approval, one hundred and ninety-six consecutively treated lung cancer patients treated with SBRT were selected for analysis. Information collected included demographics and all ionizing imaging scans one year before SBRT treatment and one year following treatment. These included chest X-rays (CXR), computerized tomography scan (CT scan), positron emission tomography scan (PET-CT scan), bone scan, ventilation-perfusion scan (VQ scan), cone-beam CT scans. In addition to the lung cancer patients, comparative data on ten prostate and breast cancer patients each was collected to get an estimate of the radiation-induced risk (RIC) in other common malignancies. For each patient, the total effective dose (mSv) was calculated by the sum of all effective doses for all scans (1 year before SBRT to 1-year post-SBRT). After calculating the total effective dose, the summed dose was used to calculate the RIC using the RadRat tool. For the study, we decided that a 1% increase in the baseline risk of radiation-induced lung cancer will be considered a significant increase. Results: Among lung cancer patients, there were 87 males (44.4%) and 109 females (55.6%). The median number of Pre-SBRT CXRs (PA/lateral) was 2 (Range: 1-22), the median number of pre-

SBRT CT scans was 2 (Range: 1-6), the median number of pre-SBRT PET-CT scans was 1 (Range: 1-4), the median number of Bone Scans or VQ scans pre-SBRT was 1. The median effective exposure dose from all scans was 72mSv (Range: 24-140.36mSv). The median excess lifetime risk (ELR) of developing lung cancer (a chance in 100,000) with a 90% uncertainty range was 57.15. The Excess Future risk (EFR), the risk from 2019 to the end of the expected lifetime of developing cancer (a chance in 100,000), showed a median of EFR mean of 73.75 (Range: 8.45-416). The total future risk (TFR, a sum of baseline and excess risk) of developing cancer, from 2019 to end of an expected lifetime was 2732.5 (Range: 808-8290), the median of TFR upper bound was 2785.5 (Range: 856-8400) and median of TFR lower bound was 2679.5 (Range: 761-8183). At 6 months, survival was 94.7% (144/152), at 1 year, 79% (94/119), at 3 years 32.5% (27/83). At five years, with survival data on 77 patients available, 9 (11.6%) were alive. Regarding the comparison of RIC from imaging before RT for patients with prostate cancer, the median total effective radiation dose from all pre-SBRT and post-SBRT scans was 20mSv (Range: 20-30mSv), and the median of mean ELR for development of RIC prostate cancer was 4.24 (per 100,000). Regarding early-stage breast cancer, the median total effective radiation dose from all pre-RT and post-RT scans was 16.56mSv (Range: 10.52-31.48mSv), and the median of mean ELR for development of RIC was 35.95 (per 100,000). Conclusion: The median excess cancer lifetime radiation-induced cancer risk for the lung cancer cohort was 0.05%, which is significantly less than the 1% risk that was determined to be clinically significant as per our study objective. The survival in this cohort of patients was poor. Enhanced imaging to enhance staging accuracy, safety during SBRT treatment, and adequate follow-up outweigh the RIC risk.

Table of Contents……Page number

Figures and Tables

ACKNOWLEDGEMENTS

I am incredibly grateful to my dissertation committee advisor Dr. Norman Kleiman, PhD for your support, ideas and guidance through the entire DrPH program. Thank you for countless hours to supervise me at every step. It was also a great honor to have Dr. Greg A. Freyer, PhD as a member of my dissertation committee. He has been instrumental in my completing this journey through his guidance and encouragement and teaching. I am also thankful to other members of the dissertation committee for their input and invaluable suggestions in making this dissertation better.

Finally, I am thankful to all the patients and treatment team that contributed the data for completion of this dissertation.

DEDICATION

I dedicate this dissertation to my Gurudev, my teacher and mentor, Jagadguru Paramhansa Acharya Mahamandaleshwar Dr. Swami Shivendra Puri Ji Maharaj for his unwavering love, guidance, blessings and inspiration to initiate and complete this project.

And this is for you Mom (Mrs. Krishna Sharma) for always teaching us the value of truth, righteousness and education. You will always be with us in our memories.

And this is for you Dad (Mr. S.P. Sharma) for your inspiration and always teaching us to place faith in divine and keep education as our highest priority.

And to my Brother Dr. Gopesh Sharma, PhD who has always encouraged and supported this effort and has been an amazing friend and guide.

To my sister-in-law Mrs. Vaishali Sharma, for her support and love and kindness. To My amazing niece Kirti Sharma and equally amazing nephew Shekhar Sharma for their love.

And finally to my dearest friend and colleague Dr. A.Gabriella Wernicke, MD, MSc who has been an amazing friend and a continuous support and help during this dissertation.

Introduction

Radiation therapy (RT) is one of the primary treatments used in the management of many cancers. RT has been in use for cancer management for over a century and has contributed to improved control rates and survival in many malignancies (1-6), including leukemia, breast, colon, head/neck, and lung cancer. Overall, cancer death rates rose throughout much of the 20th century, peaking at 215 cancer deaths per 100,000 people in 1991 (Figure 1). As of 2016, the rate has dropped 27% to 156/100,000 (1-7).

Figure 1

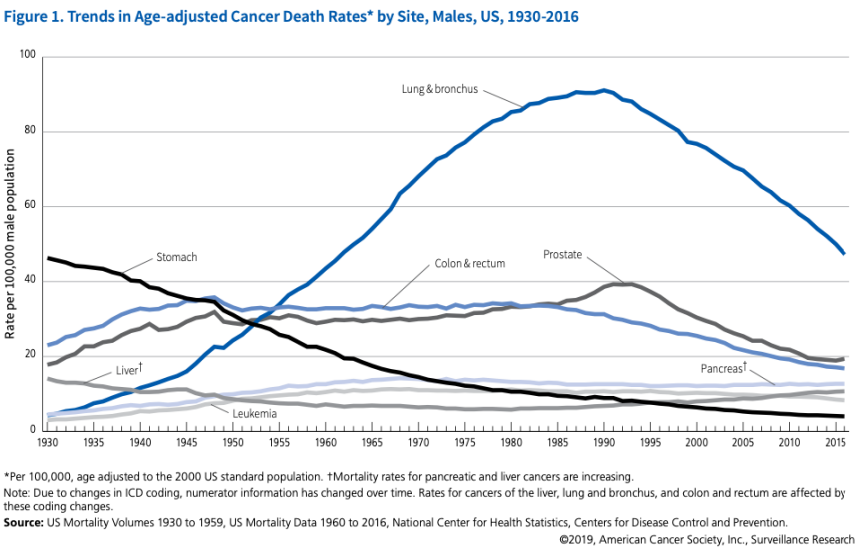

Figure 2

Figure 2. Trends in Age-adjusted Cancer Death Rates* by Site, Females, US, 1930-2016

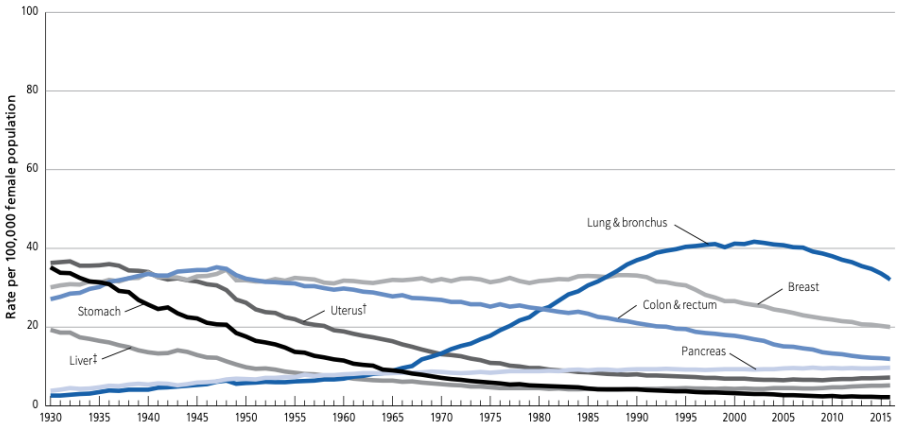

*Per 100,000, age adjusted to the 2000 US standard population. Rates exclude deaths in Puerto Rico and other US territories. †Uterus refers to uterine cervix and uterine corpus combined. ‡The mortality rate for liver cancer is increasing.

Note: Due to changes in ICD coding, numerator information has changed over time. Rates for cancers of the liver, lung and bronchus, colon and rectum, and uterus are affected by these coding changes.

Source: US Mortality Volumes 1930 to 1959, US Mortality Data 1960 to 2016, National Center for Health Statistics, Centers for Disease Control and Prevention.

Figure 1 and 2 from https://www.cancer.org/content/dam/cancer-org/research/cancer-facts-and-statistics/annual-cancer-facts-and-figures/2019/cancer-facts-and-figures-2019.pdf

Breast Cancer: In the 2019 US estimates (Figure 2), there were 268,600 new cases of invasive breast cancer diagnosed in women, 2,670 cases diagnosed in men, and an additional 62,930 cases of in situ breast lesions (ductal carcinoma in situ [DCIS] or lobular carcinoma in situ [LCIS]) diagnosed in women. The female breast cancer mortality peaked at 33.2/100,000 in 1989, declining to 20.0/100,000 in 2016, a decrease of 40% primarily due to improvements in early detection (e.g., screening) and better treatments. This translates into an estimated 348,800 fewer breast cancer deaths than would have been expected if the death rate had remained at its peak in 1989. From 2007 to 2016, breast cancer mortality declined by 1.8% per year, and it corresponds to 5- and 10-year relative survival rates for invasive breast cancer of 90% and 83%, respectively. Sixty-two percent of cases are local disease, and their 5-year survival is 99%. Survival rates have improved over time irrespective of the race but remain about 10% lower for black women (1,2,7).

Prostate Cancer: 174,650 new prostate cancer (PCa) cases were estimated to be diagnosed in the US during 2019 (7), with a 60% higher incidence in blacks than whites. In the late 1980s/90s,

incidence rates spiked with the introduction of screening with the prostate-specific antigen (PSA) blood test. In recent years, however, there has been a decreased incidence due to reduced PSA screening between 2011 to 2015. During this period, the rate decreased by about 7% per year (7). Prostate cancer mortality declined by 51%, from a peak of 39.3/100,000 in 1993 to 19.4/100,000 in 2016. This rapid reduction in PCa mortality may be due to earlier detection through PSA screening (7,8). There were an estimated 31,620 deaths from prostate cancer in 2019 (7). Ninety percent of PCa are diagnosed at a local or loco-regional stage, and 5-year survival is 100% for such patients. In contrast, the 5-year survival for patients diagnosed with distant disease is 30%, while the 10-year survival rate for all stages is 98% (7).

Lung Cancer: There were an estimated 228,150 new lung cancer cases diagnosed in the US in 2019 (6,7). Incidence has been declining since the 1980s in men, although a slower decline is observed in women, beginning in the mid-2000s, likely because of different smoking cessation patterns. From 2011 to 2015, incidence declined 3% per year in men and 1.5% per year in women (6,7). In 2019, there were an estimated 142,670 deaths from lung cancer. Lung cancer mortality is also declining, decreasing by 48% since 1990 in men and by 23% since 2002 in women, likely due to reduced smoking rates (7). From 2012 - 2016, mortality rates decreased by about 4% per year in men and 3% per year in women (7).

"The lifetime risk of developing or dying from cancer refers to the chance a person has, over the course of his or her lifetime (from birth to death), of being diagnosed with or dying from cancer" (8). Risk estimates are based on Surveillance Epidemiology and End Results (SEER) database studies that have collected data from the US population between 1975-2014 (8). Based on this data, the lifetime risk of lung cancer diagnosis in males is 6.86%, and the risk of dying

from lung cancers is 5.96%. In females, the lifetime risk of developing lung cancers is 5.95%, and the risk of dying from lung cancers is 4.72% (8).

Lung cancer screening with low-dose spiral computed tomography (LDCT) reduces lung cancer mortality by about 20% compared to standard chest x-ray among high-risk patients such as current or former (quit within 15 years) heavy smokers (6,7). Therefore, the American Cancer Society recommends annual screening for lung cancer using LDCT in adults 55 to 74 who are current or former heavy smokers and relatively good health. These individuals should receive evidence-based smoking-cessation counseling (if they are current smokers) and undergo a process of informed/shared decision making that included a description of the potential benefits, limitations, and harms associated with lung cancer screening (7).

Smoking increases the risk of lung cancer 15-30 times compared to non-smokers. Other tobacco products, such as cigars and pipes, also increase risk. Quitting smoking decreases risk but does not approach the lung cancer rates seen in non-smokers. Other contributing risk factors for lung cancer include exposure to secondhand smoke, asbestos, silica, chromium, arsenic, or diesel exhaust, as well as genetics, family history, and diet. Smokers who take beta-carotene have an increased risk of lung cancer (9). Lastly, ionizing radiation exposure increases lung cancer (9), especially exposure to radon gas (9). Excess radon exposure causes an estimated 20,000 cases of lung cancer each year (9). In addition to radon exposure, ionizing radiation exposure during RT is responsible for approximately 5% of second cancers following initial cancer treatment (9,10). Multiple factors contribute to the development of radiation-induced cancer (RIC), including age at exposure, gender, cancer type (e.g., hematopoietic v. solid cancers), radiation technique, and type of radiation exposure (10).

An estimated 228,100 cases of lung cancer occurred in 2019, some 12.9% of all cancer cases. This will result in an estimated 142,600 lung cancer deaths, 23.5% of cancer deaths overall (8). Based on 2009-2015 SEER data, only 19.5% will survive five years. 16% of patients will be diagnosed localized to the primary site, while 57% will be diagnosed with distant metastasis, and the remainder will be diagnosed with the regional disease (8). The age-adjusted incidence of lung cancer is as follows:

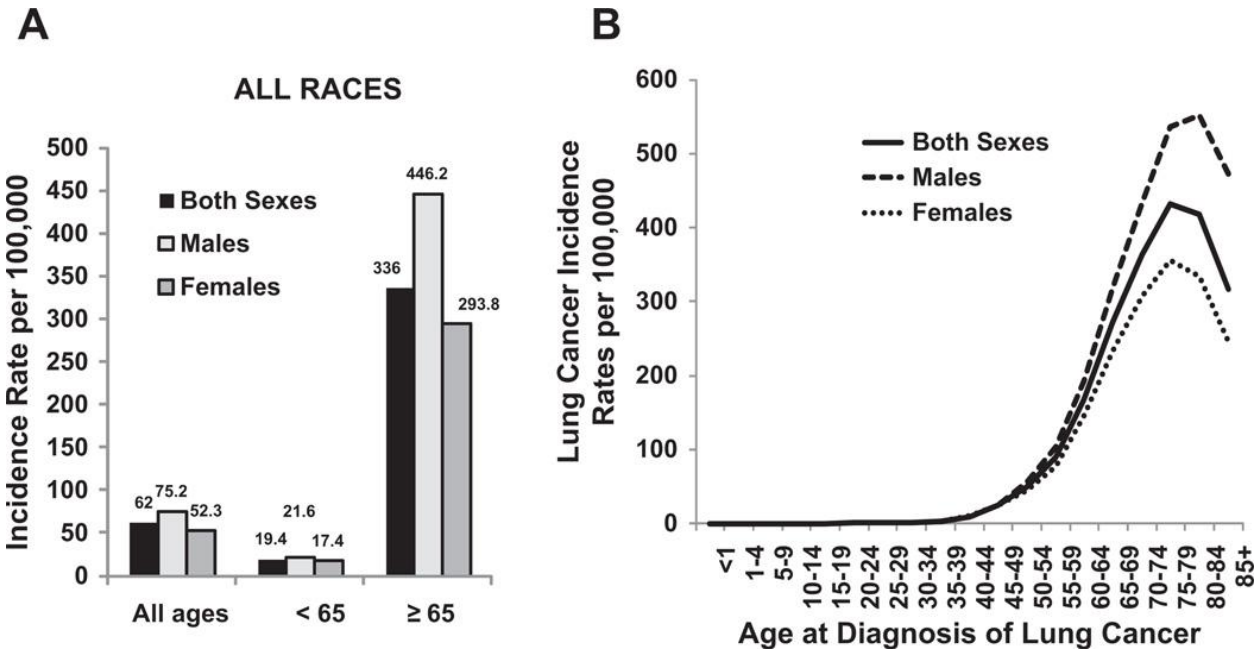

Figure 3 (A) and 4 (B): US age-adjusted lung cancer incidence by gender, age, and race. (*A*) Separated by age <65 years and age ≥65 years. (*B*) Separated by age from <1 to 851 years. Rates are per 100,000 and are age-adjusted to the 2000 US standard population. (*Data from* Howlader N, Noone AM, Krapcho M, et al., editors. SEER Cancer Statistics Review, 1975–2008. Bethesda (MD): National Cancer Institute; 2010. Available at: http://seer.cancer.gov/csr/1975_2008/, based on November 2010 SEER data submission, posted to the SEER web site, 2011.)

Imaging. There is an increasing number of imaging techniques to identify better and localize lung cancers. All such methods rely on ionizing radiation exposure (either radio-isotopes or photon/x-ray beams) to image the chest. These are briefly described below.

Chest radiographs (chest X-ray, CXR) are the most commonly used imaging modality for initial diagnosis, follow-up, and potential complications resulting from treatment. Advantages include low cost, minimal inconvenience, and low radiation exposure. Often, CXR helps determine subsequent imaging techniques utilized. CXR can be used to estimate the tumor size, assess any post-obstructive collapse, pleural effusion, or any extra-pulmonary spread. CXR imaging poses difficulty assessing invasion into the mediastinum, vessel, or nodal involvement (11).

Another imaging modality, computerized helical tomography (CT), was introduced in 1991. Helical CT has significantly improved the resolution and quality of images in thoracic imaging (12,13). Helical CT produces a single volumetric dataset within one breath-hold while the patient is moved through the CT gantry. The newer multidetector scanners (MDCT) use multiple rows of detectors that offer increased speed and better temporal and spatial resolution, with concomitant improved image quality (12,13). MDCT's enable maximum intensity projection (MIP) imaging and 3-Dimensional (3D) reconstruction. MIP enables the detection of much smaller lung nodules. MIP projects the pixels with the highest attenuation values in a 2D format (13). Multiplanar (MPR) images provide an excellent tool for accurate staging (12).

Positron emission tomography (PET), PET/CT scan, allows imaging of metabolic pathways in human tissue and is a standard option for staging lung cancer (14). PET/CT is a combined anatomic-metabolic imaging technique using integrated PET and CT scans. The first

PET/CT scan came into clinical practice in 1998 (15,16). Integrated PET/CT scans offer detection of lesions not visible on CT scans, better delineation from surrounding tissue, more precise localization, and better distinguishing between benign and malignant lesions. PET/CT is now a standard imaging modality in lung cancer staging since its very sensitive in detecting distant metastasis. CT data can be used for attenuation correction of the PET scan, and the examination session time can be significantly reduced (17).

PET uses radioisotopes such as Fluorodeoxyglucose (FDG), a D-glucose molecule in which a hydroxyl group is replaced by a positron-emitting F-18, a fluorine isotope. FDG is taken up and metabolized by cells where it's phosphorylated and becomes trapped intracellularly (14). Malignant cells have higher glucose metabolism rates than normal cells and accumulate more significant amounts of the radiolabeled FDG. Other radiopharmaceuticals are also used, such as Choline (C-11) (14).

At a cellular level, positrons traverse through tissue where they combine with an electron resulting in the generation of a pair of photons that travel in the opposite direction with an energy of 511 KeV each (15). These photons are detected by a couple of detectors located in the PET scan camera. Photons that are released are registered as decay events, and these events give a tomographic image. To measure radioactivity, the 'standardized uptake value' (SUV) is measured. $SUV = (Q \times W)/Q_{inj}$ where tumor radiotracer concentration (Q) is normalized to the injected activity (Q_{inj}) and the body weight (W) of the patient. An SUV >2.5 is usually considered suspicious for malignancy (15).

Another approach, cone-beam CT (CBCT), is also routinely used in lung cancer treatment utilizing radiation therapy, especially with hypo-fractionated regimens such as SBRT (Stereotactic body radiation therapy) (18, 19). The development of electronic portal imaging

device (EPID) led to the availability of mega-voltage (MV) images as a beam-eye view of treatment fields or as orthogonal images during RT. KV (Kilo-voltage) images have a superior image quality versus MV imaging (18). There are limitations in using 2D-KV imaging (e.g., 2D-KV uses bony anatomy as a surrogate for tumor position). Therefore this approach is challenging to use in lung SBRT, where high precision is required to reduce toxicity and target tumor (19). Several advances have partially overcome these limitations, including placement of fiducial markers, use of in-room CT scanners, and onboard kV CT, which has resulted in improved geometric localization for lung SBRT and reduced inter-fractional uncertainties (20).

Another alternative or sometimes supplement to CBCT is ExacTrac™ (Brain Lab AG, Germany), a 6D system composed of an infrared tracking system, an X-ray system, and a robotic couch capable of 6D correction positioning. Exactrac has clinical benefits over CBCT, including faster patient positioning, 6D degree of freedom, ability to monitor patient motion during the treatment, and a reduction in image-based radiation delivered to the patient (21).

Early-stage lung cancers: The American Joint Commission on Cancer TNM staging system, 8th edition (AJCC 8th edition), was implemented in January 2018. Stage classification is essential for patient care since it provides guidelines on appropriate management. A TNM classification system is utilized where T stands for characteristics of the primary tumor, N for nodal involvement, and M for (distant) metastasis. T, N, and M coalesce into stage groups. The bodies that decide on the particular definition of each TNM stage are American Joint Commission on Cancer (AJCC) in the United States and the Union for International Cancer Control (UICC) internationally (22).

Stage I and II are usually considered early-stage, non-small cell lung cancer. Management options for early-stage lung cancer include surgery, chemotherapy, and/or radiation therapy.

Surgical resection of these tumors usually involves lobectomy or wedge resection (although segmentectomy or pneumonectomy are also options) followed by chemotherapy if stage II cancer or higher (23). Following standard therapy, 60-70% of patients with early-stage lung cancer (stage I and II) survive 5-years (24). For patients that undergo surgical resection for stage I small, less invasive tumors, 5-year survival is between 80-90% (25).

For medically inoperable patients or patients who refuse to undergo surgical procedures, radiation treatment is offered. Traditionally, RT was utilized to treat early-stage lung cancer either with a 2-Dimensional (2D) or 3D technique (conventional RT) (26-30). Outcomes of patients treated with conventional RT are poor, and RT is considered an inferior option to surgical resection (26, 27). Conventional RT involved delivering radiation over 5-7 weeks, five days a week in 1.8-2 Gy fractions. The reported 5-year survival was between 6-35%, although this could be a result of selection bias (26, 27). RT dose escalation was shown in multiple studies to enhance local control and improve outcomes (28-30).

Stereotactic body radiation therapy (SBRT), also known as SABR (Stereotactic Ablative Radiation Therapy), was a significant advancement in RT delivery (31). SBRT was developed in the 1990s as an extension of stereotactic radiosurgery (SRS) techniques for brain metastasis. SBRT uses daily image guidance, target delineation, motion management, and conformal treatment planning to deliver high dose radiation to the target with a sharp dose fall-off beyond the target. Early reports of excellent outcomes using SBRT for early-stage lung cancer resulted in SBRT becoming the standard RT technique for inoperable non-small cell lung cancers. The Radiation Therapy Oncology Group (RTOG) conducted several phase I/II/III trials to determine the efficacy of SBRT in the management of NSCLC (non-small cell lung cancer) (32-34). In a landmark phase II study by Timmerman et al., 70 patients with T1/T2 inoperable NSCLC were

treated with SBRT to a total dose of 60-66 Gy in 3 fractions. The 2-year local control was >95%, although grade 3 or higher toxicity was unacceptably high for central lesions (tumor within 2 cm of tracheobronchial tree) versus peripheral tumors (32). In another phase II multicenter trial that treated patients with 60 Gy in 3 fractions (excluded central tumors), 55 evaluable patients had a median follow-up of 4 years. The 5-year local control was 80%, regional control was 62%, and there was 31% distant metastasis (33). Toxicity was acceptable, with 15 patients experiencing grade 3 toxicity and two patients experiencing grade 4 toxicity.

The use of SBRT in the management of early-stage lung cancer was initially studied and utilized for inoperable tumors. However, given the safety and efficacy of its use in stage I and II tumors, it is now increasingly used in operable NSCLC patients, and results are encouraging (35). Survival in early-stage lung cancer patients or lung cancer patients, in general, demonstrates a trend towards increased survival. Lung cancer patients are living longer for various reasons, including earlier detection, improved staging techniques, improved chemotherapy, use of immunotherapy, improved treatment techniques, including the use of SBRT, and better follow-up tools. A trend towards improved survival has been observed over the last few decades (36). With increasing survival rates, there has been increased concern about the risk of potential second cancers induced by ionizing radiation exposures during treatment. Evaluation of this potential risk is the focus of this thesis.

Why choose early-stage lung cancer patients treated with SBRT to study RT-induced cancer? As noted above, early-stage lung cancer management involves surgical resection that may include lobectomy or wedge resection, radiation therapy that commonly uses stereotactic body radiation therapy (SBRT), conventional external beam radiation, or wedge resection plus brachytherapy. Other options include radiofrequency ablation (RFA) and systemic treatments such

as chemotherapy or targeted agents (37-39). If a patient opts for radiation (e.g., SBRT), some diagnostic tests may be needed before RT that result in additional exposures to radiation such as CT scans, X-rays, and PET-CT scans. Furthermore, following treatment, diagnostic follow-up scans are recommended to evaluate disease recurrence. These may also include X-rays, CT scans, or PET/CT scans, and this follow-up imaging may continue for several years after the initial diagnosis. As noted earlier, clinical outcomes in early-stage lung cancer have improved over the last decade (40). In a population-based study in patients with stage I NSCLC during 2000-2010, 62% underwent surgery, 15% received RT, 3% received both surgery and RT, and 18% received neither surgery nor RT. For these patients, the 2-year risk of death decreased by 3.5% each year, driven primarily by improved survival in surgical and RT patients. Reported outcomes in early-stage lung cancer patients treated with older techniques were relatively poor (before utilization of SBRT), and only a minority of patients reported long-term survival (41). Also, there were limited systemic options at the time. Therefore, long-term morbidity and mortality associated with RT use, such as RIC and cardiotoxicity, were less relevant since the median 5-year survival values were much lower. With improvements in RT technology, including the use of SBRT, IGRT, and IMRT, as well as dramatic improvements in diagnostic imaging quality and therapeutic approaches, the survival of patients with early-stage lung cancer improved markedly and continues to improve. It is therefore prudent to consider and measure the risk of long-term side effects of RT, in particular, RIC, in patients treated with SBRT for early-stage disease.

SBRT to the lung entails delivering a high dose per fraction to the lung nodule without elective nodal radiation (42). An advantage of using SBRT is high conformality, reduced toxicity, and improved outcomes compared to conventional RT. High-dose conformal RT requires improved immobilization, respiratory gating during the simulation and RT delivery, and improved RT

delivery technology. Improvement in clinical outcomes in early-stage lung cancer using RT is also a result of better and more accurate diagnostic imaging technology. Although SBRT is usually safe, there are some potential side effects (43, 44). Acute side effects include radiation pneumonitis, esophagitis, fatigue, rib injury, and skin toxicity. Patients with central tumors (tumors located within 2 cm of the trachea-bronchial tree) are at a higher risk of stenosis, stricture, and fistula, and risks are proportional to the high fractional doses utilized (>20 Gy per fraction). Long-term toxicity risk includes RIC, pulmonary fibrosis, and cardiac toxicity (43, 44).

Radiation-Induced Cancers (RIC):

Historically, the initial evidence that radiation can induce adverse effects came from the first observations of Wilhelm Roentgen. He was able to cause burns on his fingers when he exposed them to X-rays (45). In 1904, Clarence Dally, an assistant in Thomas Edison's laboratory who worked extensively with x-rays, is thought to be the first person to die of RIC (46). Fritz Giesel established the first dental imaging laboratory in 1896 but unfortunately passed away in 1927 from RIC because of massive irradiation exposure to his hands (47). Other deaths that were reported during the development of X-rays were Elizabeth Ascheim (1905), Wolfram Fuchs (1907), Dr. William Egelhoff (1907), as well as many other unnamed pioneers in the use of X-ray technology (46). In addition to these historical figures, the medical literature is full of reports of RIC following radiation therapy used to treat diseases such as eczema, tinea capitis, and tuberculosis. There are reports of radiation-induced cancers in radium dial workers (47, 48). Most commonly reported RIC at the time were thyroid cancers and sarcomas (46).

The risk of RIC calculated using the ICRP (International Commission on Radiological Protection) recommendation was estimated to be 10%/Sv for high dose and high-dose-rate exposure to ionizing radiation (49). In a Statistics, Epidemiology, and End Results (SEER)

database, cancer survivors of childhood soft tissue sarcoma were found to have an increased risk of developing second cancer following chemotherapy and radiation (Observed/Expected ratio = 15.2 vs. 1.4; $p < 0.0001$) (50). Strong evidence that radiation exposure is associated with malignancy has arisen from multiple human epidemiological studies examining cancer incidence following accidental, occupational, and therapeutic exposures. These include exposures resulting from the Chernobyl nuclear power plant accident (51-54), atomic bomb survivors from Hiroshima and Nagasaki (55-58), and therapeutic or diagnostic radiation exposure (59-61). Some of the most significant and well-documented epidemiological radiation carcinogenesis studies are from the Life Span Study (LSS) of Japanese Atomic bomb survivors (62, 63). Findings from human studies have been complemented and expanded upon using a large number and variety of animal exposure models (63-66).

RIC is a stochastic phenomenon- the severity of the cancer is independent of the RT-dose. Current understanding of radiation carcinogenesis posits a linear no-threshold response, e.g., there is no dose of RT below which there is no cancer risk (67, 68). This understanding is based on the linear no-threshold (LNT) model, which theorizes that the risk of cancer development is linearly proportional to RT dose and that there is no dose at which the risk does is zero. While other models have been proposed (67,68), they are not widely accepted. The LNT theory is generally accepted by the National Council for Radiation Protection (NCRP) (69), the International Committee for Radiological Protection (ICRP) (70), the United Nations Scientific Committee on the Effects of Atomic Radiation (UNSCEAR) (71) and by the Nuclear Regulatory Commission (NRC) (71). The latest National Academy of Sciences BEIR (Biological Effects of Ionizing Radiation) report (BEIR VII) is also based on the use of the LNT model (72). For a variety of reasons, there is a pronounced lack of experimental, epidemiological, and clinical data at very low exposures, less

than 50 mSv (Fig 5), at doses relevant to diagnostic and therapeutic radiology where linearity is well characterized. This feature was consistent with solid tumor incidence for doses <1.5 Gy in the Life Span Study (73).

Figure 5 (7): Schematic representation of different possible extrapolations of measured risks a low doses. Adapted from Brenner et al. (74)

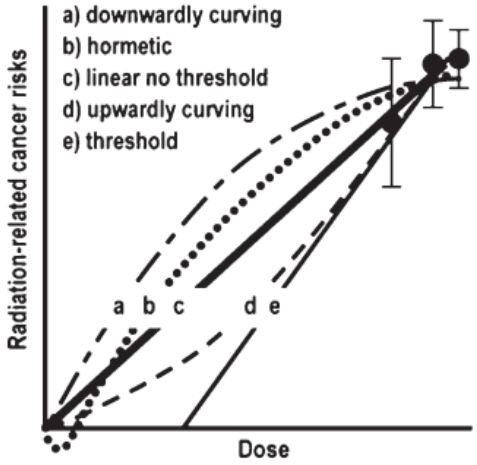

The most important epidemiological studies on which much RIC risk modeling is based was generated during the LSS study. The study cohort included a large population of some 70,000+ survivors of the Japanese atomic bombing who were initially exposed to a wide range of radiation doses. Following enrollment in the study, health outcomes for these individuals were followed for more than 50 years (75, 76) and compared to comparable unexposed matched Japanese subjects. For doses in the range of 0.1-2.5 Gy, LSS data suggests a linear relationship with solid cancers. Below this range, linearity is less clear (67). There are also concerns about the dose-response curve's shape at very high doses where other factors may affect survival. Given even larger numbers of subjects required for epidemiological studies at very low doses, below 100 mSv, it is unlikely that studies can be done to estimate cancer risk at these low exposures. Most experts feel that linear extrapolation from higher doses is reasonable (77).

Primary risk estimates in the LSS population were made from subjects exposed to relatively high dose and dose rates. Linear extrapolation to very low doses can overestimate risk. To correct this, a dose and dose-rate effectiveness factor (DDREF) was introduced (77), which was calculated using experimental laboratory data, statistical methods, and radiobiological measurements (77).

Life Span Study (LSS):

The most important source of information about RIC is the atomic bomb survivor cohort examined in the Life Span Study (LSS) (78). LSS is a longitudinal, life-long health outcomes study of some more than 70,000 survivors of the WWII atomic bombings at Hiroshima and Nagasaki. This study is being conducted by the Radiation Effects Research Foundation (RERF), a jointly funded endeavor of Japanese and US researchers (78). Findings have been used to set radiation protection standards by several national and international advisory organizations, including UNSCEAR, IAEA, NRC, ICRP, and NCRP. These guidelines are designed to minimize the probabilistic risk of cancer deaths by keeping radiation exposures 'As Low As Reasonably Achievable' (ALARA). The LSS uses the linear no-threshold (LNT) model for radiation-induced carcinogenesis to estimate risk. LNT is based on the assumption that even the smallest possible radiation dose increases RIC risk with no threshold. The excess risk is assumed to increase linearly at doses less than 1.5 Gy.

The LSS, the cohort consisted of atomic bomb survivors within 2.5 km of the epicenter of the bomb blasts and age and sex-matched controls between 2.5-10 km of the epicenter (78). Twenty-six thousand persons were registered as residents of either Hiroshima or Nagasaki in 1950 but were not in the cities at the time of the bombing. More recent LSS reports excluded these persons in the analysis because of concerns about the comparability of cohorts. The final number of subjects was 120,321 members (82,214 in Hiroshima and 38,107 in Nagasaki). In this

study, the risk of all-cause death was positively associated with radiation dose. The risk of solid cancers increases throughout life with a linear dose-response relationship. The sex-averaged excess relative risk/ Gy was 0.42 for all solid cancer at age 70 years if exposure happened at age 30. The risk increased by about 29% per decade decrease in age at exposure (95% CI: 17%, 41%). The excess relative risk (ERR) per Gy (ERR/ Gy) for total deaths was 0.22 (95% CI: 0.18, 0.26) and the risk estimate for all solid cancer was 0.47 (95% CI: 0.38, 0.56). The highest ERR was observed for cancers of the renal pelvis/ureter, breast (female only), gastrointestinal cancers, bladder, ovary, lung, colon, esophagus, gall bladder, liver, and stomach in descending order. The sex-specific ERR/ Gy in females was double that of males. The ERRs for cancers of most sites were also higher in females. ERR/ Gy for lung cancers was 0.63 (95% CI: 0.42, 0.88). Sex-averaged ERR/ Gy for lung cancers was 0.75 (95% CI: 0.51,1.03), ERR sex-ratio (f/m) was 2.7 (57,78,79,80).

LNT model (Linear no-threshold model):

The LNT dose-response model was first proposed in 1928 (81) after the publication of seminal papers by Hermann J Muller, Gilbert Lewis, and Alex Olson (82, 83). In the LNT model, the risk of inducing cancer in an irradiated tissue is proportional to the dose to that tissue, with no threshold below which there is no risk. LNT assumes that radiation can cause harm even at small doses, and the extent of harm is the same, whether it's a sum of small doses or a single large dose. LNT model has been accepted over the years because of its simplicity, and it matches the results of some observational studies of radiation carcinogenesis fairly well (84). However, there is conflicting evidence about the LNT model's accuracy based on the risk of radiation carcinogenesis reported for some epidemiologic studies. There is evidence that the model is overstating cancer risk for exposures less than 100 mSv (85). There are two additional competing

models for radiation carcinogenesis: The threshold model and the hormesis model. The threshold model assumes that very small doses of radiation are harmless. Hormesis hypothesizes that low doses of radiation are beneficial and stimulate repair mechanisms that help against disease (86). The threshold model suggests a threshold dose below which there is no risk of cancer (87). A study was performed to evaluate if non-linearity and threshold exist for atomic bomb survivors for doses of 0.01-0.05 Sv. This was done by applying the fitted statistical models to the lowest dose exposure. In this study, the estimated threshold values for solid cancer incidence was approximately 0.05 Sv, and for leukemia, it was 0.05-0.1 Sv. However, for cancer mortality, there was no threshold seen for solid cancers. However, leukemia mortality was not seen below the 0.2-0.5 Sv range (87). Regarding the Hormesis model, there are some studies showing the beneficial effect of low dose radiation (88, 89). A study on reproduction in a protozoan Tetrahymena pyriformis, a radiation dose of 0.15 mrad/d, lower than background radiation, resulted in a decreased reproduction rate. In contrast, doses that were chronically elevated above background resulted in increased reproductive rates. The authors concluded that ionizing radiation was important to maintain reproduction in T. pyriformis (88). A study was used to evaluate the effect of low dose radiation on proliferation in hematopoietic progenitor cells in a mouse model. Maximal stimulation of bone marrow cells was achieved by 75 mGy, 48 hours post-radiation, and mobilization into peripheral blood (89). However, as mentioned previously, the LNT model is useful for its simplicity and has matched models of radiation carcinogenesis well (84). Also, LSS uses the LNT model for its assessment (78), and LNT has been adopted as the model of choice by the leading nuclear regulatory agencies (78).

Radiobiology of low-LET (linear energy transfer) radiation:

Alpha particles dissipate their energy rapidly, producing short, dense tracks of ionization, and are classified as high-LET radiation. In contrast, low-LET radiation such as beta particles and gamma rays ionize the atoms in the path less frequently and produce tracks that are less densely ionized. As mentioned previously, the two main types of ionizing radiation effects are 1. Deterministic effects, and 2. Stochastic effect (90). Deterministic effects are effects that happen from cell killing, and the severity of the effects is dependent on the dose. Stochastic effects are those where the severity of the effects is not dependent on the dose. Irradiation has direct effects on deoxyribonucleic acid (DNA) through secondary electrons, and this is the dominant process associated with high-LET radiation, such as carbon ion beams (90). Low-LET Irradiation commonly causes indirect effects. Secondary electrons can interact with a water molecule to produce a hydroxyl radical, damaging the DNA molecule. Indirect action is the dominant form of interaction between biological material and less-concentrated ionizing radiation sources, such as X-rays and electrons produced by a Linac (90). Data from quantitative animal tumorigenesis and human epidemiologic studies imply that low-LET ionizing radiation acts principally as a tumor-initiating agent (91) by causing genetic mutations and initiating a carcinogenic response. Studies on the cytogenetic characterization of acute myeloid leukemia in A-bomb survivors (92) and radiotherapy-associated solid tumors (93) support a monoclonal basis for post-irradiation tumor development and suggest that the characteristics of induced tumors are similar to those of spontaneously arising neoplasms of the same type. However, an excess of complex chromosomal events and microsatellite sequence instability was observed in late-expressing myeloid leukemia arising in A-bomb survivors exposed to high radiation doses (92).

RadRAT (RadRAT available at https://irep.nci.nih.gov/radrat):

NCI has developed an online computer model (94) to assess the risk of radiation-induced cancers and the uncertainty following specific information on individual radiation exposure. The risk calculator is based on models developed by the BEIR VII (Biologic Effects of Ionizing Radiation, VII) committee. These risk models have been generated for 18 site-specific cancers. The approach that has been used in RadRAT is the Lifetime Attributable Risk (LAR). The LAR is calculated 'using the survival function for a population unexposed to radiation and is a close approximation to the more general risk of exposure-induced cancer (REIC), which is calculated using a survival function that accounts for deaths due to the same exposure to radiation for which risk is estimated.' The LAR and REIC are virtually identical for most doses of interest considered in RadRAT. The calculator estimates the LAR from the time of exposure to the end of the expected lifetime. The 'Future risk' is the sum of 'excess risk from radiation exposure' and the 'baseline risk' without that exposure. The calculator can estimate risk from a single or multiple exposures and as a sum of all exposures. The risks can be estimated for each cancer type. The following information is needed to calculate the estimated risk: 1. Sex, 2. Year of birth, 3. Exposure history: year and number of exposures, exposed organs, dose to each exposed organ, exposure rate (acute or chronic), 4. Run-specific parameters: random seed and sample size of the Monte-Carlo simulation used for the propagation of uncertainties (94).

A key component of RadRAT is that both statistical and subjective sources of uncertainty are accounted for, parameters are assigned probability distributions, and Monte Carlo simulation for uncertainty propagation (95). 'The calculator was developed using the Analytica programming software, employs Monte Carlo simulation methods with Latin Hypercube Sampling (LHS) to estimate a distribution of potential lifetime risk estimates, by taking into account statistical uncertainties in the risk parameters and subjective uncertainties in a number of

the assumptions' (96). RadRAT accounts for uncertainties in the risk model coefficients, in the transfer to the U.S. population, and the dose and dose-rate effectiveness factor (DDREF), as well as uncertainty in radiation doses, and uncertainties in the adjustments related to the minimal latency period (94).

Radiation exposure measurement from imaging:

There are three commonly used terms for radiation exposure measurement: 1. Absorbed dose, 2. Equivalent dose, and 3. Effective dose (97). Absorbed dose is the energy deposition by ionizing radiation in an absorbing medium. It's the energy imparted per unit mass, and its SI (International System of Units) unit is Joules per kilogram (also called Gray). Absorbed dose correlates well with cumulative effects, stochastic effects, and delayed effects, although it is used to determine the acute damage caused by radiation (deterministic effect) (97).

Equivalent dose is the product of the mean absorbed dose to an organ or tissue and applicable radiation weighting factors. It is computed as the sum of absorbed doses in an organ or tissue from all contributions by radiations of different types multiplied by their respective radiation qualities. The units of equivalent dose are joule per kilogram ($J\ kg^{-1}$), where the special name for the unit of equivalent dose is Sievert (Sv). It's derived from absorbed dose but takes into account the type and energy of radiation (biologic effectiveness of radiation). Equivalent dose is designated as a quantity to specify exposure limits to ensure that "the occurrence of stochastic health effects is kept below unacceptable levels and that tissue reaction is avoided" (98).

An effective dose is the weighted tissue sum of equivalent doses in all specified tissues organs and represents the stochastic health effects of low dose ionizing radiation. It takes into account not just the type of radiation (equivalent dose) but also the nature of each organ/tissue

being irradiated and enables a summation of organ doses to produce an overall calculated effective dose. The SI unit of effective dose is Sievert (Sv).

The literature review (99) estimates published effective doses from imaging commonly utilized in cancer management. In a review of various scientifically published studies, data from the United States, Canada, Japan, Australia, Western Europe, literature reviews of the United Nations Scientific Committee on Atomic Radiation, material from web sites of the U.S. FDA (Food and Drug Administration), and the Conference of Radiation Control Program directors was collected (99). The following tables give an estimate of the effective doses from various diagnostic techniques (99):

Table 1

Adult Effective Doses for Various Diagnostic Radiology Procedures

Examination	Average Effective Dose (mSv)	Values Reported in Literature (mSv)
Skull	0.1	0.03–0.22
Cervical spine	0.2	0.07–0.3
Thoracic spine	1.0	0.6–1.4
Lumbar spine	1.5	0.5–1.8
Posteroanterior and lateral study of chest	0.1	0.05–0.24
Posteroanterior study of chest	0.02	0.007–0.050
Mammography	0.4	0.10–0.60
Abdomen	0.7	0.04–1.1
Pelvis	0.6	0.2–1.2
Hip	0.7	0.18–2.71
Shoulder	0.01	. . .
Knee	0.005	. . .
Other extremities	0.001	0.0002–0.1
Dual x-ray absorptiometry (without CT)	0.001	0.001–0.035
Dual x-ray absorptiometry (with CT)	0.04	0.003–0.06
Intravenous urography	3	0.7–3.7
Upper gastrointestinal series	6*	1.5–12
Small-bowel series	5	3.0–7.8
Barium enema	8*	2.0–18.0
Endoscopic retrograde cholangiopancreatography	4.0	. . .

* Includes fluoroscopy.

Table 2

Adult Effective Doses for Various CT Procedures

Examination	Average Effective Dose (mSv)	Values Reported in Literature (mSv)
Head	2	0.9–4.0
Neck	3	. . .
Chest	7	4.0–18.0
Chest for pulmonary embolism	15	13–40
Abdomen	8	3.5–25
Pelvis	6	3.3–10
Three-phase liver study	15	. . .
Spine	6	1.5–10
Coronary angiography	16	5.0–32
Calcium scoring	3	1.0–12
Virtual colonoscopy	10	4.0–13.2

Table 3

Effective Doses for Adults from Various Nuclear Medicine Examinations

Examination*	Effective Dose (mSv)	Administered Activity (MBq)†	Effective Dose (mSv/MBq)‡
Brain (^{99m}Tc-HMPAO–exametazime)	6.9	740	0.0093
Brain (^{99m}Tc-ECD–Neurolite)	5.7	740	0.0077
Brain (^{18}F-FDG)	14.1	740	0.019
Thyroid scan (sodium iodine 123)	1.9	25	0.075 (15% uptake)
Thyroid scan (^{99m}Tc-pertechnetate)	4.8	370	0.013
Parathyroid scan (^{99m}Tc-sestamibi)	6.7	740	0.009
Cardiac stress-rest test (thallium 201 chloride)	40.7	185	0.22
Cardiac rest-stress test (^{99m}Tc-sestamibi 1-day protocol)	9.4	1100	0.0085 (0.0079 stress, 0.0090 rest)
Cardiac rest-stress test (^{99m}Tc-sestamibi 2-day protocol)	12.8	1500	0.0085 (0.0079 stress, 0.0090 rest)
Cardiac rest-stress test (Tc-tetrofosmin)	11.4	1500	0.0076
Cardiac ventriculography (^{99m}Tc-labeled red blood cells)	7.8	1110	0.007
Cardiac (^{18}F-FDG)	14.1	740	0.019
Lung perfusion (^{99m}Tc-MAA)	2.0	185	0.011
Lung ventilation (xenon 133)	0.5	740	0.00074
Lung ventilation (^{99m}Tc-DTPA)	0.2	1300 (40 actually inhaled)	0.0049
Liver-spleen (^{99m}Tc–sulfur colloid)	2.1	222	0.0094
Biliary tract (^{99m}Tc-disofenin)	3.1	185	0.017
Gastrointestinal bleeding (^{99m}Tc-labeled red blood cells)	7.8	1110	0.007
Gastrointestinal emptying (^{99m}Tc-labeled solids)	0.4	14.8	0.024
Renal (^{99m}Tc-DTPA)	1.8	370	0.0049
Renal (^{99m}Tc-MAG3)	2.6	370	0.007
Renal (^{99m}Tc-DMSA)	3.3	370	0.0088
Renal (^{99m}Tc-glucoheptonate)	2.0	370	0.0054
Bone (^{99m}Tc-MDP)	6.3	1110	0.0057
Gallium 67 citrate	15	150	0.100
Pentreotide (^{111}In)	12	222	0.054
White blood cells (^{99m}Tc)	8.1	740	0.011
White blood cells (^{111}In)	6.7	18.5	0.360
Tumor (^{18}F-FDG)	14.1	740	0.019

* DMSA = dimercaptosuccinic acid, DTPA = diethylenetriaminepentaacetic acid, ECD = ethyl cysteinate dimer, ^{18}F = fluorine 18, FDG = fluorodeoxyglucose, HMPAO = hexamethylpropyleneamine oxime, ^{111}In = indium 111, MAA = macroaggregated albumin, MAG3 = mercaptoacetyltriglycine, MDP = methylene diphosphonate, ^{99m}Tc = technetium 99m.

† Recommended ranges vary, although most laboratories tend to use the upper end of suggested ranges.

‡ From reference 74.

Tables 1-3: With Permission from: Mettler FA Jr, Huda W, Yoshizumi TT, Mahesh M. Effective doses in radiology and diagnostic nuclear medicine: a catalog. Radiology. 2008 Jul;248(1):254-63. doi: 10.1148/radiol.2481071451. Review. PubMed PMID: 18566177).

More recent publications give similar or marginally decreased effective radiation doses as above (59, 60, and 61,100,101).

Literature review: RIC with medical imaging

Multiple published studies evaluate the risk of radiation-induced cancers (RIC) from medical imaging in oncologic and non-oncologic settings. A brief review of relevant studies evaluating RIC risk from medical imaging is presented below. The studies have focused mostly

on breast and lung cancer risk from radiation exposure, although some other cancers are also discussed.

To estimate the risk of RIC in women undergoing imaging for the management of tuberculosis (TB), RIC incidence data from women with tuberculosis discharged from two sanatoria in Middlesex County, Massachusetts, between 1930-1956 was collected (102). The cancer incidence and causes of death through December 31, 1980, were calculated. Absorbed dose was calculated based on the number of fluoroscopies, reconstruction of exposure conditions, and absorbed dose estimates. Patient-related information was obtained from medical records from the original/primary hospitalization and hospitals to which the patients were subsequently transferred. All hospitals in Massachusetts were surveyed along with the available medical records. Among the 1,742 women with TB, 74 primary breast cancer cases were identified (4.2%). There were 1,044 women exposed to CXRs (chest x-rays) in management of TB, 30,932 woman-years of observation accumulated, and 55 primary breast cancers developed versus 35.8 that was expected (Observed/Expected (O/E) = 1.54; 90% CI = 1.2-1.9). The six hundred and ninety-eight patients not exposed to this number of fluoroscopies accumulated 21,486 woman-years of observation, with 19 cases observed versus 22.8 expected (O/E = 0.83; 90% Cl = 0.6-1.2). The exposed women were at an 86% increased risk of developing breast cancer than unexposed (RR = 1.86; 90% CI = 1.2-2.8). The risk was highest in the young, 15-19 year age group and was lower at older ages. The risk of developing breast cancer increased with increasing absorbed dose and was highest among those exposed to more than 3 Gy. The increased risk of breast cancer was seen after at least 15 years of follow-up. The relationship between dose and breast cancer risk was linear up to 4 Gy. The authors concluded that for patients living at least ten years, "the absolute excess risk was 5.5/1 million woman-year-rad, the

excess relative risk per rad was 0.73%". The authors also concluded that 'These data indicate that a woman's lifetime risk of breast cancer is influenced by events occurring in early reproductive life, that low-dose fractionated exposures are as effective as single exposures of the same total dose in inducing breast cancer, and that risk of radiogenic breast cancer persists for many years, and perhaps for life' (102).

A 2004 European study estimated the RIC from annual diagnostic X-rays in the UK and 14 other developed countries (103). The study used risk models after radiation exposure, frequency of exposure annually, type of radiation exposure and dose to organs and all-cause mortality and cancer incidence in population from 15 countries such as UK, Australia, Canada, Croatia, Czech Republic, Finland, Germany, Japan, Kuwait, the Netherlands, Norway, Poland, Sweden, Switzerland, and the USA. Japanese atomic bomb survivor data and linear models used in that study were utilized to determine RIC risk. For lung cancer risk, smoking history, age, and sex were included in the analysis. To determine the frequency of exposure to diagnostic CXRs, data from a worldwide survey of medical radiation was used. This data was collected between 1991-1996 as well as the one taken earlier in 1977. The data from 1991-1996 excluded age and sex information while the one from 1977 contained that information. The frequency of CT examinations was obtained from 1989 surveys of British practice and annual worldwide surveys. Mammography data was obtained from the UK national service breast screening program. Organ-specific absorbed doses were obtained from a Finnish study about x-ray exposure in the UK, a British survey of CT practice, and a mammography breast screening study. Results showed an estimated RIC from diagnostic X-ray use in the UK of 0·6% of the total risk of cancer to age 75 years in men and women, equivalent to 700 cases per year. The most common RIC cancer in men was bladder cancer, and in women was colon cancer, followed by lung and breast

cancers. The estimated annual RIC risk rose from about age 40 years and continued to rise to age 70, 2% of RIC cases were estimated before 40 years of age, and 56% cases between ages 65 and 74. Among the imaging types, CT scans were most strongly associated with RIC development, followed by barium enemas and pelvis X-rays. Radiation exposures to neonates less than one year of age were responsible for 3% of cancers versus 19% for children aged 1-14. In the UK and other developed countries, the attributable risk was 0.6%-1.8%. In comparison, the attributable risk in Japan was 3.2%, possibly a contribution from the atomic bomb exposure. However, the reason for this increased risk in Japan was not discussed by the authors (103).

In a study to evaluate cancer mortality risk in patients with scoliosis and other spine disorders exposed to imaging (104), the investigators obtained records of 5,573 female patients with a confirmed diagnosis of scoliosis, kyphosis, lordosis, or kyphoscoliosis before 20 years of age in one of 14 orthopedic medical centers in the United States during 1912–1965, collected as a part of the US scoliosis cohort study. Data on all available radiology exams included information regarding date, field, view, position, presence of an orthosis, radiograph size, whether the breast was in the radiograph beam, and radiograph machine parameters. Cumulative radiation doses to the breast, thyroid gland, lung, ovary, and bone marrow were estimated. Patients were tracked using telephone, contacts, friends, and such information was obtained on more than 94% of patients. Nineteen percent were lost to follow-up, and 16% died. In 1993, a questionnaire survey was administered to the remaining 3620 patients that were alive, and 86% participated. From this report, mortality follow-up was done, and that extended to December 31, 2004, with causes of death obtained from death certificates or through the National Death Index. The average number of radiographs per patient with any breast exposure was 22.9 (Range: 0 - 553). The estimated mean cumulative breast dose was 10.9 cGy, average and maximum doses to

the active bone marrow were 1.0 cGy, and 16 cGy, respectively, and those to the thyroid gland were 7.4 and 137 cGy, respectively. The excess absolute risk (EAR) for breast cancer was 1.8 excess deaths per 10,000 woman-years of observation, whereas the EAR for lung cancer was −0.6 excess deaths / 10,000 woman-years. There was a statistically significant 46% higher overall mortality risk compared to the general population. Cancer was listed as the primary cause for 23% of all deaths, and the overall cancer standardized mortality ratio (SMR) was 1.08 (elevated, although not statistically significant). Breast cancer was the most common cancer listed, followed by cancers of the lung, colon, and ovary. Cancer mortality was 8% more than expected (95% CI=0.97–1.20), and mortality from breast cancer was elevated (standardized mortality rate (SMR) =1.68; 95% CI: 1.38–2.02), whereas mortality rates from several other cancers were below expected, for example, the lung was SMR=0.77, cervical cancer was SMR=0.31, and liver cancer SMR=0.17 (104).

Various radiation techniques are utilized for treating breast cancer, including 2D (2-dimensional), 3D-conformal radiation therapy (3D-CRT), IMRT (intensity-modulated radiation therapy), brachytherapy. These techniques aim to deliver conformal radiation to the target while minimizing normal tissue radiation. However, the healthy tissue may receive more abundant 'low-dose' radiation that predisposes to RIC. To evaluate the risk of RIC in patients being treated for breast cancer with RT, five irradiation breast RT techniques were selected for analysis (105). These techniques included 50 Gy in 25 fractions using either physical wedge or virtual wedge, breast IMRT (Intensity-modulated radiation therapy), partial breast 3D-conformal radiotherapy (3D-CRT) to 38.5 Gy in 10 fractions, high dose rate brachytherapy delivering 34 Gy in 10 fractions, and permanent breast seed implants with palladium-103 seeds to a dose of 90 Gy. The lifetime risk and probability of developing RIC were estimated from the National Council on

Radiation Protection and Measurements (NCRP) report 116. The radiation leakage from the head of the machine was small. Larger fields resulted in a larger backscatter of electrons. For breast IMRT, internal scatter showed the most significant contribution to the total body dose. If external beam radiation therapy (EBRT) with physical wedge compensation technique, that yielded the most significant dose to solid organs like the spleen and heart that received 2,356 mSv and 3.0 Gy, respectively. Breast IMRT reduces the dose of these neighboring organs to 866 mSv and 1.4 Gy, respectively, and partial breast RT using 3D-CRT is the safest technique with doses of 130 mSv and 0.7 Gy, respectively. The dose scattered in the lung was small for IMRT and 3D-CRT, but higher for the wedge technique. A physical wedge increased the radiation dose to organs outside the treated volume by 50 - 800% compared to breast IMRT. Breast seed implant resulted in a low internal scatter, e.g., left breast irradiation using Iridium-192 HDR brachytherapy resulted in scatter to the heart was 3.6 Gy, the spleen (1,171 mSv), and the lung (2,471 mSv). Using a balloon catheter increased dose by 44%, reaching 5.2 Gy to the heart, 1,686 mSv to the spleen, and 3,558 mSv to the posterior part of the ipsilateral lung. The probability of developing RIC from various RT techniques (%/Sv) was 0.20 for the breast and 0.85 for the lung. For partial breast, the risk was 0.00% for breast RIC and 0.67% for lung RIC. With HDR catheters, it was 0.05% for breast RIC and 2.10% for lung RIC. With a physical edge, RIC breast risk was 0.34%, and lung RIC was 0.49%. Using IMRT, breast RIC was 0.04%, and lung RIC was 0.10%. Finally, using 3D-CRT, breast RIC was 0.03%, and lung RIC was 0.07% (105).

In a study to quantify the effect of reduced life expectancy on cancer risk by comparing estimated lifetime risks of lung cancer because of CT examinations in patients with and without cancer or cardiac disease (106), the following imaging exposures were measured 1. Surveillance chest and abdominal CT examinations during follow-up in patients treated for colon cancer, and

2. Coronary CT angiographic in patients with multivessel coronary artery disease who had undergone coronary artery bypass graft (CABG) surgery. The goal of the study was to estimate the ratio of lifetime lung cancer risks after radiologic examination in an individual with an average life expectancy compared to the estimated risk in the same patient with a disease-related reduced life expectancy. To estimate the ratios, the BEIR VII report was utilized. The ratio of estimated lifetime risks after surveillance CT exams in patients with colon cancer of various stages versus that in individuals with an average life expectancy compares the reduction in lifetime radiation risk due to the compromised life expectancy of the patients with colon cancer. The authors provide an example for "a 70-year-old patient with colon cancer, the estimated reduction in lifetime radiation-associated cancer risk was approximately 92% for stage IV disease, versus approximately 8% for stage 0 or I disease." A similar pattern was seen in the ratio of estimated lifetime risks of RIC lung cancer in patients who underwent CABG surgery versus individuals with an average life expectancy. For example, the estimated reduction in lifetime RIC risk was approximately 57% for a 55-year-old patient, versus only 12% for a 75-year-old patient. Patients with decreased life expectancy had decreased RIC risk (106).

A mouse model study (107) was designed to calculate the risk of RIC from multiple CT exposures, similar to the clinical situation where asymptomatic smokers and ex-smokers undergo screening that approximates the national lung screening trial (NLST) screening protocol (108). The study was also performed to hypothesize the mechanism of RIC using a mouse model. The CCSP-rtTA/Ki-ras bitransgenic mice that conditionally express the human mutant Ki-rasG12C gene in a doxycycline (DOX)-inducible and lung-specific manner were used in these experiments. Eight groups of mice were as follows: Group 1: No DOX, sham irradiation; Group 2: No DOX + 5 mGy/fraction; Group 3: No DOX + 15 mGy/fraction; Group 4: No DOX + 25

mGy/fraction; Group 5: DOX + 5 mGy/ fraction; Group 6: DOX + 15 mGy/fraction; Group 7: DOX + 25 mGy/fraction; Group 8: DOX + sham irradiation. The four weekly whole-body exposures were 5, 15, or 25 mGy plus the lung imaging exposures of 30 mGy at 3 and 6 months. This resulted in total lung doses of 80 mGy (Groups 2, 5), 120 mGy (Groups 3, 6), and 160 mGy (Groups 4, 7). In the DOX alone group, there was no significant difference ($P > 0.3$) in tumor formation. The number of tumors/mouse in radiated mice expressing the Ki-rasG12C gene was 43% greater than the unirradiated mice expressing the Ki-rasG12C gene in their lungs. In contrast, the tumor incidence in irradiated and unirradiated mice that did not express the Ki-rasG12C transgene was identical. For those mice expressing the Ki-rasG12C gene, irradiated females had significantly more tumors/mouse than irradiated males. No tumor size difference or dose-response was observed over the dose range of 80–160 mGy for either sex. Irradiated mice that did not express the Ki-rasG12C gene had a low tumor incidence not affected by exposure to CT radiation. There was no evidence to suggest that low-dose CT radiation affected the tumor growth rate (volume doubling time) or morphology. The data suggested that individuals expressing susceptibility genes have a higher carcinogenic risk from CT exposures, individuals not expressing a cancer susceptibility gene have little or no RIC risk from CT, the increased RIC risk from CT is probably due to promotion rather than initiation, and estimates of the carcinogenic risk from CT imaging that extrapolate Japanese atomic bomb survivor data (likely initiation) to low-dose CT exposures (likely promotion) using the LNT model should be viewed with caution. The LSS data suggested an increased risk of RIC in the entire population exposed to low-dose RT compared to the background risk of the unexposed population (78, 79-74). Risk among smokers was higher than non-smokers, although there was no particular genetic profile

identified in the LSS population that increased the risk of RIC of the lung after atomic bomb radiation exposure (57, 78, 79, and 80).

ITALUNG is a randomized clinical trial that showed that annual screening using a low-dose CT scan (LDCT) for four years decreases lung cancer mortality compared with usual care in high-risk patients such as smokers and former smokers. The trial included four scans, one baseline, and three repeat scans. Investigators (109) assessed the collective effective dose delivered to subjects participating in the ITALUNG trial. The trial included smokers aged 55-69 years with at least 20 pack-year smoking history and no prior history of cancer. The collective effective dose delivered to nine hundred ten males (mean age 61.1 years) and four ninety-six females (mean age of 60.6 years), who underwent screening with LDCT formed the basis of this report and was obtained by adding the effective doses associated with LDCT examinations, chest FDG-PET examinations, and CT-guided biopsy procedures. The dose from LDCT examinations was based on acquisition protocols used in each CT scanner, the air CT dose index values reported in the database of the CTDosimetry (release 1.0.2, http://www.impactscan.org/) software. The RIC risk was assessed using the National Radiological Protection Board (NRPB) and in ICRP publications 60 and 103 and using the BEIR VII report, which allows estimation according to gender and age. The number of potential radio-induced tumors in adult subjects is 0.035/Sv, according to NRPB, 0.048/ Sv, according to ICRP 60, and 0.041/ Sv, according to ICRP 103. The total number of LDCT examinations was 6320, a mean of 5.9 LDCT examinations/subjects over four years. Ninety-five chest FDG-PET scans were carried for the management of suspicious nodules or annual repeat screening rounds. Thirty-eight CT-guided FNA procedures were carried out in 34 subjects. The average collective effective dose in the subjects was 8.02Sv for short volume acquisition and 8.91Sv for long volume acquisitions. The

cumulative effective dose with chest FDG-PET scans was 0.66 Sv, mean collective effective dose associated with CT- guided FNA procedures was 0.06Sv. The average collective effective dose in subjects considering LDCT examinations was between 8.75 and 9.36 Sv, and the mean effective dose/subject over four years was between 6.2 and 6.8 mSv. The mean number of RIC ranged between 0.12-0.33/1000 subjects (109). According to BEIR VII, the RIC risk was 0.12 - 0.13/1000 males and 0.31-0.33/1000 females. In conclusion, the individual effective dose in this 4-year lung cancer screening trial with annual LDCT was very low. This low rate of RIC matches the results of my study, which also showed a clinically insignificant risk of RIC with images performed within the two years around SBRT (0.05%). The population in my study is already diagnosed with cancer and is generally older.

In a study to evaluate lung cancer risk from breast cancer radiation (110), fifteen patients with early-stage breast cancer patients were planned for radiation treatment. The prescription dose for the standard fractionation schedule was 5000 cGy in 2 Gy fractions, and for the hypo-fractionated schedule, the prescribed dose was 4256 cGy in 16 fractions. Dose-volume histograms (DVHs) of the target and healthy tissues were calculated. Differential DVH data for the ipsilateral lung was then analyzed using a 'Fortran program' that utilizes a biologically-based mathematical model of spontaneous and radiation-induced carcinogenesis. In a differential DVH, the radiation dose is split into bins of 1 cGy, and the model formalism allows the predicted lifetime risk of RIC to be estimated for each bin. These estimates are summed to generate risk predictions for the entire DVH for each plan. Model-predicted absolute RIC for lung cancer for each year after RT were adjusted by the probability of the patient to survive up to the given year, and these results were added to obtain lifetime absolute risk (LAR). The LAR was compared with average lifetime absolute risks for similar individuals receiving no RT. The mean predicted

LAR of lung cancer for standard fractionation was 4.86% +/− 0.43% in the supine position and 1.99% +/− 0.18% in the prone position for a mean difference 2.87%. An analysis of hypo-fractionated plans revealed that the mean predicted LAR of lung cancer was 4.78% +/− 0.43% in the supine position and 1.88% +/− 0.17% in the prone position ($p<0.001$). There was no difference in the relative risk of RIC between standard versus hypo-fractionated schedules in either the supine (RR 1.05, 95% CI 0.97-1.14) or prone positions (RR 1.01, 95% CI 0.88-1.15). Prone breast irradiation is associated with a significantly lower predicted risk of secondary lung malignancy (110).

A retrospective study was conducted in Taiwan (111) to assess cancer risk from radiation exposure for coronary artery disease (CAD). This cohort study was conducted based on the Longitudinal Health Insurance Database 2000 (LHID2000) from the NHIRD of Taiwan that included 1 million individuals enrolled in LHID2000. Subjects with CAD were identified by ICD-9-CM code and records collected from 1997-2010. Subjects without cancers before medical radiation exposure were included to correlate the effect of radiation on carcinogenesis. Patients that were selected in this study had patients that received myocardial perfusion scintigraphy (MPS), coronary angiography (CA), cardiac ventriculography (CV), computed tomographic coronary angiography (CTCA), and percutaneous transluminal coronary angioplasty (PTCA) accompanied medical radiation exposure including medical/dental radiography, conventional and interventional fluoroscopy, and nuclear medicine procedures. The control cohort included patients that underwent electrocardiography or echocardiography for the diagnosis of CAD, accompanied by most of the medical radiation procedures except MPS, CA, CV, CTCA, and PTCA. The demographics were 10,367 vs. 8,310 males exposed vs. unexposed, respectively, 8,330 vs. 10,799 females exposed vs. unexposed. The average age at examination was 61.5±15.7

and 59.7±15.6 in males exposed/control subjects, 63.8±11.6 and 60.6±14.1 years in females exposed/control subjects, respectively. The total cancer cases were 565 in exposed males versus 433 cases in unexposed males. Three hundred eighty-nine cancer cases in females were exposed vs. 452 in the unexposed female. 93.5% of patients that underwent medical procedures for CAD were over 40 years of age. The average numbers of all medical radiation procedures were 36.9 and 33.5 in the male exposed/control subjects and 41.9 and 36.6 in the female exposed/ control subjects. The age-adjusted incidence rate ratio (AA-IRR) was calculated. The risk of breast cancer (AA-IRR=1.85, 95% CI: 1.14-3.00) is significantly increased with cardiac procedures. The relative risk of RIC of the lung is significantly increased more than five cardiac diagnostic/therapeutic procedures and those with 1-5 procedures compared to no exposure (RR=2.2 and 1.9, 95% CI: 1.2-3.9 and 1.1-3.3, respectively). The exposure-dependent risk was found in breast cancer among those cumulated more than five procedures and 1-5 procedures compared with those with no cardiac exposure (RR=3.3 and 1.8, 95% CI: 1.1- 10.4 and 1.0-4.1, respectively) (111). In conclusion, cancer risks of the breast and lung were increased with the exposure levels of cardiac imaging or therapeutic procedures for CAD.

In a retrospective analysis of a ten year, observational lung cancer screening trial (COSMOS study), high-risk participants (age >50, smoking history with ⩾20 pack-years, and no history of cancer in the past five years) underwent annual LDCT for ten consecutive years (112). Patients with clinically significant findings on LDCT underwent additional exams for further work-up. The COSMOS was conducted in 2004-15. After completing the study, all examination results were collected from the radiology information-picture archiving and communication system (RIS-PACS) and analyzed at Radimetrics (Bayer Healthcare), commercially available software for monitoring and tracking patient radiation exposure. Total

estimated organ dose and effective dose were calculated as the sum of the doses of each LDCT examination and PET CT scans for each patient. The LAR of cancer incidence was derived from an equivalent dose table of the National Research Council's Biological Effects of BEIR VII report. Over the ten years, 5203 high-risk subjects underwent 42,228 LDCT scans and 635 PET-CT scans. The median effective dose measured at the baseline was 1.0 mSv for men and 1.4 mSv for women. Median cumulative effective doses from both LDCT and PET-CT scans at the 3rd, 5th, and 10th year of screening were 3.0 mSv, 5.2 mSv, and 9.3 mSv for men, respectively, and 4.2 mSv, 7.2 mSv, and 13.0 mSv for women, respectively. The lifetime attributable risk (LAR) of lung cancer after ten years of CT screening was 5.5/10000 participants for women starting screening at age 50-54, versus 1.4/10000 participants for men starting screening aged 65 and older. The number of lung and other primary cancers induced by ten years of LDCT screening was 1.5 and 2.4, respectively, which results in a theoretical risk of primary carcinoma of 0.05% (2.4/5203). The LAR of lung cancer was four times greater for women aged 50-54 years versus older men aged 65 and older (106). Estimates of lung cancer over ten years yielded one radiation-induced lung cancer that would be expected for every 173 lung cancers diagnosed. One radiation-induced cancer is expected for every 108 (259/2.4) lung cancers detected through screening. The authors concluded, 'Radiation exposure and cancer risk from low dose CT screening for lung cancer, even if non-negligible, can be considered acceptable in light of the substantial mortality reduction associated with screening' (112).

In a Brazilian study (113) evaluating RIC in women undergoing breast radiation using MCNPx code (Monte Carlo N-particle eXtended code) (114), a female phantom was adapted for whole breast radiation therapy simulation. MCNP code is general-purpose, continuous energy, generalized geometry, time-dependent, Monte Carlo radiation transport code designed to track

many particle types over broad ranges of energies. MCNPx code is capable of simulating particle interactions over 34 different particles and many heavy ions. Two tangential beams with the same weight were simulated, following 3D conformational radiation therapy (3D-CRT), and the mean absorbed dose to the body organs was calculated (prescription dose 50 Gy in 25 fractions). The highest risk of second cancers was determined to be in the contralateral breast, followed by leukemia, lung, and stomach cancer. The risk of a secondary RIC for the Brazilian population ranged between 2.2–1.7% and 0.6–0.4% for the ages of 35 years and 80 years, respectively (114).

A Four-Dimensional (4D) CT scan is which is an advanced technique to acquire a sequence of 3DCT for respiration signal, which could be used to monitor the lesion motion in patients, has been widely utilized in radiation therapy as well as for diagnosis. 4DCT is frequently used in SBRT planning and delivery. Investigators quantified and compared radiation dose to organs at risk with 4DCT scans versus conventional 3DCT scans using Monte Carlo simulation and investigated RT dose as a function of patient size (115). One hundred and two patients treated between 2007-2017 were included in this study. The mean age of patients was 65 (Range: 6-93y). A 16-slice Brilliance Big Bore CT scanner (Philips Medical System) was used, and a thoracic 4D helical plus 3D axial scans were acquired. Varian real-time position management system v1.7 was used in the 4DCT acquisition, and organ doses from the 3DCT and cine 4DCT imaging were calculated using Monte Carlo simulation. The function of estimated relative risk (ERR) in BEIR VII models was used to calculate the cancer risk. The average of the mean dose to thoracic organs was in the range of 7.82-11.84 cGy/4DCT scan versus 0.64-0.85 cGy/3DCT scan. The mean dose delivered to the whole body per 4DCT scan was 12.8-fold

higher versus each 3DCT scan. The relative risk of cancer increased (with a ratio of 15.68:1) resulting from 4DCT scans compared to 3DCT scans (115).

There are case-reports of radiation-induced cancers that happen years after radiation exposure. Radiation-induced sarcoma (RIS) is a rare late-onset complication of radiation therapy, usually developed in 8.4–10 years (116,117). A published case report from 2019 reported a 10-year survivor with stage IV EGFR-mutated NSCLC who had undergone palliative radiation therapy three times for recurrent cancer. Such reports are infrequent because patients with stage IV NSCLC are unlikely to survive ten years. RIS was located on the edge of the irradiation region of the second sacral vertebra. The total dose was 30 Gy in 10 fractions in the field, but RIS arose in the region exposed to a very low dose of around 2 Gy (118), which supports the LNT model discussed above.

RIC can potentially be reduced when delivering therapeutic radiation. In a planning study to evaluate whether a radiation plan can reduce RIC in women being treated for breast cancer, three commonly used RT techniques were compared: IMRT, Volumetric modulated arc therapy (VMAT), or Field-in field. The lowest excess absolute risk (EAR) for the contralateral breast RIC, Contralateral lung RIC, and Ipsilateral lung RIC were achieved with field-in-field technique, which reduced the EARs by 77%, 88%, and 56% relative to those with IMRT, and by 77%, 84%, and 58% relative to those with VMAT, respectively (119).

A study aimed to assess the RIC risk after radiotherapeutic management of Hodgkin's lymphoma (HL) using involved field radiation therapy (IFRT) versus involved site radiation therapy (ISRT) (120). Twenty consecutive patients with supra or infra-diaphragmatic HL underwent a planning CT scan. For each patient, two planning target volumes (PTVs) were generated, one for ISRT and the other for IFRT, based on recommendations of the international

lymphoma radiation oncology group (ILROG) (121). The Excess absolute risk (EAR) and lifetime attributable risk (LAR) for the induction of RIC of organs at risk after RT was estimated. Moreover, the calculated LAR for each studied organ compared to the corresponding baseline risk for patients unexposed to this RT. For supra-diaphragmatic HL, the LARs for developing RIC for lung, mouth, and pharynx were found 1.2–1.3 times higher than the baseline risk of the unexposed population. The LARs for the development of thyroid and breast cancer were 1.2–2.6 times lower than baseline risk. Using the involved site technique (ISRT), which treats a smaller volume, the LARs for the lung, mouth, breast, and thyroid cancer induction were 1.2–3.9 times lower, while those for pharyngeal cancer were found 1.1 times higher than the baseline risk. The LAR for RIC with involved-field RT (IFRT) that treats a bigger area versus ISRT, RIC was found 0.50%–8.02%, depending on the organ at risk and the calculation model, and for ISRT technique was 0.50%–5.19%. For HL below the diaphragm, the LAR for RIC with IFRT was 0.20%–9.28%, whereas the corresponding range with ISRT was 0.86%–6.01% (121). Estimated cancer risks for breast, lung, thyroid, colon, and rectal with ISRT was significantly less compared to IFRT. The risk of RIC for lung, mouth, pharynx, rectum, and colon was more than 1.2 times higher than the negligible risk for IFRT.

Regarding excess cancer risk from radiation in children, a study estimated the lifetime excess cancer risks for children that had an atrial septal defect (ASD) repair, a patent ductus arteriosus (PDA) repair, or a pulmonary valvuloplasty (122) since it involves various cardiac catheterization procedures using imaging. The study included children who were all participants of the “Coccinelle” cohort study that investigated the incidence of leukemia in the long run and solid cancers among children treated in France with a cardiac catheterization procedure (CCP). Excess radiation during CCPs is due to fluoroscopy used to obtain hemodynamic images of the

circulatory system. This is typically associated with effective radiation doses from 3 -15 mSv, although it can result in doses exceeding 50 mSv for some complex procedures. The study population was 1175 children who underwent 1251 CCP in 2009 -2013. The median age of children at CCP was 8.7 years for ASD closure, 2.7 years for PDA occlusion, and one month for pulmonary valvuloplasty. Radiation exposure was most to the lungs and breasts with estimated median equivalent doses 3 - 17 mSv and 1 to 16 mSv respectively, depending on the type of procedure and patient age. Median doses were 2 - 9 mSv to the esophagus, 1 - 5 mSv to active bone marrow, stomach, liver, and pancreas, and below one mSv to the other organs. Pulmonary valvuloplasty had the highest median projected lifetime attributable risks (LARs), 5 – 12/1000 (0.5-1.2%) procedures in girls and 1 – 2/1000 (0.1-.2%) procedures in boys. PDA occlusion, median LARs ranged from 4 -7/1000 (0.4-0.7%) in girls and 0.5–1/1000 (0.05-0.1%) in boys, depending on the age group. Median LARs ranged between 0.3 and 1.4 (atrial septal defect closure), 0.6 and 5.0 (PDA occlusion), and 1.0 and 12.0 (pulmonary valvuloplasty)/1000 procedures, depending on patient sex and age at treatment. These numbers show the RIC risk of 0.4% - 6.0% of children's total lifetime cancer risk. For the 10% of procedures with the highest radiation exposures, LARs reached 4.2 /1000 (0.4%) in boys and 22.2/1000 (2.2%) in girls. In boys, lung cancer accounted for 70% - 80% of the projected LARs, whereas in girls, it accounted for 20% - 60% and breast cancer for 30% - 80% of the excess risks, depending on the type of procedure and patient age (122).

To quantify the impact on cancer risk of diagnostic imaging procedures and the associated dose, a French study estimated the number of new cancer cases in adults in France in 2015 attributable to RIC (123). The analysis focused on the risk of RIC occurring in adults >30 years of age. Interventional diagnostic procedures, specifically coronarography and cerebral

angiography, X-rays (including mammography) and CT scans, constituted exposure to external medical radiation, with nuclear medicine considered as internal irradiation exposure from one of the following: 99mTc Phosphates (bone scan), 20ITI Thallous chloride (myocardium), 99mTc Tetrofosmin (myocardium), 99mTc Sestamibi (myocardium), 99mTc MAA (Lung perfusion) and 18F-FGD-PET. Therapeutic irradiation was excluded from the analysis. The average annual radiation dose delivered to each organ in milligray (mGy) was estimated by combining the frequency of X-rays, CT scans, and interventional radiology procedures by sex and age group. As is generally accepted for radiation-induced solid malignancies, a 10-year latency period was assumed between exposure and cancer diagnosis. Therefore, the excess relative risks (ERR) were estimated by sex and age group for 2015 using lifetime cumulative organ dose exposures estimated at the year 2005, from medical imaging using the risk models described in the BEIR VII report. The dose-risk relationship was linear for all cancer sites, except for leukemia, for which a linear-quadratic relationship was assumed. Specifically, the ERRs were computed for cancers. Both the BEIR VII risk models and the organ doses per procedure were available: bladder, female breast, colon, liver, lung, stomach, esophagus, and thyroid. Also, PAF (population attributable fractions) were calculated. The PAF refers to the fraction of all cases of a particular disease in a population attributable to a specific exposure. Among men, the highest ERR related to cumulative external medical imaging exposure was for leukemia. Among the other cancer sites, the ERRs among men did not differ substantially. In women under the age of 75, the highest ERR from cumulative exposure to external medical imaging was for bladder cancer, and after this age, the highest ERR was for leukemia. There were 346,000 estimated new cancer cases in adults in France in 2015, of which 2300 cases (940 among men, 1360 among women) were attributable to diagnostic imaging, which was 0.7% of all newly diagnosed cancer

cases (0.5% for men, 0.9% for women). The leading diagnostic RIC were female breast (n = 560 cases), lung (n = 500 cases) and colon (n = 290 cases) cancers. The authors concluded that compared to other risk factors, the contribution of medical diagnostic imaging to the cancer incidence is small, and the benefits largely outweigh its harms (123).

In another study in estimating RIC risk from therapeutic radiation for breast cancers (124), the authors estimated organ doses for three-dimensional conformal radiotherapy (3D-CRT) and a multi-field IMRT technique with a Monte Carlo-based treatment planning system. IMRT uses a highly conformal technique that generally is shown to spread lower doses around versus 3D-CRT. In the next step, based on these doses, RIC risks were calculated for the lung, breast, and esophagus. For more distant organs, the authors applied results from the atomic bomb survivors of Hiroshima and Nagasaki. The prescribed dose to the whole breast was 50.4 Gy plus an additional boost of 16 Gy to the tumor bed. Cancer risks were derived by applying published, organ-specific risk models, and estimates from the dose-volume histograms (DVH) of nearby organs. DVH for each organ is a calculation in radiation planning that shows the dose to each contoured organ. For 3D-CRT, the relative risk was 1.4, and the highest for lung cancer. For the IMRT plan, the relative risk was higher for the contralateral breast, compared with the 3D-CRT plan. For right-sided breast therapy, high relative risks of 1.2 were for 3D-CRT without wedges and 1.4 for multifield IMRT for the liver. However, as liver cancer is infrequent, the total contribution of liver cancer to the entire risk is low. Estimated risks to colon, uterus, and pancreas were comparable to lung and contralateral breast (124).

In another study to evaluate RIC from breast cancer therapeutic radiation using different RT techniques, including accelerated partial breast radiation (APBI), lifetime attributable risks were calculated using BEIR VII (125). APBI treats the resected tumor bed

rather than the whole breast, which is another standard RT option. Measurements of the scatter dose for various RT techniques were performed using custom-made tissue-equivalent breast phantoms. Whole breast radiotherapy used a regimen of 42.5 Gy in 16 fractions. Beam angles were optimized to reduce the contralateral breast and lung dose. The dose was measured in the lungs, contralateral breast, thyroid, esophagus, colon, ovaries, and the uterus using ThermoLuminescent dosimeters (TLDs) distributed uniformly over the organs and Gafchromic film for the lungs. The lungs got the highest mean doses (50 to 200 cGy) depending on the RT technique. The mean doses to the other organs remained well below 70 cGy except for the esophagus, which received more than 100 cGy with the 3D-APBI. The mean doses to the ovaries and uterus ranged between 1 to 8 cGy. As expected, Whole breast radiotherapy delivered the highest doses versus all APBI techniques that resulted in lower doses to the lungs and contralateral breast. The Cyberknife techniques (a different radiation delivery machine that uses a robotic arm and has more degrees of freedom) showed a slightly higher dose to the abdominal organs than other APBI techniques. The lungs carried the highest LAR, with a 3.8% lifetime risk of lung RIC for whole breast radiotherapy at age 50 years. The LARs for the uterus were lower than 1/1000th of the LARs of the lungs. The relative risk for women exposed at age 40, 50, 60, and 80 years were compared to non-irradiated breast cancer patients of the same age. Selecting a threshold of 50% relative risk increase as being clinically significant, only whole breast RT and the VMAT technique significantly increased RIC risk of lung cancer. If a 10% increase in relative risk is considered clinically significant, there was an increased risk of lung RIC for all techniques of all ages. At a 10% threshold, there is also an increased risk of esophagus cancers, although absolute numbers were small. The risks of secondary malignancies of the thyroid, contralateral breast, ovaries, and uterus were close to the baseline (125).

Another planning study (126) to estimate the risk of RIC in the lungs and the contralateral breast, in the case of left-sided breast cancer patients treated with RT, comparing 3D-CRT and 2 VMAT (volumetric arc therapy) approaches. VMAT is a highly conformal planning technique that may scatter low dose around the target to achieve high conformality. Planning CT scans of 20 patients presenting with stage I/ II left breast cancer after breast-conserving surgery were randomly selected from the institutional database. The clinical target volume (area of the breast at risk of microscopic disease) was delineated for whole-breast irradiation according to the Radiation Therapy Oncology Group (RTOG) recommendations with a prescription of 40.05 Gy in 15 fractions of 2.67 Gy. RTOG is the radiation body that sets guidelines for RT planning. Three plans per patient were generated: 1. 3D-CRT field in field plan, 2. The VMAT_full plan using the RapidArc technique (Varian Medical Systems, delivers RT in a short time) and 3. The VMAT_tang, a full VMAT plan optimized with avoidance sectors. Each of these planning techniques has a different low dose RT dose scatter around the target. Excess absolute risk (EAR) was estimated using linear, linear-exponential, plateau, and full model (which uses a carcinogenesis model, epidemiologic data induction if cancer, and accounts for cell repopulation/ repair during the radiation therapy). The EAR differences between 3D-CRT and VMAT_tang were highly significant for the contralateral breast; however, the absolute difference did not reach 1 case of 10,000 patient-years (criteria for significance). Concerning the risk of RIC induction, 3D-CRT and VMAT_tang could be considered equivalent. The VMAT_full technique presented a significantly higher RIC risk to the contralateral organs, and the absolute difference between VMAT_full and the other techniques was 5 to 6 cases over 10,000 patient-years (126). These studies again suggest a risk of RIC from the treatment of breast cancer with external beam radiation.

A modeling study (127) was done to calculate the RIC in a non-malignant situation, a non-malignant shoulder syndrome. Shoulder syndrome affects the shoulder joint causing pain and a loss of motion. Duplay described this benign disease in 1872 with the term periarthritis humero-scapularis. Treatment options include physiotherapy, non-steroidal anti-inflammatory drugs, direct injection of steroids, extracorporeal shock wave therapy, open or arthroscopic surgery, or radiation therapy. The Monte Carlo N-particle (MCNP) radiation transport code was employed to model a medical linear accelerator emitting 6 MV photon beams. This was combined with a computational androgynous phantom to represent the patient's irradiation for non-malignant shoulder syndrome. A two-field technique was used to simulate the radiation therapy in the region of the shoulder using two opposing anteroposterior (AP) and a posteroanterior (PA) treatment field. Monte Carlo simulations were used to find the average radiation dose received by all critical organs (based on the BEIR-VII report). The average dose was calculated for the following ten organs: stomach, colon, liver, lung, prostate, urinary bladder, thyroid, female breast, uterus, and ovary. For each selected organ, the lifetime attributable risk for cancer development was calculated by multiplying the average dose by an organ- age- and gender-specific risk factor derived from the BEIR-VII report. RIC risk assessments were made by assuming patients to be 50- and 60-year-old males and females. Monte Carlo calculations resulted in an average range of 0.7–48.4 mGy for a total target dose of 6 Gy. The use of smaller field sizes resulted in a mean dose reduction of 14.0 ± 3.6% (range: 9.8–19.4%). The lifetime probabilities for 50-year-old males undergoing RT in the region of shoulder ranged from (2.4×10^{-4})% to (2.7×10^{-3})%, whereas the corresponding range for patients treated at the age of 60 years was (1.4×10^{-4})% to (2.2×10^{-3})%. The LARs for female patients was estimated to be (1.4×10^{-4})% to (2.8×10^{-2})% depending upon the patient's age at the time of RT and the organ of

interest. The probability of lung cancer, as estimated with the non-linear mechanistic model, was 0.11% - 0.16% by the age and gender of the exposed patient. The corresponding risk range obtained with the linear model was 0.12–0.18%. The lung cancer risks were 36–64 times less than the lifetime intrinsic risk (127).

Lung cancer screening (LCS) refers to screening for lung cancer using low-dose CT (LDCT) systems with up to 64 detector rows. However, contemporary wide-area detector CT scanners may considerably suppress the radiation burden from CT imaging. A study (128) aimed to determine the absorbed dose to all radiosensitive organs of individuals of different body habitus with various CT scanners. The comparison was between a standard LCS LDCT examination on a modern 256-slice CT scanner, a single LCS 256-slice LDCT study and estimate the theoretical cumulative risk of radiation-induced cancer for a typical cohort to be subjected to repeated annual LCS 256-slice LDCT studies versus the calculated intrinsic risk of being diagnosed with cancer at the age of enrollment in a CT-based LCS program. Chest CT was performed to scan and cover the chest region from the lung apex to below the diaphragm. Mathematical anthropomorphic phantoms representing the internal human anatomy was generated by Bodybuilder software package version 1.3 (White Rock Science, White Rock, NM, USA). This software allows the generation of standard humanoid phantoms representing average-size individuals. Doses to all radiosensitive organs/tissues were derived for different scans as ‘normalized values to free-in-air CT dose-index’ at the isocenter. The risk of developing RIC at any time after the age at exposure, known as life-attributable risk (LAR), was estimated for a single 256-slice LDCT chest examination for adults of varying body mass index and age at exposure (range: 55-80 years).

Organ/tissue-specific LARs associated with this LDCT was estimated from organ doses and organ-specific RIC risk factors available in the literature for the estimation of radiation-induced cancer risk following low-level exposures to ionizing radiation. Linear interpolation was employed to derive risk factors for the age range 55–80 years with a '1-year step'. The radiation-induced cancer LARs for lung, colon, stomach, bladder, liver, thyroid, breast (females), uterus (females), ovary (females), prostate (males), leukemia, and the remainder of organs were determined. The total estimated RIC risk for a specific adult subjected to a single lung cancer screening LDCT examination at a specific age was determined as the sum of all corresponding organ-specific LARs. Cumulative LARs from annual LDCT exposures from the age of 55 or 65 years till the age of 80 years was derived by adding up the LARs of LDCT exposures performed till the age of 80 years. The estimated cumulative LAR was compared to the corresponding baseline lifetime intrinsic risk (LIR) of being diagnosed with cancer at any time during remaining life as provided by the National Cancer Institute (NCI). The effective dose from the standard lung cancer screening 256-slice LDCT examination to normal BMI, overweight and obese populations (high BMI) in equal numbers of males and females was estimated to be 0.77, 0.72, and 0.63 mSv, respectively. The effective dose for a typical screening cohort was estimated to be 0.71 mSv. The cumulative LAR of cancer from repeated annual scans from the age of 55 years to 80 years was found to increase the baseline LIR of cancer by 0.11 % and 0.27 % for the typical LCS male and female population, respectively. The RIC LAR from a single LDCT study was found to increase the nominal LIR of cancer in average-size 55-year-old males and females by 0.008 % and 0.018 %, respectively. Cumulative radiation-induced cancer risk of cancer from repeated annual scans from 55–80 years was found to increase the nominal LIR of cancer by 0.13 % in males and 0.30 % in females (128).

To eliminate confounding in the study, a propensity-matched analysis (129) was conducted to compare the incidence of radiation-induced radiation pneumonitis and RIC for breast cancer patients treated with IMRT/VMAT (intensity-modulated radiation therapy/volumetric arc therapy). A total of ninety breast cancer patients were enrolled, of which 32 patients were treated with IMRT and 58 with VMAT. Patients received either IMRT/VMAT with a simultaneous integrated boost technique, a boost plan built within the primary radiation plan. SIB is a radiation planning technique of adding additional radiation to the high-risk region at the same time as primary radiation treatment rather than adding a separate boost dose at the end of primary treatment. IMRT patient treatments were planned with a six or 7-field plan, while VMAT used a five/six-partial-arc plan. The prescribed doses were 63 Gy to planning target volume and 51 Gy to subclinical disease area delivered at 1.7–2.1 Gy per fraction using SIB. Schneider's full models of organ equivalent dose (OED) and excess absolute risk (EAR) were used for the carcinoma induction analyses. The risk equivalent dose is a dose-response-weighted tissue dose value that is proportional to the risks. The RIC was evaluated for the spinal cord, contralateral breast, contralateral lung, ipsilateral lung, liver, and stomach, all of which were assigned parameter values obtained from Schneider's full risk models. The EAR was calculated for patients from the age of exposure to 70 years of age. VMAT only showed a significantly lower OED and EAR compared to IMRT of the ipsilateral lung ($p \leqslant 0.01$). However, the values of OED and EAR in the contralateral lung and breast were slightly higher in VMAT than in IMRT patients ($p \leqslant 0.05$). The authors concluded that VMAT is a rational radiotherapy option for breast cancer patients, based on its reduced potential for inducing secondary malignancies and radiation pneumonitis complications compared to IMRT (129). Currently, both techniques

are utilized in breast cancer radiation planning, although 3D-CRT is still the most commonly used.

Another breast radiation planning study compared and estimated the risk of ischemic heart disease and RIC between two radiotherapy techniques (3D-CRT or VMAT) in free-breathing (FB) and DIBH (deep inspiratory breath-hold) from RT for left-sided breast cancer (130). Computed tomography data sets of 10 patients with left-sided early-stage breast cancer were used in the study. All patients were treated with 3D-CRT in DIBH (helps minimize target movement with breathing during RT delivery) following breast-conserving surgery. Patients had to undergo two planning CT scans acquired on a CT simulator, and target volume and organs at risk (OAR) were contoured using the treatment planning software Oncentra® (Nucletron, Elekta, Sweden). Four different treatment plans were generated for each patient: for both techniques, 3D-CRT and VMAT, two plans were created based on CT scans free-breathing (FB) and deep inspiratory breath-hold (DIBH). The prescribed dose was 50 Gy in 25 fractions. There was no significant difference in 10-year excess RIC risk when comparing 3D-CRT plans in DIBH and FB ($P = 0.95$). In contrast, in VMAT plans, the predicted EAR of RIC was significantly increased when the DIBH maneuver was applied ($P = 0.02$). The 10-year EAR for RIC lung cancer was significantly influenced through the use of VMAT, which was correlated with a significant increase in radiation-induced lung cancer risk as compared to 3D-CRT plans in DIBH plans ($P = 0.007$) and FB plans ($P = 0.005$). The baseline risk for lung cancer had the most definite impact on EAR estimation: medium-risk patients showed substantially lower 10-year EAR values for Radiation-induced lung cancer than high-risk patients (0.08% vs. 0.67% in 3D-CRT FB plans) (130).

The majority of radiation treatments for patients with various cancers are given using photons. The use of protons (a heavy particle) is gaining popularity since it delivers a more conformal RT given its 'Bragg-peak' effect. Bragg-peak is the sharp radiation dose fall off beyond the target. In a comparison of RIC risk between photons and protons, patients with thymoma/thymic carcinoma requiring adjuvant radiation therapy after surgical resection and treated with double-scattered proton beam radiation therapy (DS-PBT) between 2011 and 2016 were enrolled in a registry study allowing prospective collection of treatment data, toxicity, and clinical outcomes (131). Ten consecutive patients with completely resected stage II thymic malignancies were selected for evaluation of RIC, and two plans were generated for each patient. And in each, the average 4D CT scan was used for plan optimization and dose calculation. Excess absolute risks of second cancers from radiation for proton and photon plans were determined by use of previously reported models of organ-specific radiation-induced cancer incidence based on organ equivalent dose (OED) as described by Schneider et al. All patients were treated with 1.8-Gy daily fractions, and the median total radiation dose was 50.4 Gy. Proton and photon plans provided similar coverage, although proton plans resulted in more significant sparing of OARs compared with photon plans. The mean lung and heart dose and the maximum esophagus dose were lower with protons. Significantly more excess RIC per 10,000 patients per year were predicted with photon therapy compared with proton therapy. This included higher rates of esophagus, lungs, breast, skin, stomach, and thyroid cancers. In total, 17.3 excess RICs per 10,000 patients per year were predicted with photons, whereas 2.8 excess RICs were predicted for DS-PBT, for 14.5 excess RICs from photon therapy compared with proton therapy. Authors conclude that 'For patients with thymoma diagnosed at the median national age, five

excess secondary malignancies / 100 patients would be avoided by treating them with protons instead of photons' (131).

Another study in HL patients (132) assessed the probability for RIC induction after involved site radiation therapy (ISRT) in patients with mediastinal HL by combining dosimetry data from radiation treatment with the appropriate risk models. These RIC risk assessments with ISRT were compared with conventional involved field radiation therapy (IFRT). Six female and five consecutive male patients that required irradiation to the mediastinum for HL were included. All patients were in a supine position, and two plans that corresponded to the IFRT technique and ISRT technique were generated. Models such as mechanistic, plateau, and bell-shaped models were used to estimate lifetime attributable risk (LAR) of developing malignancies by using patient-specific organ equivalent dose (OED). The LAR estimates were compared with the nominal risks for unexposed people. The LAR range for lung RIC estimated with the mechanistic, plateau, and bell-shaped models was 1.65–2.79%, 1.77–3.34%, and 1.78–3.31%, respectively. The LAR calculation for breast RIC induction was 0.16–2.36%, 0.17–2.37%, and 0.17–2.24%, LAR range for esophagus RIC was 0.21–0.41% as per the mechanistic model. The mechanistic model led to smaller LAR estimates for lung RIC versus LARs derived from the plateau and bell-shaped models. For each specific HL patient, the difference between the minimum and maximum LARs of lung RIC induction was 7.7% -19.5%, for breast RIC induction was 2.0–8.2%. The LARs for developing lung RIC were 1.8–4.4 times lower than the respective baseline risks; for breast RIC, it was 5.3–67.8 times smaller than the baseline probabilities and for esophagus RIC, 1.1–3.8 times lower compared to baseline risk values. The estimated LAR for lung and breast cancer RIC risk due to ISRT was lower than IFRT irrespective

of which model was used for analysis ($P < 0.05$). However, there was no significant difference between the LARs for esophageal RIC estimated by the ISRT and IFRT plans ($P = 0.63$) (132).

A study (133) evaluated the exposure from diagnostic imaging for lung cancer. Diagnosis of lung cancer is a drawn-out process requiring multiple imaging and biopsies. The cumulative radiation dose received by patients undergoing staging and investigations for curative treatment for primary lung cancer between December 2012 and March 2014 was calculated. Retrospective data were obtained from electronic records, including patient demographics, stage/type of cancer, information on all imaging investigations involving ionizing radiation between the first diagnostic investigation and the start of definitive treatment was gathered. The total effective radiation dose was calculated for each patient, and lifetime attributable risk (LAR) was estimated. The mean cumulative dose of radiation received by 80 patients undergoing investigation for curative treatment with surgery or chemoradiation was 27.6 mSv±0.9. Patients that either received surgery or chemoradiation received comparable doses, surgery 28.6mSv, chemo-radiation 25.8 mSv, $p=0.89$. This was significantly higher than those who received the best supportive care since imaging is minimized in patients on supportive care or hospice. When stratified by stage, the effective dose of radiation received was higher for early-stage disease than for those with metastatic disease (mean=26.9 mSv for stage I, 24.6 mSv for stage II, 22.3 mSv for stage III, and 14.4 mSv for stage IV), which is expected since prognosis is poor in stage IV disease and effort is made to focus on the quality of life of patient since the cure is not possible. There was a correlation between body mass and effective dose ($p<0.05$), but no significant correlation with patient age ($p=0.52$). For patients undergoing treatment with curative intent, the median number (range) of investigations undertaken was CT staging was 1 (Range: 0–4), CT head was 1 (Range: 0–2), CT-guided biopsy was 1 (Range: 0–3), and positron emission

tomography (PET)-CT was 1 (Range: 0–2). The mean LAR of malignancy for those receiving treatment with curative intent was 0.059%, which means that 5.9 in 10,000 long- term survivors would be expected to develop a RIC as a direct consequence of diagnostic imaging investigations. The lung-specific risk was 0.019% (133). This risk estimate should be clinically insignificant, given the grave prognosis of lung cancer.

A meta-analysis published in 2017 (134) estimated the RIC risks of modern breast cancer radiotherapy since several studies have been published estimating the risk with various RT techniques. Randomized studies on women with long-term follow-up were used to derive rate ratios (RRs) for incident RIC cancers and causes of death before a recurrence of breast cancer and excess rate ratios (ERRs) / Gy for incident primary lung cancer. These ERRs / Gy values were combined with lung and heart doses from modern radiation and population-based modern lung cancer and cardiac mortality rates in smokers and nonsmokers to estimate the absolute risks of contemporary breast RT for cancer. The meta-analysis involved a systematic review of lung and heart doses from 2010 to 2015 and breast cancer RT regimens. A 'typical modern dose will be an unweighted average' calculated for all published mean whole-lung doses (average of ipsilateral and contralateral lung doses). Data were obtained from trials that began before 2000 of RT versus no RT or RT versus additional surgery in early breast cancer or ductal carcinoma in situ (DCIS). For every woman, information was obtained about patient and tumor characteristics, delivered treatment, time to recurrence, time to any contralateral breast cancer or another second cancer before recurrence, and date last known to be alive or date and cause of death. To estimate absolute risks for women, the ERRs / Gy were multiplied by typical modern lung and heart doses and applied to the current smoker and nonsmoker population mortality rates in 5-year age groups. The baseline death rate from lung cancer was taken from nonsmokers in the American

Cancer Society Cancer Prevention Study II. The review of all breast cancer radiotherapy dosimetry reports between 2010 - 2015 identified 214 reports. The average of the lung doses was average ipsilateral 9.0 Gy and average contralateral lung 2.4 Gy and mean of the two doses of the two lungs, the typical modern technique and planned whole-lung dose was 5.7 Gy. Compared to the contemporary doses, lung and heart doses were higher in the trials: 10 Gy whole lung and 6 Gy whole heart, ipsilateral lung 17.6 Gy, contralateral lung 1.6 Gy, whole lung 9.6 Gy. The main risks noted in the trial were contralateral breast cancer, lung cancer, leukemia, esophageal cancer, and heart disease. The RR for contralateral breast cancer was 1.20. The contralateral breast cancer RR was higher in the old trials of orthovoltage radiotherapy, RR, 1.57, than in the other trials. In trials, the absolute 15-year increase in contralateral breast cancer risk was 1.0%. Older techniques of RT resulted in higher estimates of the exposure of normal tissues to RT and, therefore, higher risks of RIC. The significant excess is in the first decade after radiotherapy. The incidence RR, radiotherapy versus control, for RIC other than breast or lung was 1.19. The main values were leukemia RR, 1.71, and esophageal cancer RR, 2.42, with the majority of cases occurring in the trials in which radiotherapy involved the internal mammary chain and supraclavicular fossa. Estimated absolute risks from modern radiotherapy were lung cancer, approximately 4% for long-term continuing smokers, and 0.3% for nonsmokers (134). These estimates suggest a less than 1% risk of RIC with modern techniques in non-smokers, which is clinically acceptable, given the survival benefit in the long term seen with breast RT for breast cancer.

In a study to evaluate the individual organ doses and the corresponding effective doses, to calculate the potential RIC from cardiac CT angiography (135), investigators collected patient characteristics and radiation dose data for 100 patients who underwent elective, nonemergency,

contrast-enhanced cardiac CT angiography. Patients were indicated to undergo CT angiography at the institution for the following reasons: Patients who presented with symptomatic chest pain and were deemed at intermediate risk for coronary artery disease (CAD), which was defined as a combination of atypical clinical presentations, non-pathological (stress) EKG findings (i.e., normal EKG / negative T-wave), in-conclusive risk factor profiles (i.e., hypertension, diabetes mellitus, nicotine abuse, presence of familial coronary atherosclerosis, cholesterol) and negative troponin T enzyme levels. Radiation doses are recorded by the CT scanner automatically, and dosimetry data for all subjects were retrieved using the Agfa IMPAX workstation (Agfa-Gevaert Group). Organ doses were converted to organ RIC risk values using patient age and sex-specific data published in BEIR VII. For each patient, investigators calculated the total cancer RIC risk by multiplying the computed organ dose by the corresponding age- and sex-dependent cancer risk coefficient. The effective dose for this group of patients ranged from 12 to 42 mSv, with a mean of 25.1 ± 4.9 mSv. Most patients received effective doses within the range of 20–31 mSv. The mean RIC induction risk in men was 0.065 ± 0.016%, with most patients falling in the range between 0.044% and 0.086%. The mean RIC induction risk in women was higher with the risk of 0.176 ± 0.050%, with most women falling in the range between 0.13% and 0.26%. For both sexes, risks from the 10th percentile to the 90th percentile covered a two-fold risk range. There was mostly overlap between men and women; the female 10th percentile risk of 0.13% was substantially higher than the male 90th percentile risk of 0.086%. The ratio of the median female to male risk was 2.6. There was a marked difference between risks for men and women, and this difference increased in younger patients. For men, the cancer incidence risk was 0.080% for a 40-year-old, which decreased to 0.071% for a 60-year-old. For women, the cancer incidence risk was 0.24% for a 40-year-old, which decreases to 0.16% for a 60-year-old. In men and women,

about 3/4th of the RIC risk was from lung cancer. Inclusion of the remaining less sensitive organs exposed during cardiac CT angiography examinations would likely increase the cancer induction risk by ~20% (135).

A systematic review (136) of the epidemiological studies evaluated the dose-response relationship for second radiation-induced solid cancer risks after high-dose fractionated RT. The authors first reviewed the shape of the dose-response relationship for each second cancer site to assess whether the data support a linear relationship, a plateau, or a down-turn in risk at high doses. Also, a comparison was made of the magnitude of the risk per unit of RT dose from the high-dose fractionated exposures with age and sex-matched risk estimates from the Japanese atomic bomb survivors that received acute lower-dose radiation exposure (<2 Gy). Other studies that were included in the review were the epidemiological studies with an outcome of RIC solid cancer that had data on details of RT treatment, specifically the estimated dose delivered to the site that developed RIC for each patient. Potentially eligible studies were identified from searching PubMed (search terms "radiotherapy," "dose," "subsequent malignancy"), from review articles and references in identified studies. For each eligible study, the following data was extracted: cohort size, average (and mean/median) age at first cancer diagnosis, age at second cancer diagnosis, estimated absorbed dose to the second cancer site in the cohort, the relative risk (or odds ratio) and 95% confidence interval for second cancer in relation to each category of radiation dose, and the estimated continuous dose-response relationship expressed as the excess relative risk per Gray (ERR/ Gy) and its 95% confidence interval, dose-response relationship with non-linear dose-response curves such as linear-exponential or linear-quadratic, and any associated tests of statistical significance. To estimate the magnitude of the impacts of cell killing at high doses and fractionation on the RIC, authors compared the dose-response estimates from

these radiotherapy studies with estimates from radiation exposure using the risk models used by the BEIR VII committee. Twenty-eight eligible studies included 3,434 patients who developed a RIC with average absorbed organ doses in the non-cases ranging from 5–165 Gy. The majority of the studies were case-control studies, many of which were nested case-control studies within a cohort, such as the Childhood Cancer Survivor Study. More than 50% of the studies were of childhood cancers. Three studies evaluated second breast cancers after RT with the average age at exposure between 6 years and 22 years and maximum absorbed organ doses of 60–80 Gy to the breast. All three studies found approximately linear dose-response relationships with breast cancer risk and no evidence of a downturn at risk, even at doses of 30 Gy or more. The ERR/ Gy varied from 0.13 to 0.27, 5–16 fold lower than the prior estimates. An interesting effect modifier was RT to the ovary of at least 5 Gy, which significantly reduced the risk of radiation-related breast cancer in both studies where such treatment was common. The mechanism was possibly the ablation of ovarian function, which suppresses the hormonal stimulation of the breast tissue. Two studies of second lung cancer were identified with a similar average age at exposure (49–50yrs). In the study of lung cancer after breast cancer, there was some evidence of increased risk with increasing dose, and the ERR/ Gy was 0.2 at an average attained age of 68 years. In the larger study of 227 lung cancer cases after Hodgkin's lymphoma treatment, the ERR/ Gy was similar in magnitude, 0.15. Maximum doses were more than 60 Gy, but there was no evidence of departure from a linear dose-response relationship ($p>0.5$). Overall the ERR/ Gy was 5–10 times smaller than in the LSS study with a similar age at exposure and attained age. Overall, when all other solid cancer sites were considered, there was no clear evidence of non-linearity in the dose-response in the direction of a reduction in risk at high doses such as 60 Gy or higher. The exception was thyroid cancer, for which there was a plateau in risk in one study and a definite

downturn in another above 20 Gy. The ERR/ Gy was generally considerably lower after fractionated high-dose radiotherapy than after the acute lower-dose exposure experienced by the Japanese atomic bomb survivors (LSS study), in the range of 5– 10 fold lower for most second solid cancer sites. For most cancer sites, the relative risk at 40 Gy of developing a second solid cancer was typically in the region of 5–10 times higher than the risk in the patients who did not receive radiotherapy or those who received very low doses (136).

A study aimed to evaluate the incidence and characteristics of RIC in patients with prostate cancer that undergo RT (137). In this study, 150 patients were included, of which a total of 117 patients underwent definitive RT for primary prostate cancer, and 33 patients underwent adjuvant or salvage radiotherapy after radical prostatectomy. The authors evaluated the incidence and previous history of multiple malignancies and the influence of these factors on survival. The incidence of subsequent malignancies was compared with the baseline estimated incidence, which was calculated using age-matched incidence data of the general population, as published by the National Cancer Center, Japan. They applied the incidence table 'Cancer Incidence by Age and Site (2007)' to the age of the present 150 cases. Differences in subsequent disease incidence in relation to the national average were analyzed using Fisher's two-tailed exact test. In addition to prostate cancer, 26 patients (17 %) had multiple primary cancers, 9 had prior malignancies, 2 had concurrent malignant tumors, and 16 had subsequent malignant tumors, including one patient who had both preceding and subsequent cancers. Twenty-two patients had two primary malignancies, three patients had three, and one patient had four, including prostate cancer treated by radiotherapy. Associated non-prostate primary sites consisted of 7 colon, six lung, five stomach, four urinary bladder, two ureter, two lymphocyte, two skin, one plasma cell, one kidney, and one bile duct. The interval between preceding cancer and prostate cancer was

10–300 months (median, 60 months), and the lead time was 13–83 months (median, 44 months) after prostate cancer to the next malignancy. Of the 150 patients, 20 (13 %) died within ten years. The cause of death was recurrent prostate cancer in 11 patients, another primary cancer in 7 patients, and cardiovascular disease in 2 patients. The incidence of subsequent malignancies is mentioned in relation to the estimated incidence of 'Cancer Incidence by Age and Site' (2007)'. The observed incidence was significantly higher than the estimated incidence at four years in ureter cancer (P = 0.045) and malignant lymphoma (P = 0.035), and higher in urinary bladder cancer, although not significantly (P = 0.072) (137). This suggests the potential of radiogenic risk even with treatment in prostate cancer.

A study compared the risk of RIC in children undergoing craniospinal irradiation (138) utilizing either photons or electrons or protons or the combination. This radiation treatment is delivered to patients with a risk of cancer recurrence in the craniospinal axis (brain/spine), and radiation is delivered to prevent that recurrence. Six pediatric patients aged 5–11 years, three girls, and three boys, having undergone CSI as part of the treatment of medulloblastoma, were selected for this study. An experienced oncologist individually delineated all structures applied in the analysis. For all techniques mentioned in this study, a typical field arrangement included a combination of two spinal fields and two oblique opposing cranial fields with the patients in a prone position. For patients, less than about 15 years of age, the skeleton's bone growth is still an ongoing event, and age-specific target volumes, including the entire vertebrae, were defined for the proton plans to prevent asymmetric growth due to sharp dose gradients in the vertebral body. A radiation dose of 23.4 Gy administered in 13 fractions was applied to the CTV, this being the conventional RT prescription when treating standard-risk medulloblastoma. For the proton treatment plans, a biologically weighted dose of 23.4 Gy was utilized. The dose-volume

distributions for each organ were evaluated using the following models: a linear no-threshold (LNT) risk, an observed response with no further increase in risk above a threshold of 4–5 Gy, and an organ-specific linear-exponential response. For lifetime attributable risk (LAR) estimates, the BEIR VII report was used. Significant variations were seen in the region beyond the distal end of the spinal volume, where little or almost no dose was deposited when applying protons. The dose to the organs at risk varied considerably depending on the treatment technique, with distinctively lower doses to all organs at risk for the proton techniques (attributed to the 'Bragg peak' effect mentioned above). The volumes receiving doses below 5 Gy was reduced with the proton techniques, and also moderately reduced in the volumes receiving doses between 5 and 20 Gy. The highest risks were found with the linear dose-risk relationship and most patients and most organs, while substantially lower risks were predicted from the linear-exponential and plateau model. OED (organ equivalent dose) results for the proton techniques were, in general, significantly lower than for the photon and electron techniques (typically 4–8 times lower). Variations between the electron and photon treatments showed that the OEDs for the lungs from the electron technique was higher using all models. For the liver, colon, and thyroid; however, the OED for the photons was larger than the electrons.

Nonetheless, the risk for these organs was similar for both techniques using the non-linear models. In the lungs, the IMPT (intensity-modulated proton therapy) technique resulted in slightly higher doses in the range up to 10 Gy and, therefore, higher OEDs. Overall, the values of absolute increase in cancer risk compared favorably to proton for all patients and all organs included in the LAR analysis: lungs, stomach, colon, liver, thyroid, and bladder. The electron technique resulted in the highest risk for the lungs, which in the 8-year-old female patient, ranged from 2% to 36% according to the linear-exponential model and from 8% to 100% from the linear

model. The DS proton technique resulted in the lowest estimates for the lungs in this patient for a linear-exponential and linear model with corresponding risks of 0–7% and 3–40%, respectively.

In contrast, the risk for colon RIC was lower than the LAR estimated for the lungs; with all patients and all models included, the LARs for the colon ranged up to 35% for the photon technique and up to 5% for the IMPT. The total accumulated risk with photons, including all organs, was about six times higher than the proton techniques by all models. For the linear-exponential model, the nominal accumulated risks were 25% and 22% for the photon and electron techniques. The corresponding values for the IMPT and DS protons (double-scattering protons) were 4% and 3% (138).

To explore the long-term outcomes of female survivors of a childhood cancer treated with chest irradiation to understand the incidence of RIC risk for breast cancer, the role of both the delivered dose of radiation and the volume of exposed breast tissue in contributing to breast cancer risk in childhood cancer survivors was analyzed (139). The CCSS (Childhood Cancer Survivor Study) was used for this study. The CCSS is a retrospective cohort study with longitudinal follow-up of survivors of childhood cancer treated at 26 institutions in the United States and Canada. Eligibility for participation in the CCSS included 1. the diagnosis of cancer before age 21 years, 2. initial treatment between 1970 and 1986, and 3. alive at five years after diagnosis of leukemia, CNS tumor, Hodgkin or non-Hodgkin lymphoma, Wilms tumor, neuroblastoma, soft tissue sarcoma, or bone tumor. The subjects of this study were female participants who had received chest irradiation within five years of their childhood cancer diagnosis. The definition of chest irradiation included treatment with any one of the following fields: mantle, mediastinal, hemithorax, whole-lung irradiation (WLI), posterior thoracic/paravertebral, abdominal (with extension above the diaphragm), and total-body

irradiation (TBI). Of the CCSS participants, 1,230 patients met these criteria. The complete radiation treatment information for all, but seven participants was ascertained. Treatment information included radiation to the ovaries and chemotherapeutic exposures, including alkylating agent chemotherapy. Breast cancers, invasive cancers, or ductal carcinoma in situ were initially identified through self- or proxy reports. The diagnosis was confirmed by pathology reports, if available, or by other medical records. New breast cancers in deceased persons were ascertained through family members and the National Death Index. Only the first primary breast cancer diagnosis was included in the analysis. There was a high risk of breast cancer in women treated with RT dose >20 Gy, although 10 to 19 Gy also showed an elevated risk of breast cancer (SIR, 30.6; 95% CI, 18.4 to 50.9). The cumulative incidence of breast cancer in women who received WLI was similar to those who received mantle field irradiation and elevated compared with women who were treated with mediastinal field irradiation. The incidence rate ratios adjusted for dose were 1.8 (95%CI, 0.9 to 3.7; P=.07) for comparing WLI with mantle field irradiation and 3.4 (95% CI, 1.6 to 7.2; P=.001) for comparing WLI with mediastinal irradiation. Women treated with mediastinal irradiation had a significantly reduced risk of breast cancer relative to women treated with similar doses of mantle field radiation (incidence rate ratio adjusted for dose, 0.5; 95% CI, 0.3 to 0.9; P= .013). However, their risk was still significantly increased compared to the general population. Treatment with an irradiation field that included the ovaries decreased the risk of breast cancer. This decrease remained statistically significant after adjusting for the dose of chest radiation (adjusted incidence rate ratio, 0.3; 95% CI, 0.2 to 0.7; P = .003). In contrast, treatment with alkylating agent chemotherapy did not materially modify breast cancer risk (adjusted incidence rate ratio, 1.1; 95% CI, 0.8 to 1.4; P=.75). Among women diagnosed with breast cancer after childhood cancer,

62 died after a breast cancer diagnosis. Thirty of these deaths were attributable to breast cancer. All-cause mortality at 5 and 10 years was 15% (95% CI, 11 to 22) and 32% (95% CI, 25 to 40), respectively; breast cancer-specific mortality was 12% (95% CI, 8 to 18) and 19% (95% CI, 13 to 25) at 5 and 10 years, respectively. There was no difference in survival by the dose of chest radiation used for childhood cancer (139).

Regarding lung cancer screening, a study sought to calculate the potential risk of radiation-induced lung cancer from three annual lung CT screens for asymptomatic individuals starting at age 30, 40, and 50 years (140). The authors then estimated the level of screening efficacy that would be required to outweigh these risks and also estimated the risk of radiation-induced breast cancer. Estimates were developed for never smokers and current smokers. The authors used the BEIR VII committee's risk model for radiation-induced incident lung cancer to calculate risks according to smoking status. The model was based on the data from the study of the Japanese atomic bomb survivors. The BEIR VII committee recommended that "greater weight be given to the excess absolute risk model (weight=0.7) than to the excess relative risk model (weight=0.3) because a detailed analysis of smoking and radiation in the Japanese atomic bomb survivors found evidence that the effects appeared to be additive rather than multiplicative". Lung cancer rates were estimated for never smokers using results from the Cancer Prevention Study II. For current smokers, the Bach lung cancer risk model was used, assuming 40 cigarettes per day smoking history. 'CT-Expo software' was used to calculate age- and sex-specific organ doses and effective doses based on the screening protocol used in the National Lung Screening Trial. The mean radiation dose to the lung from a helical low-dose lung CT was estimated to be 3.9 mGy (range 2.7-6.1 mGy) for females and 3.8 mGy (range 2.6-5.9 mGy) for males, and the mean effective doses were 1.3mSv and 1.0mSv, respectively. The risk of

radiation-induced lung cancer remains elevated indefinitely after radiation exposure. Regarding lung cancer mortality, incidence-based mortality rates were estimated using the smoking and age-specific incidence rates for the relevant screening period multiplied by 90% (the estimated probability of dying from lung cancer in the absence of screening). A two-year (range 1-4 years) mean sojourn time (the period during which the disease is preclinical but detectable by screening) was assumed based on the findings from a recent study that estimated this parameter data from six published lung CT screening studies. Hence, the cumulative incidence-based mortality rate for each three year screening period was the sum of the rates for the screening ages plus rates for the following two years. For never smokers the excess lifetime risk of radiation-induced lung cancer mortality from annual lung CT screening from age 30-32 was estimated to be 3 deaths (90% credibility interval, 2-5) / 10,000 women screened (0.03%) and 1 (0.3-2) death / 10,000 men (0.01%) screened. For current smokers the risks were approximately two-fold higher: 5 deaths (2-12) per 10,000 women (0.05%) and 2 deaths (1-4) per 10,000 men screened (0.02%). Given the low baseline rates of lung cancer before 50 years of age, for annual screening from ages 40-42 or 50-52, the estimates were similar in magnitude to those for screening age 30-32. The estimated cumulative risk of lung cancer mortality without screening was relatively low for each screening period because lung cancer incidence rates are still low at these ages, even for current heavy smokers. Hence, the potential number of lung cancer deaths that could be prevented by CT screening at these younger ages was also relatively low. The mortality reduction required to outweigh the radiation risks was high. For male never-smokers the estimates were:125% (40%-300%) age 30-32 years, 70% (30%-190%) age 40-42 years and 25% (10%-70%) age 50-52 years, and for male current-smokers:70%(20%-120%) age 30-32 years, 10%(3%-20%) age 40-42 years and 2%(1%-4%) age 50-52 years. These figures were 2-3 times

higher for females because of the higher radiation risks. The authors concluded that before age 50, the mortality reduction from lung CT screening that is required to outweigh the radiation risk might be substantial, and in some cases, unattainable (i.e.,>100%) (140).

A study was performed to estimate the risk of RIC during lung cancer treatment with radiation using one of the three radiation techniques, IMRT, VMAT, and TOMO, using the concept of OED (organ equivalent dose) for RIC (141). Investigators randomly selected five patients with lung cancer who were to be treated with IMRT. These patients underwent treatment planning CT scans of the chest to identify targets and normal healthy organs. An Eclipse (Varian Medical Systems) and Hi-Art (TomoTherapy, Madison, WI, USA) planning system were used to plan IMRT, VMAT, and TOMO for this group of patients. The age range was 56 to 71 years old, with an average age of 67. All patients are stage III of non-small cell lung cancer (NSCLC) cases, and PTV volumes are varied from 64 to 890 cc. The targets in the five lung cancer patients were defined per the report of the International Commission on Radiation Units and Measurements (ICRU 50). A four-dimensional computed tomography image was obtained during the CT scan by using a Philips brilliant big bore CT with Varian real-time patient monitoring system (RPMS). Each patient received a total dose of 50–63 Gy, using different fractionation schemes, to the iso-center. All treatment plans used 4-9 beams for IMRT, single or double arcs for VMAT, and a helical beam for TOMO. A radio-photoluminescence glass dosimeter (RPLGD) is newly introduced as a substitution of the thermoluminescence dosimeter (TLD), which was commonly used for in-vivo measurement. In this study, the authors used commercially available RPLGD. An RPLGD measured the absorbed dose by detecting the orange light (500 ~ 700 nm) from the dosimeter when 365 nm of mono-energetic light was exposed to the irradiated dosimeter. In all treatments, a photon of 6 MV energy (Clinac 21iX; Varian Medical Systems,

USA) was used for IMRT and VMAT. Secondary radiation was assessed by measuring the ionization of the photon beam as a function of distance from the iso-center because the contribution of the secondary neutron dose is negligible in 6MV photon beams. These measurements were performed using two RPLGDs set at various distances from the beam iso-center on a solid phantom at SAD 100 cm. From statistical data on Japanese atomic bomb survivors and medically exposed patients, the "Excess Absolute Risk" (EAR) index per 10,000 persons per year from Schneider et al. was used to estimate the RIC. The average % scattered dose for prescription dose for five patients at 20, 35, 50, 65 and 80 cm from the isocenter was 1.04±0.56, 0.30±0.20, 0.21±0.18, 0.09±0.06 and 0.06±0.04% for IMRT, 0.80±0.36, 0.25±0.11, 0.11±0.04, 0.06±0.02 and 0.04±0.01% for VMAT, 0.34±0.10, 0.18±0.04, 0.11±0.03, 0.09±0.02 and 0.07±0.02% for TOMO. The scattered secondary dose is decreased as the distance from the in-field region is increased. Also, the scattered secondary dose depends on the modality. TOMO (VMAT) has about 30% (80%) of scattered secondary dose comparing to a scattered secondary dose of IMRT at a 20 cm distance from the iso-center.

Moreover, the secondary scattered dose decreases as the distance from the iso-center increases resulting from the fact that the secondary scattered dose at 80 cm distance from the iso-center is about 20 times lower than the dose measurement at 20 cm for IMRT and VMAT. TOMO has a relatively low secondary dose around the target area, although the monitor unit of TOMO treatment cases is higher and close to the values of IMRT and VMAT. As predicted from the measurements of the secondary scattered dose, TOMO has a relatively low OED for most of the organs compared to the other modalities, and this OED difference from modality decreases when the position of the organ gets further away from the field edge. The authors concluded that OED based estimation suggests that the secondary cancer risk from TOMO is less than or

comparable to the risks from conventional IMRT and VMAT (141). This study differs from my study in various aspects: My study evaluated radiation exposure from imaging before and after SBRT, and we excluded actual SBRT dose. Also, the patients in this study are performed in stage III cancer versus my study, which was performed in early-stage lung cancer since SBRT is an option for early-stage disease. This study compared IMRT versus VMAT versus Tomotherapy, planning techniques to treat lung cancer versus my study that used only SBRT.

A modeling study (142) estimated the RIC with image guidance for radiation therapy for cancers. All the cancer patients treated with radiotherapy at a New England hospital from September 1, 2009, to April 30, 2014, were reviewed. Patients treated without any image-guidance or computed tomography (CT) scans and patients treated with total body irradiation or with large blocks protecting the brain, lungs or RBM, were excluded from this study. A total of 4,832 patients whose brain, lungs, or RBM were irradiated by at least one of the three image-guidance modalities kV-CBCT (kilo-voltage cone-beam CT), kVPI (kilo-voltage portal imager), and MVPI (mega-voltage portal imager) were included. An 'EGSnrc/BEAMnrc code' was used to simulate the photon beams emanated from the X-ray sources of CT, kVPI, MVPI, and kVCBCT systems, respectively. MCSIM, an EGS4/BEAM user code, was used to calculate the 3D dose distributions in patient anatomy with multiple source models as beam input for each imaging procedure. To convert Monte Carlo simulations into the absolute dose, the absorbed dose was first measured at the iso-center of an acrylic ball phantom of 5 cm in diameter with a calibrated EXRADIN A12 ionization chamber for the specific scan protocol. Using the standardized empirical functions, mean organ doses of 4,832 patients from 142,824 imaging procedures were estimated and summed up. The lifetime attributable risk (LAR) of cancer incidence was based on BEIR VII models was calculated to quantify the probability of cancer

incidence with the cumulative imaging doses in IGRT. Overall, from 2009-2013, there was a steady rise in the number of new patients and imaging procedures each year, followed by a decline in 2014. Compared to the prior year, the total number of imaging procedures increased by 52.1%, 26.6%, 14.7%, and 6.8%, respectively, from 2010 - 2013. The decline of imaging procedures in 2014 was primarily due to the decrease of new patients treated in the first months of 2014. KVCBCT, MVPI, and kVPI accounted for 14.1%, 24.1, and 58.1% of all the 142,824 imaging procedures performed on 4,832 patients. The average CT, kVCBCT, MVPI, and kVPI scans per patient were 1.1, 4.2, 7.1, and 17.2, respectively. For both males and females, the averaged LAR of incidence for brain and lung cancers decreased with age. However, the LAR of leukemia incidence showed a regular decrease in young groups, followed by a "hump" in senior groups. The hump peaked around 65 years old for males mainly due to the more frequent kVCBCT scans in prostate IGRT, whereas it peaks around 45 years old for females due to the increased IGRT in RT of pelvic lesions. Regardless of age, a significant difference was observed for the LAR of both RIC lung cancer and leukemia incidence between the males and females ($p < 0.001$) but was not present in the LAR of brain cancer incidence ($P = 0.063$). The associated mean (range) LAR of cancer incidence/100,000 persons was 78 (0–2798), 271 (1–8948), and 510 (0–4487) for brain cancer, lung cancer, and leukemia, respectively (142).

A study determined the characteristics and risk factors in Hodgkin lymphoma (HL) survivors (143) who developed lung cancer (LC) by performing a comparison between them to the ones who were diagnosed with other second primary neoplasms. Investigators retrospectively analyzed 604 patients treated for HL between 1967 and 2012. Radiotherapy (RT) treatment was applied in most patients with involved-field RT. Patients were followed-up with clinical control and image evaluation three times per year in the first two years after finishing HL treatment,

twice per year until they had completed five years, once per year until ten and, finally, once every two years when surpassing ten years after the end of treatment. Every diagnosis of new hematological tumors, including non-Hodgkin lymphoma or leukemia or primary solid tumors, such as breast cancer, sarcoma, digestive tract tumors (esophageal, gastric or colorectal cancer), thyroid cancer, gynecological cancer (cervical or endometrial), lung cancer or mesothelioma and others was included as a second neoplasm. In the lung cancer group, malignant mesothelioma was considered as a serous lung membrane tumor, and none of the patients diagnosed had any known exposure to asbestos (a risk factor for mesothelioma). When RIC was diagnosed, RT dose and fields applied as part of HL treatment were analyzed to determine whether the new primary tumor had appeared in a previously irradiated region. Of 604 patients, 558 were finally included in the analysis. In all, 90 (14.9 %) were found to have developed second neoplasms, 27 (30.0 %) lung cancer (2 of them mesothelioma), and 63 (70.0 %) other types of tumors. The latter included 13 (14.4 %) leukemia, 10 (11.1 %) non-Hodgkin lymphoma, 10 (11.1 %) breast cancer, 10 (11.1 %) sarcoma, 5 (5.5 %) digestive tract tumors, 5 (5.5 %) thyroid cancer, 3 (3.3 %) gynecological cancer and 7 (7.7 %) other tumors. Five (5.5 %) patients developed a third primary tumor. The remaining 468 patients diagnosed with HL did not develop second cancer. No differences were found between groups concerning HL histology subtypes. In the analysis of HL stage at diagnosis in lung cancer, other second neoplasms (SN) and non-second neoplasms group, 7 (25.9 %), 32 (50.8 %), and 166 (35.5 %) patients, respectively, were found to have advanced stages (III or IV) with statistically significant differences between the groups with second tumors ($P = 0.024$). The RT fields applied (supra- or infra-diaphragmatic), total nodal irradiation, or other extended fields such as mantle and lumbo-aortic fields, IFRT) also had a similar distribution in the chosen sample, whether they were applied alone or combined with

combined modality treatment (P = 0.22). The majority of the IFRT treatments were mediastinal involved RT and were included in the supradiaphragmatic field group, but most (n = 20) were in the non-solid neoplasm group. Statistically significant differences were found in mean RT doses with 43.6 Gy (standard deviation [SD] 13.3) in lung cancer, 39.7 Gy (SD 16.7) in other SN, and 37.3 Gy (SD 6.0) in the non-SN group (P = 0.002) with an increased risk of lung cancer and other SN being found with doses higher than 42 Gy. The relative risk associated with RT in patients who developed leukemia, solid tumors or both was 4.1 (95 % CI 0.8–20.1 P = 0.08), 3.1 (95 % CI 1.6–6.1 p\0.001) and 2.8 (95 % CI 1.5–5.1 P = 0.001), respectively. Most solid tumors in both SN groups occurred in previously irradiated fields, with 81.8 % in lung cancer and 88.5 % in other SN (P = 0.78). A median time elapsed until the diagnosis of SN of 16.5 and 11.0 years, respectively (P = 0.04). Male predominance was found in the lung cancer group; however, no difference was found when comparing the SN versus non-SN groups. Cigarette smoking was associated with lung cancer in 84.6 % of the patients, and to other SN is 48.9 %. Overall, 90 % of lung cancer group patients died due to the second primary tumor, and 92 % in the other SN group (143).

In a Danish study (144), the authors evaluated the occurrence of second primary solid non-breast cancer among Danish women treated for early breast cancer with postoperative radiotherapy using modern standards in radiation. The incidence of RIC among women treated with radiotherapy was compared to both the general Danish female population and to those who were non-irradiated. Data were supplied by the Danish Breast Cancer Cooperative Group (DBCG), which has been established in 1977 to ensure uniform national diagnostic and therapeutic breast cancer guidelines. Since then, women in Denmark diagnosed with primary, unilateral loco-regional breast cancer is included in a nationwide clinical database under the

DBCG containing information regarding tumor characteristics and patient follow-up. Treatment interventions, including surgery, systemic treatment, and RT, are recorded for patients treated according to DBCG guidelines. To attain risk estimates for RIC reflecting RT practice at the time, investigators excluded 132 women treated with orthovoltage X-rays. All irradiated women were treated on linear accelerators. The final cohort included 46,176 women. The cohort was divided into two groups according to whether the patients had been prescribed postoperative radiotherapy or not. The majority of patients allocated to post-mastectomy RT were treated with a combined 3-field anterior electron/photon technique consisting of an electron field to the chest wall ± the internal mammary chain combined with photon fields against the lateral chest and supraclavicular fossa. The median absorbed dose in the target volume was 48–50 Gy, given in 24–25 fractions over five weeks. All patients treated with breast-conserving surgery (BCS) received postoperative radiotherapy to the residual breast. The majority of these patients were treated with tangential photon fields of the conserved breast combined with a boost to the tumor bed, primarily with electrons. The median absorbed dose in the target volume was 48–50 Gy, given in 24–25 fractions over 4.5—5 weeks, followed by a boost to the tumor bed of 10– 24 Gy over 5–12 fractions. The second primary cancers were identified by linking the cohort to the national Danish Cancer Registry. Since 1943, all incident cases of cancer in Denmark have been reported to the Registry on notification forms from all clinical departments and departments of pathology and forensic medicine, supplemented with death certificates. Tumors diagnosed since 1978 have been classified according to the International Classification of Disease, 10th revision (ICD-10), and the International Classification of Diseases for Oncology, third edition (ICD-O-3). All types of second solid cancers except non-melanoma skin, ill-defined- and second-breast-cancers were included as an outcome. The second cancers were classified into two subgroups: (1)

sites potentially associated with radiation exposure (RT associated); and (2) sites not associated with radiation exposure (non-RT-associated). This grouping of cancer sites was based on considerations of how close the anatomical relation was to the treatment field and on a review of the literature. The attributable risk associated with radiotherapy was estimated by dividing the number of excess cancers by the total number of cancer cases. The excess absolute risk (EAR) related to radiotherapy was calculated as the number of excess cancers associated with radiotherapy divided by the person-years at risk and then multiplied by 10,000. The study cohort included a total of 46,176 patients. Overall, 51% of the women received postoperative radiotherapy, while 49% did not. Irradiated women were younger at breast cancer diagnosis and more frequently treated with chemotherapy and hormone therapy than non-RT women. A total of 2358 second primary cancers developed during the follow-up period. Among the irradiated women, 928-second primary cancers develop, whereas 784 cancers were expected (standardized incidence ratio [SIR] 1.18; 95% CI 1.11–1.26). One thousand four hundred thirty-second primary cancers were observed among the non-irradiated women, whereas 1350 cancers were expected (SIR 1.06; 95% CI 1.01–1.12). The adjusted HR for all second primary was 1.10 (95% CI 1.01–1.21, P = 0.03). For second cancer classified as RT-associated, a significantly elevated SIR was found among irradiated women based on 226-second cancers (SIR 1.18, 95% CI 1.03–1.35), while the SIR among the non-irradiated women was close to 1, based on 328-second cancers (SIR 1.02; 95% CI 0.91–1.14). The adjusted HR for the RT associated sites was 1.34 (95% CI 1.11–1.61, P = 0.002). For the cancer sites classified as non-RT-associated, SIRs were increased among both radiotherapy-treated (SIR 1.19; 95% CI 1.10–1.28) and non-treated patients (SIR 1.07; 95% CI 1.01–1.14), but there was no excess risk associated with radiotherapy HR 1.04 (95% CI 0.94–1.16). Radiotherapy-treated women had significantly elevated SIRs for ovarian

and uterus cancer, but when comparing irradiated women with non-irradiated, there was no increased risk associated with RT for both ovarian (HR 1.11; 95% CI 0.82–1.51) and Uterus cancer (HR 0.93; 95% CI 0.71–1.23). A significantly increased incidence of CNS cancer was observed among irradiated women compared with both the general female population and with non-irradiated women. In both cases, though, the risk was only significantly increased 1–4 years after treatment (SIR 1.58; 95% CI 1.13–2.16) and (HR 2.51; 95% CI 1.39–4.56). The addition of chemotherapy and radiation gave a higher HR than that seen for 'RT only,' but these HRs were not significantly different (P = 0.40). For the RT-associated sites, the risk increased with time since treatment and was significantly greater than one for the periods 10–14 (HR 1.55; 95% CI 1.08–2.24) and 15 or more years after treatment (HR 1.79; 95% CI 1.14–2.81). Lung cancer contributed 86% of the second cancers in this category. The risk of non-lung cancer was significantly increased for the time 10–14 years after treatment (HR 2.74; 95% CI 1.05–7.15). Among the irradiated women, the attributable risk related to radiotherapy was 9% for all second solid cancers, and the corresponding excess absolute risk was 6 cases per 10,000 person-years. For the RT-associated sites, the attributable risk related to radiotherapy was 25%, and the corresponding excess absolute risk was 4 cases per 10,000 person-years (144).

To compare the risk of RIC using neutrons versus photons (145), a cohort study was done in a group of patients treated with hypofractionated preoperative ionizing radiation therapy and using neutron brachytherapy using Californium-252 (252-Cf) sources for breast cancer in comparison with patients treated with conventional ionizing radiation therapy. Between 1987 and 1996, 991 female patients with operable breast cancer were treated. All patients underwent surgical resection (either radical mastectomy or breast-conserving), received adjuvant systemic and radiation therapies (either conventional or combined hypo-fractionated external and internal

radiotherapy) at the Institute of Oncology, Vilnius University during the period January 1987 - 1996. The schedule of radiotherapy was divided into two groups. Of the 832, 621 patients (74.6%) received 2.0 Gy daily fractions for 25 fractions to a total dose of 50 Gy to the treated breast and was designated the conventional (CRT) group. A cohort of 211 patients underwent preoperative hypofractionated external beam radiotherapy (EBRT) (7 Gy twice or 4–5 fractions by 5 Gy), postoperative EBRT (10–14 Gy, 2 Gy/fraction), and brachytherapy by 252-Cf. Neutron sources were indicated for patients with inner and central breast-located tumors after surgery. The follow-up time (person-years at risk) for second cancers for each individual began one year after the date of initial cancer diagnosis and ended at the date of diagnosis of any second cancer, last known vital status, death, or the end of the study, whichever occurred first. Follow-up for second malignancies was mainly conducted through direct contact with the patients at regular visits at out-patient clinics. For this study, data were collected retrospectively. The information on second malignancies was collected from the Cancer Registry of the Institute of Oncology, Vilnius University, by record linkage. The Cancer Registry of the Institute of Oncology, Vilnius University, has kept information on the date of diagnosis, histology, stage, and death for all patients in Lithuania since 1978. The occurrence of any subsequent RIC cancer was ascertained by pathology, reports, hospital or physician records, or death certificates. Pathology reports confirmed 82.5% of second breast cancer cases. The median time interval between the initial diagnosis and the second primary cancer was 7.4 years (range, 3–24 years). The most common types of second non-breast cancer malignancies were gynecological malignancies (39 cases, 25.2%) and gastrointestinal cancers (24 cases, 15.9%). The total numbers of second primary cancers were 112 in CRT patients and 38 in hypofractionated patients. Sporadic mediastinum cancer occurred among patients who received hypofractionated radiotherapy with HDR-

brachytherapy for internal lymph nodes using 252-Cf sources. One case of mediastinal lymphoma occurred for a CRT-treated patient > 20 years after radiotherapy. The age-adjusted incidence rate for second breast malignancies was 6 per 1000 person-years, and 15 cases per 1000 person-years of other primary cancer malignancies. A higher than expected second primary cancer was observed in all patients given combined therapy compared with the general female population (SIR 1.3, 95% CI 1.1– 1.5). The observed number of second RIC primary cancers was also higher than expected for lung (SIR 3.8, 95% CI 2.0–6.7) and stomach cancer (SIR 2.0, 95% CI 1.0–3.4). There was a significantly elevated risk of second primary breast cancer (SIR 2.1, 95% CI 1.4–2.9) in the first nine years after diagnosis. The SIR of lung cancer was 4.7 in the first nine years after diagnosis and 3.4 for ⩾ten years after diagnosis. There was a significant increase in the risk of second primary cancers compared with the general population (SIR 1.3, 95% CI 1.1 – 1.5). For second breast cancer, no raised relative risk was observed during the period ⩾ten or more years after radiotherapy. Compared with the CRT group, hypofractionated RT patients had a not statistically significant higher risk of breast cancer. Increased relative risks were explicitly observed for age at initial diagnosis of <50 years (HR 2.9, 95% CI 1.6–5.2) and for obesity (HR 2.8, 95% CI 1.1–7.2) (145).

An interesting study (146) was done to quantify RIC risks to the lung and the breast in female patients, for early-stage NCSLC patients who receive definitive SBRT, and to compare radiation-induced secondary cancer risks with different SBRT delivery techniques. The authors retrospectively selected ten patients with early-stage NSCLC, five men and five women, who previously received definitive SBRT treatment at their institution. Before treatment planning, each patient received computed tomography (CT) scans in the thoracic region with a 3 mm slice thickness in the helical mode. Three CT scans were performed for each patient while the patient

was in shallow free-breathing and at the end of the inspiration and expiration phases, respectively. In a treatment planning system (Eclipse 8.2, Varian Medical Systems, Inc., Palo Alto, CA), the 3 CT image sets were registered rigidly. The contours of critical organs, including the lungs, heart, spinal cord, and esophagus, were drawn on the free-breathing CT images. They generated the five treatment plans for each patient using two 3D-CRT techniques and three arc-based IMRT techniques.

At low-dose levels, estimation of the excess absolute risk (EAR) for the incidence of the solid tumor was generally performed, assuming a linear relationship between the cancer incidence rate and irradiated dose. At higher dose levels, the carcinogenetic effect is expected to be suppressed because of cell sterilization. With each OED model, the average EAR increases with the prescribed dose, whereas the slopes of the curves gradually decrease with dose with both the plateau and linear-exponential models. Including all the delivery techniques, with the prescription dose range from 30-70 Gy, the average EAR ranged from 11.6 to 18.7, from 10.4 to 17.0, and from 17.3 to 41.8 (unit: cancer incidence/10,000 patients/ year) with the linear-exponential, plateau, and linear models, respectively. For a given dose level and given delivery technique, the linear model gave significantly higher EAR estimates than the other models, whereas the plateau model gave significantly lower EAR estimates (2-tailed P-value for paired t-tests b .05). With each of the 3 OED models, the VMAT-2 technique showed the lowest average EAR values. However, the difference in EAR was not statistically significant for a given prescription dose level in the range of 30 to 70 Gy. The 3D-CRT plans showed significantly lower monitor units (MU) than the rotational intensity-modulated radiation therapy plans. Using a linear exponential model, at a prescription dose of 50 Gy, the average RIC lung EAR estimation ranged from 15.7 ± 5.3 -16.0 ± 6.5 per 10,000 patients per year with the five delivery

techniques. The average EAR estimation for the breast RIC ranged from 18.0 ± 14.0 to 21.0 ± 15.0 / 10,000 patients per year. The secondary cancer risk increased approximately linearly with the mean organ dose. The 3D-CRT plans showed significantly higher secondary cancer risk for the ipsilateral lung and lower risk for the contralateral lung than the hypofractionated and VMAT plans (146). Similar to my study, this study (146) evaluated patients that received SBRT for lung cancer. However, this study evaluated and compared RIC between 3D-CRT versus IMRT/VMAT plans, while my study evaluated RIC from scans the precede and follow SBRT treatments. My study did not calculate the scatter from the SBRT treatment itself.

Regarding the mechanism of tumor progression and invasion with low dose RT, the A549 cell model of human adenocarcinoma was exposed to 0, 2, 4 and 6 Gy of RT and cultured for 24-48 hours (147). Wound healing and Transwell assays were performed to detect invasion and CXCL1, and p65 expression was blocked using a lentiviral vector. Exposure to 6 Gy resulted in apoptosis, while RT to 4 Gy resulted in upregulation of CXCL1 and NF-kB signaling pathway, thereby promoting invasion and migration (147). Additional studies have proposed the mechanism of radiation-induced tumorigenesis, including alteration in cytogenetics, gene expression, DNA repair, and genomic instability (148-152). Table 5 lists select studies of radiation-induced cancers from medical imaging.

Conclusion: Most of the studies discussed as a part of literature search in the last decade have been done in patients undergoing diagnostic radiology exams, exposure to low dose radiation exposure, modeling studies, or radiation exposure as a part of radiation treatment for cancers. As we see above, the risk of RIC is generally low, although the risk escalates in pediatric groups. None of the studies shed light on the extent of RIC from all the imaging performed before and following lung SBRT for lung cancer. If patients develop lung cancer, how

much radiation is ‘too much’ when used to diagnose lung cancer, imaging to treat lung cancer using SBRT, and then imaging during follow-up after lung cancer treatment. I present the innovation in the project that I propose and specific questions that need to be answered.

Innovation

Over the last decade, there has been a trend towards increased utilization of imaging both as a diagnostic and staging modality and to perform CT-guided biopsies and in follow-up after the patient completes treatment (153). Until the 1990s, RT delivery utilized fluoroscopic films for simulation and only a few portal images at the beginning of selected treatment fractions. This protocol has changed dramatically over the last decades. The development of 3D-conformal therapy, Intensity-modulated Radiotherapy (IMRT), and frameless stereotactic radiosurgery has resulted in the need for Image-Guided Radiation Therapy (IGRT). IGRT involves multiple imaging procedures for planning, simulation, setup, and intra and inter-fraction monitoring (154). IGRT has resulted in more conformal RT delivery and better outcomes (155). Finally, after RT treatment completion, regular and frequent imaging is recommended for response evaluation and post RT complications. Since the patients receiving this RT exposure are cancer patients, there is little effort to limit imaging for RIC risk-reduction since these patients already have ‘cancer.' There is some truth to that because RIC latency is assumed to be decades. However, the survival in lung cancer patients has improved (156,157), and the risk of RIC in this cohort of patients is real and needs to be measured.

In this study, I propose to quantitate the imaging utilized in lung cancer patients for their diagnosis, calculate the total radiation exposure, and finally measure the increased cancer risk in these patients.

My study is novel because it considers all ionizing radiation exposure in early-stage lung cancer patients done for cancer diagnosis, SBRT treatment, and up to 1 year of follow-up after completion of SBRT. This study considers the ionizing radiation exposure resulting from IGRT (e.g., cone-beam CT scans) commonly used in contemporary RT management. There have been many reports measuring radiation exposure and cancer risk diagnostic imaging in non-oncologic settings (158-162). However, there is no published study to date that measures the total ionizing radiation exposure in lung cancer patients from diagnosis, treatment, and follow-up. Also, this study calculates the total RIC risk from imaging during SBRT treatment such as CBCT, simulation scans, and in addition to the pre-and-post-SBRT imaging. This study then calculates the survival at six months, one year, three years, and five years after treatment. This estimates the risk of RIC (latency 10-15 years) versus the actual survival in the cohort and whether the RIC risk is clinically significant. Such a study has not been published previously.

Specific Aims

The specific aims of the study are as follows:

Aim. 1). To quantify the total radiation exposure of patients undergoing SBRT for lung cancer from initial diagnosis to 1 year after completion of curative treatment. *I hypothesize that patients have a significant radiation exposure in the year before initial diagnosis, during radiation treatment, and following RT up to 1 year after RT completion.*

Aim. 2). To assess the increase in RIC risk resulting from this exposure. *I hypothesize that there is a significant increase risk of RIC in these patients compared to baseline*.

Methods

Institutional review board (IRB) approval was obtained before data collection. Consecutively treated patients with early-stage NSCLC treated from 2013-2018 were selected

for data collection. Eligibility included: Patients with non-small cell lung cancer or small cell lung cancer, patients with localized disease that were candidates for curative stereotactic body radiation therapy, a minimum follow-up of 1 year after completion of radiation, availability of records about work-up and follow-up at least one year before SBRT or 1-year post-treatment, radiation treatment records including information about image-guidance during SBRT. Data collected included the number of scans that utilize ionizing radiation (CT, CXR, PET-CT, exacttrac, cone-beam CT, bone scan, VQ scan (ventilation quotient scan). Also, demographic variables that were collected included age, sex, age of first treatment, Karnowski Performance Status (KPS), age at exposure to diagnostic scans, the dose of therapeutic RT (SBRT dose). The KPS describes a patient's functional status as a comprehensive 11-point scale correlating to percentage values ranging from 100% (no evidence of disease, no symptoms) to 0% (death) (163). Outcomes data collected included mortality at six months, one year, three years, and five years after completion of radiation.

Once the total number of scans and types of ionizing imaging (excluded MRIs) were obtained, the total effective dose from each scan was calculated based on institutional standards.

To get a comparative estimate of radiation exposure in patients receiving radiation for breast and prostate cancer, a sample of 10 each of consecutively treated early-stage prostate and breast cancer patients were also analyzed and excess lifetime risk (ELR) calculated. Breast cancer patients are at risk of radiation-induced lung cancer, other breast cancer, skin cancer, among other possible RICs. Prostate cancer patients are at risk of radiation-induced second prostate cancer, rectal, or another pelvic malignancy. This RIC risk was calculated for radiation-induced lung cancer in the breast cancer cohort and radiation-induced prostate cancer in the prostate cancer cohort.

Table 4: Effective doses for each scan

Imaging (ref)	mSv	mrem
CXR - AP	0.02	2
CXR - LAT	0.04	4
CT CHEST	8	800
CT-pelvis	10	1000
PET-FDG	14	1400
LUNG-VQ SCAN	2	200
BONE SCAN	4.2	420
Bone density	0.001	0.1
CBCT	2	
exactrak	1	
Mammogram (4 views)	0.7	70
Sentinel node for breast nodal sampling (63)	0.12	12

For each patient, the total effective dose (mSv) was calculated by the sum of all effective doses for all scans (1 year before SBRT to 1-year post-SBRT). After calculating the total effective dose, the summed dose was used to calculate the RIC using the RadRat tool. The RadRat online tool (***https://irep.nci.nih.gov/radrat***) requires the full exposure (in mGy or mSv), whether the exposure was acute or chronic, the organ of exposure, the gender of the subject, and the year in which the exposure happened. The report that is generated after this information is entered includes excess lifetime risk (risk from the time of exposure to the end of expected lifetime, calculated as chance in 100,000), excess future risk, baseline future risk, and total future risk (calculated as chance in 100,000, defined as risk from the year of data entry to end of expected lifetime).

In clinical oncology, patients presenting with lung cancer face a life-threatening illness; curing their cancer patients is the top priority. However, given the improving survival in early-

stage lung cancer patients, RIC becomes a relatively significant variable that needs to be addressed. Given the high frequency of imaging used in lung cancer patients, a potential source of RIC, we determined that a 1% increase in the baseline risk of radiation-induced lung cancer will be considered a significant increase. Also, we will evaluate survival data in the patients selected for this study. The imaging ordered is as per institutional standards.

Statistical Analysis: Descriptive data measurements will include percentage, percentiles, central tendency such as mean median and mode, and standard deviation. Normality will be assumed. Data will be expressed as a frequency for the nominal variables and the mean ± standard deviation (SD) for the continuous variables.

Power Calculation: *Sample size justification:* The lifetime risk of developing lung cancer for males is 6.85%, and for females, it is 5.95%. We will consider an increase in the risk of 1% as significant. Conservatively assuming a 0.2 correlation between lifetime risk and radiation exposure, with a two-tailed test and alpha=0.05, this study will achieve 80% power to detect a slope of 1% with a sample size of 191 patients. Since approximately 200-300 patients are eligible from our institution, this study should be > 80% powered to detect this increase in risk. PASS 16 (164) was used for calculations.

Results

One hundred and ninety-six consecutively treated early-stage lung cancer patients, with adequate follow-up and documentation, were selected for the study. There were 87 males (44.4%) and 109 females (55.6%). Race distributions are as follows; 72 Hispanic (36.7%), 33 Whites (16.8%), 29 Asian (14.7%) and 20 blacks (10.2%). The race of 42 patients (21.4%) was not identified (Figure 6).

Figure 6:

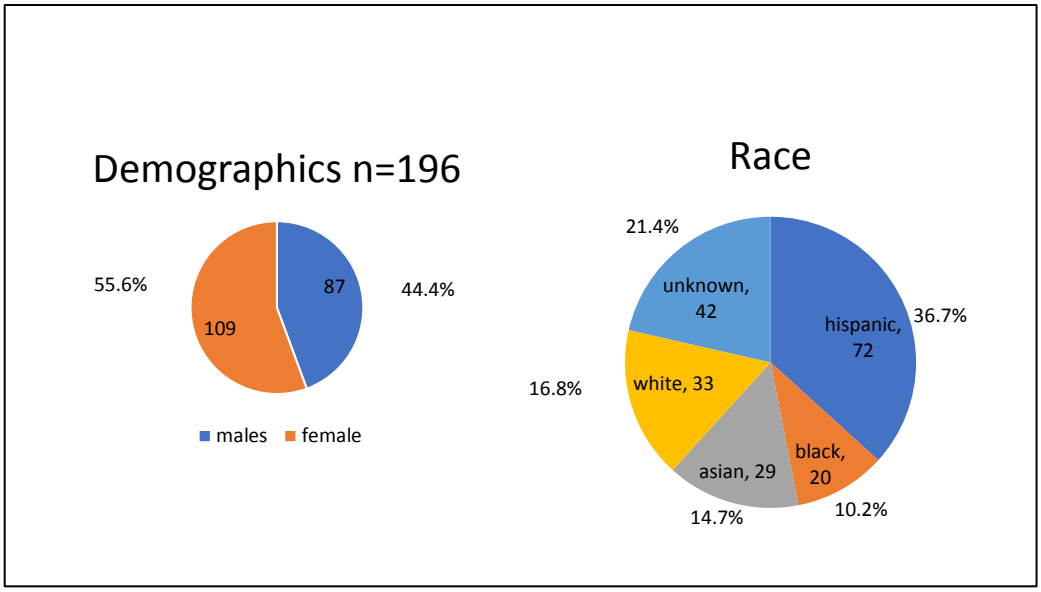

Histologic distributions of the lung tumors were 58 adenocarcinomas (29.5%), 21 squamous cell carcinomas (10.7%), 16 labeled as non-small cell lung cancer (8.1%), and 101 where histology was not specified (51.5%). Although all patients were treated with SBRT, a curative treatment used commonly for early-stage lung cancer, the distribution of stages were as follows; 149 stage I (76%), 3 stage II (1.5%), 12 stage III (6.1%), 13 stage IV (6.6%) and 19 (9.6%) where the stage was not mentioned (Figure 7).

Figure 7

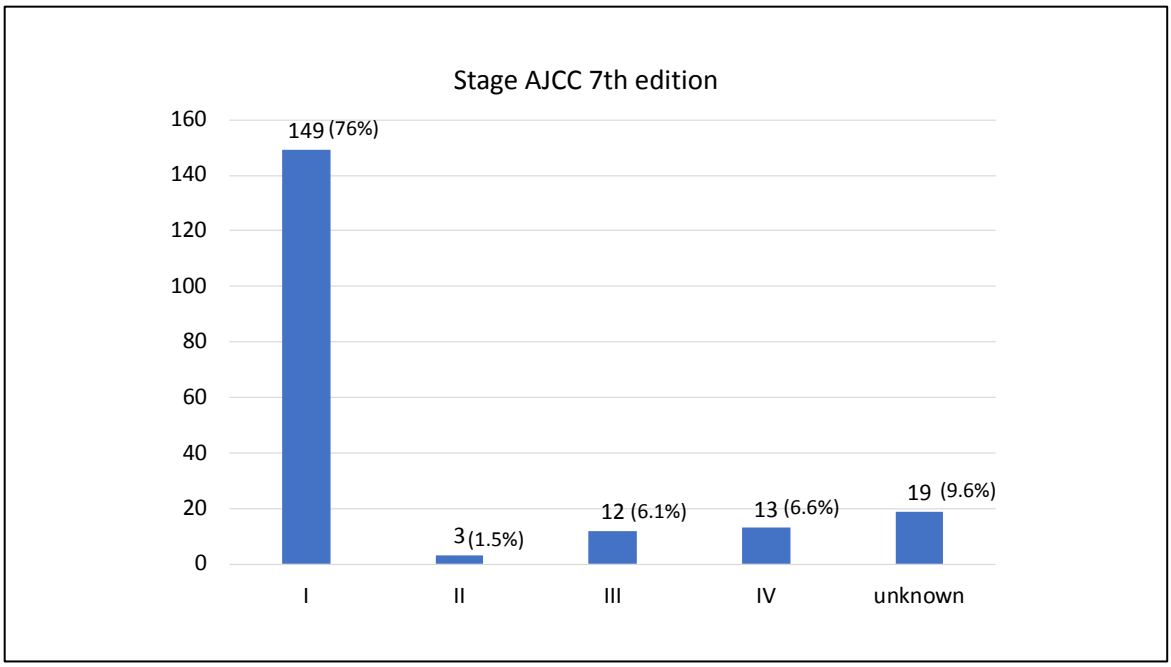

The median age of patients was 77y (Range: 53-93y), median KPS was 70 (range: 50-90), median weight was 161.9 lbs. (Range: 66-305.5lbs).

For SBRT delivery, the median dose was 50 Gy (Range 10-60 Gy), the median dose per fraction was 10 Gy/fraction (Range: 4.5-20 Gy/f). The median number of RT fractions was 5 (Range: 1-6).

Median number of Pre-SBRT CXRs (PA/lateral) was 2 (Range: 1-22), with the median effective radiation exposure dose of 0.12mSv (Range: 0.06-1.32mSv). The median number of pre-SBRT CT scans was 2 (Range: 1-6) with the median effective exposure dose of 16mSv (Range 8-48mSv). The median number of pre-SBRT PET-CT scans was 1 (Range: 1-4) with an effective exposure dose of 14 mSv (Range: 14-56 mSv). The median number of Bone Scans or VQ scans pre-SBRT was 1 (Range: 1-2) with a median effective dose of 2mSv (Range: 2-4.2 mSv).

Planning for SBRT required one simulation CT scan with an effective exposure dose of 8mSv. During SBRT delivery, the median number of CBCTs was 5 (Range: 1-10) with a median

effective exposure of 10mSv (Range: 2-20mSv). The median number of pre-SBRT delivery exactrac was 5 (Range: 2-14), and median exposure with this imaging was 5mSv (Range: 2-14mSv).

Median post-SBRT CXRs was 2 (Range: 1-16) with a median exposure dose of .12mSv (Range: 0.06-0.96mSv). The median number of post-SBRT CT scans was 2 (Range: 1-6), resulting in median effective exposure of 16mSv (Range: 8-48mSv). The median number of post-SBRT PET-CT scans was 1 (Range: 1-4) with a median effective exposure of 14mSv (Range: 14-56mSv).

The median effective exposure dose from all scans was 72mSv (Range: 24-140.36mSv).

Using the RadRat calculator, excess lifetime risk (ELR) of developing lung cancer (a chance in 100,000) with a 90% uncertainty range was calculated. The median of ELR mean was 57.15 (Range: 1.91-409) with a median of ELR upper bound of 97.9 (Range: 4.93-809) and median of ELR lower bound was 24.4 (Range: 0.174-219). The Excess Future risk (EFR), the risk from 2019 to end of the expected lifetime of developing cancer (a chance in 100,000), showed a median of EFR mean of 73.75 (Range: 8.45-416), with a median of EFR upper bound of 125.5 (Range: 21.3-823) and median of EFR lower bound of 29.65 (Range: 1.13-223). The Baseline Future risk (BFR) of developing cancer (a chance in 100,000), the risk from 2019 to end of expected lifetime showed a median of BFR mean of 2701 (Range: 745-8199), the median of BFR upper bound of 2747 (Range: 757-8295) and median of BFR lower bound of 2656 (Range: 733-8104). The total future risk (TFR, a sum of baseline and excess risk) of developing cancer from 2019 to the end of the expected lifetime was calculated (a chance in 100,000). The Median of TFR mean was 2732.5 (Range: 808-8290), the median of TFR upper bound was 2785.5 (Range: 856-8400), and the median of TFR lower bound was 2679.5 (Range: 761-8183).

Regarding survival outcomes in these patients (Figures 8-11), we calculated survival at six months, one year, three years, and five years. At six months, survival data on 152/196 patients were available, and survival was 94.7% (144/152). At one year, of the 119 patients with survival data, 79% (94/119) were alive. At three years, 83 patients with survival data were available; survival was 32.5% (27/83). At five years, most patients were either lost to follow up or had not reached the five year follow-up time, and survival data on 77 patients were available. Of the 77 patients, 9 (11.6%) were alive at five years.

Figure 8

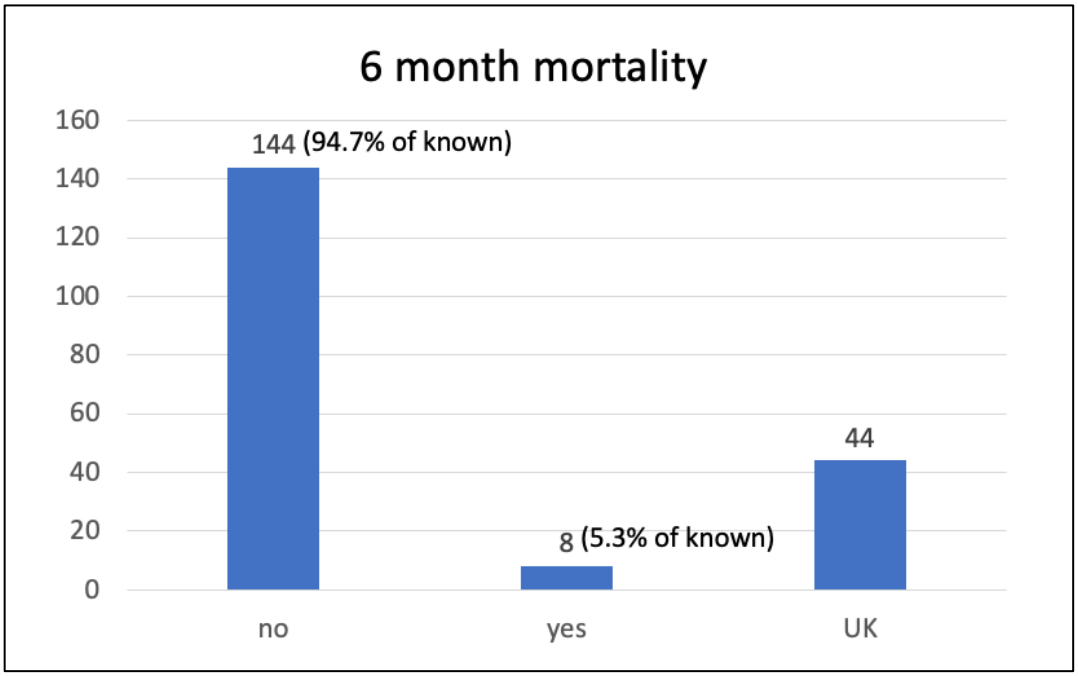

UK: unknown

Figure 9

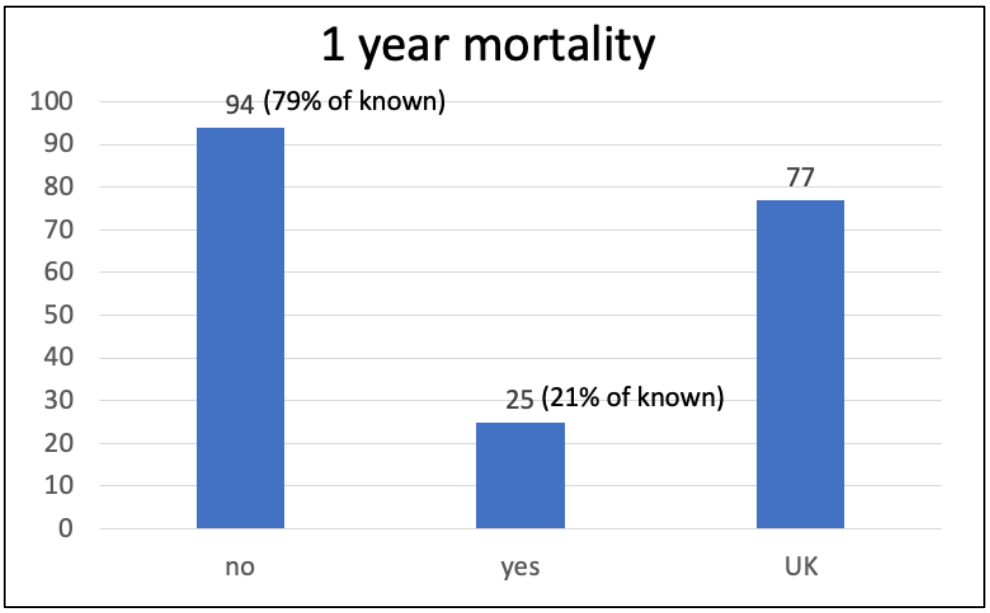

UK: unknown

Figure 10

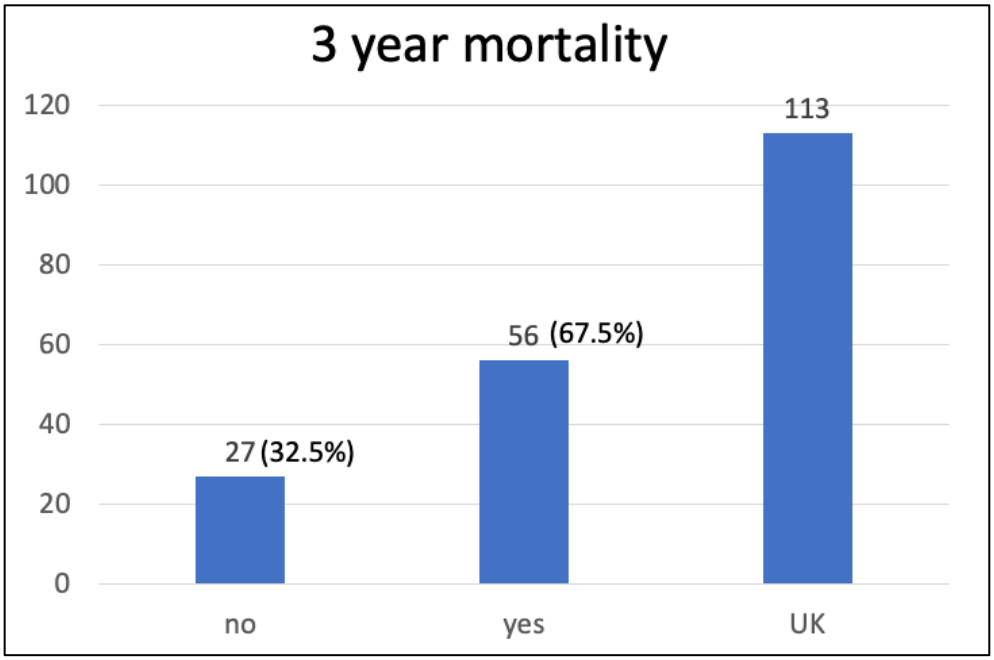

UK: unknown

Figure 11

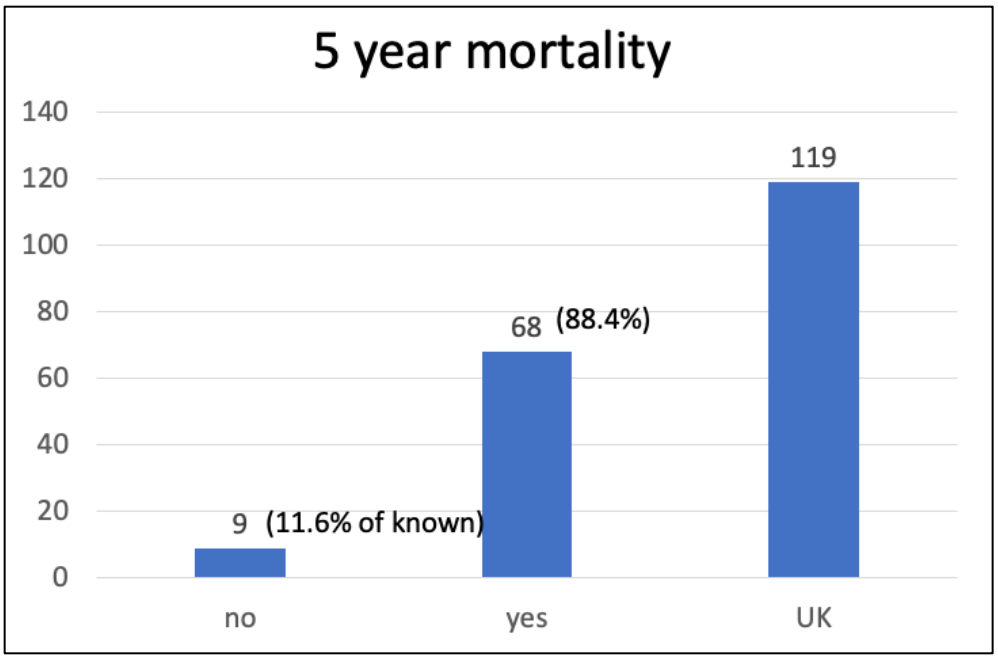

UK: unknown

Comparison estimates of ELR in prostate and breast cancer patients.

Patients with prostate cancer (biopsy-proven) were staged using MRI and PSA. Of the ten patients, 2 received a bone scan as a staging procedure, and one patient received a CT scan of the abdomen and pelvis before SBRT. All patients received 5 SBRT treatments to a total dose of 42.5 Gy, except one who received a total of 35 Gy. The median total effective radiation dose from all pre-SBRT and post-SBRT scans was 20mSv (Range: 20-30mSv). The median of mean ELR for the development of RIC prostate cancer was 4.24 (per 100,000).

Patients treated with radiation for early-stage breast cancer were staged using a median of 2 mammograms before radiation and one mammogram after completing radiation. Eight of 10 patients had a sentinel nodal biopsy using Technetium scan, 4/10 patients received a CXR. All patients received a CT simulation, and 5/10 patients received a bone scan after completion of radiation. Each patient received a dose of 42.4 Gy in 16 fractions. The median total effective radiation dose from all pre-RT and post-RT scans was 16.56mSv (Range: 10.52-31.48mSv). The

median of mean ELR for the development of radiation-induced lung cancer was 35.95 (per 100,000).

Discussion

The median of ELR mean was 57.15 (Range: 1.91-409 /100,000), which brings the median risk of 0.05%. This is significantly less than the 1% risk that was hypothesized to be clinically meaningful. The upper range of this ELR mean is 409. The risk in that situation will be 0.4%. Based on the assumptions and uncertainties in the study, it appears that the risk of RIC from non-therapeutic imaging immediately before and after SBRT for lung cancer is small. Also, the risk of mortality in this group of patients is high, and imaging used for SBRT management will likely result in enhanced management and benefits outweigh the risk. Although survival in early-stage lung cancer has improved in recent years, survival is still poor compared to other slower going cancers such as breast cancer and prostate cancer. In this cohort of subjects, patient survival data showed a 5-year survival of 11.6%. Since RIC latency for solid cancers is generally ten years or more, the risk of RIC is clinically not significant, given poor survival and long latency.

To further evaluate these findings, RIC risk in early-stage breast and prostate cancer patients from imaging radiation exposure was also estimated. The median of mean ELR for development of RIC prostate cancer was 4.24 (per 100,000), which is 0.004%, and the median of mean ELR for development of RIC in breast cancer 35.95/100,000 (0.03%). Both these risks are relatively small compared to the significant benefit in local control and survival due to radiation treatment. Median survival in patients treated for localized prostate and breast cancer is higher than 95% at ten years. Therefore, the benefit of treatment far outweighs the risk of treatment. The benefits of reducing the toxicity of radiation treatment are apparent. Based on this study's results,

the increasing use of imaging and modern techniques that involve ionizing radiation to deliver therapeutic doses hold a significant benefit and low risk of RIC in this group of patients.

Other limitations of the study include different makes and models of imaging machines for imaging scans (2013-2018) that may have different radiation effective doses, the uncertainties in the assessment of cancer risk using the LNT model, variation in the cone-beam scan machines, assumptions regarding absorbed dose to the lung, lack of long term follow-up in a set of patients either because they were lost to follow-up or patients not reaching the three and 5-year follow-up (patients treated in the last 1-2 years). Our study did not include the radiation exposure RIC risk during radiation delivery (high therapeutic doses), where the LNT model's accuracy is questionable.

The patient cohort in this study were all treated with a curative intent with SBRT. This cohort matches the patient population treated with SBRT for lung cancer across the country (7-9). SBRT is commonly used for patients with early-stage (Stage I/II) lung cancer. The stages included in our study was stage I-IV. This stage distribution is because several of these patients may have been diagnosed with higher stage disease and subsequently developed a new stage I/II lung cancer and was deemed to be curable with SBRT. Decisions about treating with SBRT is made after discussion in the multidisciplinary thoracic team. The workup and treatment techniques for SBRT treatment was standardized and included standard pre-SBRT and post-SBRT imaging as well as imaging for accurate SBRT delivery. The work-up consists of imaging to diagnose and treat with SBRT, and follow-up imaging after SBRT is similar across age groups, including young patients with good KPS. Exceptions may be made in older patients with poor KPS when occasional treatments may be given without a biopsy. However, patients may undergo additional imaging for suspicious nodules or for complications developing due to biopsies such

as pneumothorax, work-up for pneumonia, or pulmonary embolism that are common in these clinical situations. Some of the patients received a large number of CXRs due to complications or disease progression and hospital admission that required a CXR every day for a significant portion of the hospital stay. Histology of NSCLC, race, and sex of patient usually does not impact the SBRT technique-work-up leading up to SBRT. Image guidance during SBRT and follow-up imaging after completing SBRT is generally not affected by these three factors. Use of SBRT in small cell lung cancer is infrequent but is occasionally offered to patients with localized disease that are not candidates for chemotherapy, conventional radiation, or surgery.

The median age in this cohort was 77 years. This is a typical age to develop lung cancer and are commonly treated with SBRT. SBRT is most frequently used for patients that are not surgical candidates due to existing co-morbidities. This has several implications for our study: the three and 5-year survival is expected to be lower than patients with early-stage lung cancer treated with surgery. The excess risk of RIC is expected to be lower, given the advanced age at exposure. The risk of RIC as per the *radrat* tool is dependent on age at exposure, female sex, and the quantity of low dose exposure. Exposure at a younger age is expected to increase the risk of developing RIC, while exposure at an older age is expected to have a lower risk.

Median KPS (Karnowski performance status) in our cohort was 70, indicating a relatively low-performance status. The KPS is scored as follows: 100 – Normal; no complaints; no evidence of disease, 90 – Able to carry on normal activity; minor signs or symptoms of the disease, 80 – Normal activity with effort; some signs or symptoms of the disease, 70 – Cares for self; unable to carry on normal activity or to do active work, 60 – Requires occasional assistance, but can care for most of their personal needs, 50 – Requires considerable assistance and frequent medical care, 40 – Disabled; requires special care and assistance, 30 – Severely disabled;

hospital admission is indicated although death not imminent, 20 – Very sick; hospital admission necessary; active supportive treatment necessary, 10 – Moribund; fatal processes progressing rapidly, 0 – Dead. Surgery is generally preferred for KPS of higher than 70. Also, a lower KPS indicates a poor long term survival, and the risk of RIC is less relevant in this setting. However, most patients with early-stage breast cancer are women, with higher KPS and a higher chance of long term survival, and RIC risk is an important consideration in such patients.

The median SBRT dose was 50 Gy in 5 fractions. The SBRT dose for early-stage lung cancer is the standard dose that has been determined by multiple studies determining adequate dose for tumor ablation (42). As discussed previously, the LNT model is usually used for doses less than 1-1.5 Gy. The dose of SBRT for lung cancer that results in good local control is a BED (Biologically equivalent dose) is greater than 100 Gy (42). Some of the patients in our cohort did not receive the full SBRT dose either due to patient preference to stop radiation or disease progression and at the physician's discretion. The upper range of SBRT dose in our study was 60 Gy that was due to the utilization of 20 Gy per fraction, which was the dose used in the initial SBRT phase II/III studied (42,165).

A typical sequence of events before diagnosing early-stage lung cancer is either a CXR for an unrelated reason (e.g., occupational health check or motor vehicle accident), cough, weight loss, or another medical reason. A nodule may be identified on the CXR that leads to further work-up, including a CT scan followed by a CT guided biopsy, which confirms cancer. Subsequently, a PET-CT scan is performed for staging purposes. During this workup for cancer, additional imaging may be required due to complications or other findings on CXR or CT scan. For example, a patient may develop pneumothorax after a CT-guided biopsy, resulting in further imaging for management. After completing SBRT, routine follow-up imaging usually includes

CT chest, PET-CT scan to evaluate for treatment response, usually performed starting 3-4 months after completion of SBRT. Also, depending on the follow-up scan results, new nodules may need to be evaluated and need imaging and CT-guided biopsies. Also, some patients that develop pneumonia or pneumonitis due to RT or systemic treatments, including immunotherapy, may require imaging and follow-up scans. Since malignancy is a hypercoagulable state, the development of pulmonary embolism is not uncommon and may require CT scans and ventilation/perfusion scans for diagnosis. A bone scan may be performed on suspicion of bone metastasis.

SBRT planning requires a simulation CT scan that is performed for each patient before treatment. After simulation scan, additional imaging in the form of Cone-beam CT scan and exactrac is performed at each treatment fraction for image guidance.

Radrat calculator gives a value of the excess lifetime risk of developing RIC from exposure to the end of expected lifetime and has been described above. It also provides a calculation of excess future risk (EFR) of RIC calculated from the time the analysis was done (2019 onwards) and gives the total excess risk, the sum of baseline future risk, and excess future risk. The EFR risk from 2019 to the end of the expected lifetime of developing cancer (a chance in 100,000) showed a median of EFR mean of 73.75 (Range: 8.45-416) or 0.07%, with a median of EFR upper bound of 125.5 (Range: 21.3-823) [0.12%] and median of EFR lower bound of 29.65 (Range: 1.13-223) [0.02%]. The percentage of excess lifetime risk is not clinically significant.

Survival data from our cohort of patients showed an approximate survival of 94.7% at six months, 79% at one year, 32.5% at three years, and 11.6% at five years. Although this survival is lower at three and 5-year time point, it could be due to higher staged patients that received SBRT

for new nodules, retrospective nature of the study, a group of patients have not reached the three and 5-year time point, and therefore that data is unavailable. The survival data available at 3 and 5 year time points show that the RIC risk from imaging required for SBRT management of lung cancer is not clinically significant. The development of novel therapeutics such as immunotherapy may further enhance these patients' survival, and we may need to revisit the RIC in the coming decades as patients live longer. Also, an important factor that affects outcomes in lung cancer management includes genetics, although ethnic and racial disparities also have a role (166)

But even if the increase in RIC risk from diagnostic imaging and image guidance in early-stage lung cancer treated with SBRT is not clinically significant, it was questioned whether RIC risk from imaging before or after RT is clinically significant in prostate and breast cancer. We calculated an estimate of RIC risk from imaging before and post-radiation treatment in patients with early-stage prostate and early-stage breast cancer. In our patient cohort, patients with prostate cancer were treated with SBRT (5 fractions), while patients with early-stage breast cancer were treated with hypofractionated radiation (15 fractions). These RT techniques are a part of standard options for early-stage prostate and breast cancer. The median of mean excess lifetime risk for development of RIC prostate cancer was 4.24/100,000 (0.004%), and RIC for development of lung cancer from breast RT was 35.95/100,000 (0.03%). The survival of patients with early-stage prostate cancer is close to 100% in patients that receive RT and more than 90% for patients diagnosed with early-stage breast cancer (167,168). Therefore, the benefits of treating these cancers far outweigh the RIC risk.

Significance

The results of the study assuming the LNT model for RIC suggest a clinically non-significant increase in the risk of radiation-induced lung cancers. The small increase in excess lifetime risk of RIC from pre-and-post-SBRT imaging is less than 1% in a set of patients with early-stage lung cancer. In contrast, improvement in imaging for staging, accurate radiation delivery, post-treatment follow-up imaging has resulted in significant improvement in patient outcomes in the last decade. With further advancement in technology, effective radiation doses from newer machines are likely to be smaller, thereby further reducing the risk of RIC. The preliminary data on RIC risk in early-stage breast cancer and prostate cancer suggests a clinically insignificant risk from pre-radiation and post-radiation imaging. This study suggests that an effort to improve radiation delivery, reduced toxicity, and improved safety should continue even if it increases exposure to ionizing radiation. The benefits outweigh the risk of this radiation exposure. Increased imaging does not always mean increased exposure to ionizing radiation. For example, there is a recent increase in MRI imaging in diagnosis and radiation delivery, such as PET-MRIs and MRI-linacs (169, 170). An advantage of PET-MRI is reduced radiation exposure and enhanced soft-tissue contrast (169). In oncologic imaging, there have been several comparative studies between PET/MRI and PET/CT, and these studies have either reported that PET/CT and PET/MRI perform equally well or that PET/MRI has some advantages (171). However, at this time, the cost is higher than installation and maintenance compared to PET-CT (172). In the future, we expect imaging technology resulting in higher resolution, accurate radiation delivery, and reduced ionizing radiation exposure.

References

1. Welch HG, Prorok PC, O'Malley AJ, Kramer BS. Breast-Cancer Tumor Size, Overdiagnosis, and Mammography Screening Effectiveness. N Engl J Med. 2016 Oct 13;375(15):1438-1447. PubMed PMID: 27732805.

2. Worni M, Akushevich I, Greenup R, Sarma D, Ryser MD, Myers ER, Hwang ES. Trends in Treatment Patterns and Outcomes for Ductal Carcinoma In Situ. J Natl Cancer Inst. 2015 Sep 30;107(12):djv263. doi: 10.1093/jnci/djv263. Print 2015 Dec. PubMed PMID: 26424776; PubMed Central PMCID: PMC4707192.

3. Hu CY, Bailey CE, You YN, Skibber JM, Rodriguez-Bigas MA, Feig BW, Chang GJ. Time trend analysis of primary tumor resection for stage IV colorectal cancer: less surgery, improved survival. JAMA Surg. 2015 Mar 1;150(3):245-51. doi: 10.1001/jamasurg.2014.2253. PubMed PMID: 25588105.

4. Newman JR, Connolly TM, Illing EA, Kilgore ML, Locher JL, Carroll WR. Survival trends in hypopharyngeal cancer: a population-based review. Laryngoscope. 2015 Mar;125(3):624-9. doi: 10.1002/lary.24915. Epub 2014 Sep 15. Review. PubMed PMID: 25220657.

5. Chen Y, Wang H, Kantarjian H, Cortes J. Trends in chronic myeloid leukemia incidence and survival in the United States from 1975 to 2009. Leuk Lymphoma. 2013 Jul;54(7):1411-7. doi: 10.3109/10428194.2012.745525. Epub 2012 Dec 5. PubMed PMID: 23121646; PubMed Central PMCID: PMC5525971.

6. Shin JY, Yoon JK, Marwaha G. Progress in the Treatment and Outcomes for Early-Stage Non-Small Cell Lung Cancer. Lung. 2018 Jun;196(3):351-358. doi: 10.1007/s00408-018-0110-1. Epub 2018 Mar 17. PubMed PMID: 29550987.

7. https://www.cancer.org/content/dam/cancer-org/research/cancer-facts-and-statistics/annual-cancer-facts-and-figures/2019/cancer-facts-and-figures-2019.pdf

8. https://seer.cancer.gov/archive/csr/1975_2014/

9. https://www.cdc.gov/cancer/lung/basic_info/risk_factors.htm

10. Dracham CB, Shankar A, Madan R. Radiation induced secondary malignancies: a review article. Radiat Oncol J. 2018 Jun;36(2):85-94. doi:10.3857/roj.2018.00290. Epub 2018 Jun 29. PubMed PMID: 29983028; PubMed Central PMCID: PMC6074073.

11. MacDonald SL, Hansell DM. Staging of non-small cell lung cancer: imaging of intrathoracic disease. Eur J Radiol. 2003 Jan;45(1):18-30. Review. PubMed PMID: 12499061.

12. Honda O, Johkoh T, Yamamoto S, Koyama M, Tomiyama N, Kozuka T, Hamada S, Mihara N, Nakamura H, Müller NL. Comparison of quality of multiplanar reconstructions and direct coronal multidetector CT scans of the lung. AJR Am J Roentgenol. 2002 Oct;179(4):875-9. PubMed PMID: 12239028.

13. Peloschek P, Sailer J, Weber M, Herold CJ, Prokop M, Schaefer-Prokop C. Pulmonary nodules: sensitivity of maximum intensity projection versus that of volume rendering of 3D multidetector CT data. Radiology. 2007 May;243(2):561-9. PubMed PMID: 17456878.

14. Pauwels EK, McCready VR, Stoot JH, van Deurzen DF. The mechanism of accumulation of tumour-localising radiopharmaceuticals. Eur J Nucl Med. 1998 Mar;25(3):277-305. Review. PubMed PMID: 9580862.

15. Sihoe AD, Yim AP. Lung cancer staging. J Surg Res. 2004 Mar;117(1):92-106. Review. PubMed PMID: 15013719.

16. De Wever W, Stroobants S, Verschakelen JA. Integrated PET/CT in lung cancer imaging: history and technical aspects. JBR-BTR. 2007 Mar-Apr;90(2):112-9. Review. PubMed PMID: 17555071.

17. Antoch G, Stattaus J, Nemat AT, Marnitz S, Beyer T, Kuehl H, Bockisch A, Debatin JF, Freudenberg LS. Non-small cell lung cancer: dual-modality PET/CT in preoperative staging. Radiology. 2003 Nov;229(2):526-33. Epub 2003 Sep 25. PubMed PMID: 14512512.

18. Esposito M, Maggi G, Marino C, Bottalico L, Cagni E, Carbonini C, Casale M, Clemente S, D'Alesio V, Fedele D, Giglioli FR, Landoni V, Martinotti A, Nigro R, Strigari L, Villaggi E, Mancosu P. Multicentre treatment planning inter-comparison in a national context: The liver stereotactic ablative radiotherapy case. Phys Med. 2016 Jan;32(1):277-83. doi: 10.1016/j.ejmp.2015.09.009. Epub 2015 Oct 20. PubMed PMID: 26498378.

19. Ikushima H, Balter P, Komaki R, Hunjun S, Bucci MK, Liao Z, McAleer MF, Yu ZH, Zhang Y, Chang JY, Dong L. Daily alignment results of in-room computed tomography-guided stereotactic body radiation therapy for lung cancer. Int J Radiat Oncol Biol Phys. 2011 Feb 1;79(2):473-80. doi: 10.1016/j.ijrobp.2009.11.009. Epub 2010 Apr 14. PubMed PMID: 20399032.

20. Borst GR, Sonke JJ, Betgen A, Remeijer P, van Herk M, Lebesque JV. Kilo-voltage cone-beam computed tomography setup measurements for lung cancer patients; first clinical results and comparison with electronic portal-imaging device. Int J Radiat Oncol Biol Phys. 2007 Jun 1;68(2):555-61. Epub 2007 Mar 29. PubMed PMID: 17398021.

21. Clemente S, Chiumento C, Fiorentino A, Simeon V, Cozzolino M, Oliviero C, Califano G, Caivano R, Fusco V. Is ExacTrac x-ray system an alternative to CBCT for positioning patients with head and neck cancers? Med Phys. 2013 Nov;40(11):111725. doi: 10.1118/1.4824056. PubMed PMID: 24320433.

22. Detterbeck FC. The eighth edition TNM stage classification for lung cancer: What does it mean on main street? J Thorac Cardiovasc Surg. 2018. Jan;155(1):356-359. doi: 10.1016/j.jtcvs.2017.08.138. Epub 2017 Sep 28. PubMed PMID: 29061464.

23. Ginsberg RJ, Rubinstein LV. Randomized trial of lobectomy versus limited resection for T1 N0 non-small cell lung cancer. Lung Cancer Study Group. Ann Thorac Surg. 1995 Sep;60(3):615-22; discussion 622-3. PubMed PMID: 7677489.

24. Flehinger BJ, Kimmel M, Melamed MR. The effect of surgical treatment on survival from early lung cancer. Implications for screening. Chest. 1992 Apr;101(4):1013-8. PubMed PMID: 1313349.

25. Travis WD, Brambilla E, Rami-Porta R, Vallières E, Tsuboi M, Rusch V, Goldstraw P; International Staging Committee. Visceral pleural invasion: pathologic criteria and use of elastic stains: proposal for the 7th edition of the TNM classification for lung cancer. J Thorac Oncol. 2008 Dec;3(12):1384-90. doi: 10.1097/JTO.0b013e31818e0d9f. PubMed PMID: 19057261.

26. Dosoretz DE, Katin MJ, Blitzer PH, Rubenstein JH, Salenius S, Rashid M, Dosani RA, Mestas G, Siegel AD, Chadha TT, et al. Radiation therapy in the management of medically inoperable carcinoma of the lung: results and implications for future treatment strategies. Int J Radiat Oncol Biol Phys. 1992;24(1):3-9. PubMed PMID: 1324899.

27. Qiao X, Tullgren O, Lax I, Sirzén F, Lewensohn R. The role of radiotherapy in treatment of stage I non-small cell lung cancer. Lung Cancer. 2003 Jul;41(1):1-11. Review. PubMed PMID: 12826306.

28. Zhang HX, Yin WB, Zhang LJ, Yang ZY, Zhang ZX, Wang M, Chen DF, Gu XZ. Curative radiotherapy of early operable non-small cell lung cancer. Radiother Oncol. 1989 Feb;14(2):89-94. PubMed PMID: 2540510.

29. Cox JD, Azarnia N, Byhardt RW, Shin KH, Emami B, Pajak TF. A randomized phase I/II trial of hyperfractionated radiation therapy with total doses of 60.0 Gy to 79.2 Gy: possible survival benefit with greater than or equal to 69.6 Gy in favorable patients with Radiation Therapy Oncology Group stage III non-small-cell lung carcinoma: report of Radiation Therapy Oncology Group 83-11. J Clin Oncol. 1990 Sep;8(9):1543-55. PubMed PMID: 2167952.

30. Kong FM, Ten Haken RK, Schipper MJ, Sullivan MA, Chen M, Lopez C, Kalemkerian GP, Hayman JA. High-dose radiation improved local tumor control and overall survival in patients with inoperable/unresectable non-small-cell lung cancer: long-term results of a radiation dose escalation study. Int J Radiat Oncol Biol Phys. 2005 Oct 1;63(2):324-33. PubMed PMID: 16168827.

31. Blomgren, H., Lax, I., Göranson, H. et al. Journal of Radiosurgery (1998) 1: 63. https://doi.org/10.1023/B:JORA.0000010880.40483.c4

32. Timmerman R, McGarry R, Yiannoutsos C, Papiez L, Tudor K, DeLuca J, Ewing M, Abdulrahman R, DesRosiers C, Williams M, Fletcher J. Excessive toxicity when

treating central tumors in a phase II study of stereotactic body radiation therapy for medically inoperable early-stage lung cancer. J Clin Oncol. 2006 Oct 20;24(30):4833-9. PubMed PMID: 17050868.

33. Timmerman R, Paulus R, Galvin J, Michalski J, Straube W, Bradley J, Fakiris A, Bezjak A, Videtic G, Johnstone D, Fowler J, Gore E, Choy H. Stereotactic body radiation therapy for inoperable early stage lung cancer. JAMA. 2010 Mar 17;303(11):1070-6. doi: 10.1001/jama.2010.261. PubMed PMID: 20233825; PubMed Central PMCID: PMC2907644.

34. McGarry RC, Papiez L, Williams M, Whitford T, Timmerman RD. Stereotactic body radiation therapy of early-stage non-small-cell lung carcinoma: phase I study. Int J Radiat Oncol Biol Phys. 2005 Nov 15;63(4):1010-5. Epub 2005 Aug 22. PubMed PMID: 16115740.

35. Kann BH, Verma V, Stahl JM, Ross R, Dosoretz AP, Shafman TD, Gross CP, Park HS, Yu JB, Decker RH. Multi-institutional analysis of stereotactic body radiation therapy for operable early-stage non-small cell lung carcinoma. Radiother Oncol. 2019 May;134:44-49. doi: 10.1016/j.radonc.2019.01.027. Epub 2019 Feb 1. PubMed PMID: 31005223.

36. Lu T, Yang X, Huang Y, Zhao M, Li M, Ma K, Yin J, Zhan C, Wang Q. Trends in the incidence, treatment, and survival of patients with lung cancer in the last four decades. Cancer Manag Res. 2019 Jan 21;11:943-953. doi: 10.2147/CMAR.S187317. eCollection 2019. PubMed PMID: 30718965; PubMed Central PMCID: PMC6345192.

37. McDonald F, De Waele M, Hendriks LE, Faivre-Finn C, Dingemans AC, Van Schil

PE. Management of stage I and II nonsmall cell lung cancer. Eur Respir J. 2017 Jan 3;49(1). pii: 1600764. doi: 10.1183/13993003.00764-2016. Print 2017 Jan. Review. PubMed PMID: 28049169.

38. Tsang MW. Stereotactic body radiotherapy: current strategies and future development. J Thorac Dis. 2016 Jul;8(Suppl 6):S517-27. doi: 10.21037/jtd.2016.03.14. Review. PubMed PMID: 27606082; PubMed Central PMCID: PMC4990666.

39. Paleiron N, Bylicki O, André M, Rivière E, Grassin F, Robinet G, Chouaïd C. Targeted therapy for localized non-small-cell lung cancer: a review. Onco Targets Ther. 2016 Jul 5;9:4099-104. doi: 10.2147/OTT.S104938. eCollection 2016. Review. PubMed PMID: 27462164; PubMed Central PMCID: PMC4940012.

40. Kapadia NS, Valle LF, George JA, Jagsi R, D'Amico TA, Dexter EU, Vigneau FD, Kong FM. Patterns of Treatment and Outcomes for Definitive Therapy of Early Stage Non-Small Cell Lung Cancer. Ann Thorac Surg. 2017 Dec;104(6):1881-1888. doi: 10.1016/j.athoracsur.2017.06.065. Epub 2017 Oct 26. PubMed PMID: 29106887.

41. Falkson CB, Vella ET, Yu E, El-Mallah M, Mackenzie R, Ellis PM, Ung YC. Radiotherapy With Curative Intent in Patients With Early-stage, Medically Inoperable, Non-Small-cell Lung Cancer: A Systematic Review. Clin Lung Cancer. 2017 Mar;18(2):105-121.e5. doi: 10.1016/j.cllc.2016.10.008. Epub 2016 Oct 27. Review. PubMed PMID: 27908621.

42. Parashar B, Singh P, Christos P, Arora S, Desai P, Wernicke AG, Delamerced M, Boothe D, Nori D, Chao K. Stereotactic body radiation therapy (SBRT) for early stage lung cancer delivers clinically significant radiation to the draining lymph nodes. J

Radiosurg SBRT. 2013;2(4):339-340. PubMed PMID: 24383044; PubMed Central PMCID: PMC3874935.

43. Malhotra A, Wu X, Chugh A, Mustafa A, Matouk CC, Gandhi D, Sanelli P. Risk of Radiation-Induced Cancer From Computed Tomography Angiography Use in Imaging Surveillance for Unruptured Cerebral Aneurysms. Stroke. 2018 Dec 7:STROKEAHA118022454. doi: 10.1161/STROKEAHA.118.022454. [Epub ahead of print] PubMed PMID: 30580703.

44. McKeown SR, Hatfield P, Prestwich RJ, Shaffer RE, Taylor RE. Radiotherapy for benign disease; assessing the risk of radiation-induced cancer following exposure to intermediate dose radiation. Br J Radiol. 2015;88(1056):20150405. doi: 10.1259/bjr.20150405. Epub 2015 Oct 14. Review. PubMed PMID: 26462717; PubMed Central PMCID: PMC4984935.

45. Radiochemistry and Nuclear Chemistry Book. ISBN 978-0-7506-7463-8. 3rd Edition, 2002. DOI https://doi.org/10.1016/B978-0-7506-7463-8.X5000-6.

46. Sansare K, Khanna V, Karjodkar F. Early victims of X-rays: a tribute and current perception. Dentomaxillofac Radiol. 2011 Feb;40(2):123-5. doi: 10.1259/dmfr/73488299. PubMed PMID: 21239576; PubMed Central PMCID: PMC3520298.

47. Polednak A. P. (1978). Bone cancer among female radium dial workers. Latency periods and incidence rates by time after exposure: brief communication. Journal of the National Cancer Institute, 60(1), 77–82. https://doi.org/10.1093/jnci/60.1.77

48. Adams, E. E., & Brues, A. M. (1980). Breast cancer in female radium dial workers first employed before 1930. Journal of occupational medicine. : official publication of the Industrial Medical Association, 22(9), 583–587.

49. 1990 Recommendations of the International Commission on Radiological Protection. Ann ICRP. 1991;21(1-3):1-201. PMID: 2053748

.

50. Cohen RJ, Curtis RE, Inskip PD, Fraumeni JF Jr. The risk of developing second cancers among survivors of childhood soft tissue sarcoma. Cancer. 2005 Jun 1;103(11):2391-6. PubMed PMID: 15852362.

51. Gábora K, Bărbuş E, Peştean C, Larg MI, Bonci EA, Bădulescu CI, Piciu A. Radiation induced thyroid carcinoma in Romania - effects of the Chernobyl fallout, a systematic review of observational studies. Clujul Med. 2018 Oct;91(4):372-375. doi: 10.15386/cjmed-1046. Epub 2018 Oct 30. Review. PubMed PMID: 30564011; PubMed Central PMCID: PMC6296726.

52. Bogdanova TI, Saenko VA, Brenner AV, Zurnadzhy LY, Rogounovitch TI, Likhtarov IA, Masiuk SV, Kovgan LM, Shpak VM, Thomas GA, Chanock SJ, Mabuchi K, Tronko MD, Yamashita S. Comparative Histopathologic Analysis of "Radiogenic" and "Sporadic" Papillary Thyroid Carcinoma: Patients Born Before and After the Chernobyl Accident. Thyroid. 2018 Jul;28(7):880-890. doi: 10.1089/thy.2017.0594. PubMed PMID: 29989861; PubMed Central PMCID: PMC6112184.

53. Ojha J, Dyagil I, Finch SC, Reiss RF, de Smith AJ, Gonseth S, Zhou M, Hansen HM, Sherborne AL, Nakamura J, Bracci PM, Gudzenko N, Hatch M, Babkina N, Little MP, Chumak VV, Walsh KM, Bazyka D, Wiemels JL, Zablotska LB. Genomic

characterization of chronic lymphocytic leukemia (CLL) in radiation-exposed Chornobyl cleanup workers. Environ Health. 2018 May 2;17(1):43. doi: 10.1186/s12940-018-0387-9. PubMed PMID: 29720177; PubMed Central PMCID: PMC5930419.

54. Bazyka D, Finch SC, Ilienko IM, Lyaskivska O, Dyagil I, Trotsiuk N, Gudzenko N, Chumak VV, Walsh KM, Wiemels J, Little MP, Zablotska LB. Buccal mucosa micronuclei counts in relation to exposure to low dose-rate radiation from the Chornobyl nuclear accident and other medical and occupational radiation exposures. Environ Health. 2017 Jun 23;16(1):70. doi: 10.1186/s12940-017-0273-x. PubMed PMID: 28645274; PubMed Central PMCID: PMC5481966.

55. Ozasa K. Epidemiological research on radiation-induced cancer in atomic bomb survivors. J Radiat Res. 2016 Aug;57 Suppl 1:i112-i117. doi: 10.1093/jrr/rrw005. Epub 2016 Mar 13. PubMed PMID: 26976124; PubMed Central PMCID: PMC4990102.

56. Ozasa K, Grant EJ, Kodama K. Japanese Legacy Cohorts: The Life Span Study Atomic Bomb Survivor Cohort and Survivors' Offspring. J Epidemiol. 2018 Apr 5;28(4):162-169. doi: 10.2188/jea.JE20170321. Epub 2018 Mar 17. PubMed PMID: 29553058; PubMed Central PMCID: PMC5865006.

57. Grant EJ, Brenner A, Sugiyama H, Sakata R, Sadakane A, Utada M, Cahoon EK, Milder CM, Soda M, Cullings HM, Preston DL, Mabuchi K, Ozasa K. Solid Cancer Incidence among the Life Span Study of Atomic Bomb Survivors: 1958-2009. Radiat Res. 2017 May;187(5):513-537. doi: 10.1667/RR14492.1. Epub 2017 Mar 20. PubMed PMID: 28319463.

58. Smoll NR, Brady Z, Scurrah K, Mathews JD. Exposure to ionizing radiation and

brain cancer incidence: The Life Span Study cohort. Cancer Epidemiol. 2016 Jun;42:60-5. doi: 10.1016/j.canep.2016.03.006. Epub 2016 Mar 31. PubMed PMID: 27038588.

59. Smith-Bindman R, Wang Y, Chu P, Chung R, Einstein AJ, Balcombe J, Cocker M, Das M, Delman BN, Flynn M, Gould R, Lee RK, Yellen-Nelson T, Schindera S, Seibert A, Starkey J, Suntharalingam S, Wetter A, Wildberger JE, Miglioretti DL. International variation in radiation dose for computed tomography examinations: prospective cohort study. BMJ. 2019 Jan 2;364:k4931. doi: 10.1136/bmj.k4931. PubMed PMID: 30602590; PubMed Central PMCID: PMC6314083.

60. Paiva FG, do Carmo Santana P, Mourão AP. Evaluation of patient effective dose in a PET/CT test. Appl Radiat Isot. 2019 Mar;145:137-141. doi: 10.1016/j.apradiso.2018.12.024. Epub 2018 Dec 20. PubMed PMID: 30599383.

61. Dabrowska M, Przybylo Z, Zukowska M, Kobylecka M, Maskey-Warzechowska M, Krenke R. SHOULD WE BE CONCERNED ABOUT THE DOSES OF IONIZING RADIATION RELATED TO DIAGNOSTIC AND FOLLOW-UP IMAGING IN PATIENTS WITH SOLITARY PULMONARY NODULES? Radiat Prot Dosimetry. 2018 Jan 1;178(2):201-207. doi: 10.1093/rpd/ncx099. PubMed PMID: 28981871.

62. Fry RJM, Storer JB. External radiation carcinogenesis. In: Lett JT, ed. Advances in radiation biology, volume 13. New York, NY: Academic Press; 1987. pp. 31–90.

63. Sasaki MS, Endo S, Hoshi M, Nomura T. Neutron relative biological effectiveness in Hiroshima and Nagasaki atomic bomb survivors: a critical review. J Radiat Res. 2016 Nov;57(6):583-595. Epub 2016 Sep 10. Review. PubMed PMID: 27614201; PubMed Central PMCID: PMC5137296.

64. Showler K, Nishimura M, Daino K, Imaoka T, Nishimura Y, Morioka T, Blyth BJ, Kokubo T, Takabatake M, Fukuda M, Moriyama H, Kakinuma S, Fukushi M, Shimada Y. Analysis of genes involved in the PI3K/Akt pathway in radiation- and MNU-induced rat mammary carcinomas. J Radiat Res. 2017 Mar 1;58(2):183-194. doi: 10.1093/jrr/rrw097. PubMed PMID: 27738081; PubMed Central PMCID: PMC5571612.

65. Rivina L, Schiestl R. Mouse models for efficacy testing of agents against radiation carcinogenesis—a literature review. Int J Environ Res Public Health. 2012 Dec 27;10(1):107-43. doi: 10.3390/ijerph10010107. Review. PubMed PMID: 23271302; PubMed Central PMCID: PMC3564133.

66. Imaoka T, Nishimura M, Iizuka D, Daino K, Takabatake T, Okamoto M, Kakinuma S, Shimada Y. Radiation-induced mammary carcinogenesis in rodent models: what's different from chemical carcinogenesis? J Radiat Res. 2009 Jul;50(4):281-93. Epub 2009 Jun 9. Review. PubMed PMID: 19506345.

67. Majer M, Knežević Z, Saveta M. Current trends in estimating risk of cancer from exposure to low doses of ionising radiation. Arh Hig Rada Toksikol. 2014 Sep 29;65(3):251-7. doi: 10.2478/10004-1254-65-2014-2425. Review. PubMed PMID: 25205689.

68. Vaiserman AM. Radiation hormesis: historical perspective and implications for low-dose cancer risk assessment. Dose Response. 2010 Jan 18;8(2):172-91. doi:10.2203/dose-response.09-037.Vaiserman. PubMed PMID: 20585444; PubMed Central PMCID: PMC2889502.

69. Evaluation of the Linear-Nonthreshold Dose-Response Model for Ionizing Radiation. Bethesda, MD: National Council on Radiation Protection and Measurement (NCRP); 2001. NCRP report no. 136.

70. The 2007 Recommendations of the International Commission on Radiological Protection. ICRP publication 103. Ann ICRP. 2007;37(2-4):1-332. PubMed PMID: 18082557.

71. United Nations Scientific Committee on the Effects of Atomic Radiation (UNSCEAR) 2000 Report: Sources and Effects of Ionizing Radiation—Annex I: Epidemiological Evaluation of Radiation-Induced Cancer. New York, New York: United Nations; 2000.

72. NCR, Health risks from exposures to low levels of ionizing radiation: BEIR VII Phase 2. National Research Council, Washington DC: National Academy Press; 2006.

73. Shah DJ, Sachs RK, Wilson DJ. Radiation-induced cancer: a modern view. Br J Radiol. 2012 Dec;85(1020):e1166-73. doi: 10.1259/bjr/25026140. Review. PubMed PMID: 23175483; PubMed Central PMCID: PMC3611719.

74. Brenner DJ, Doll R, Goodhead DT, Hall EJ, Land CE, Little JB, Lubin JH, Preston DL, Preston RJ, Puskin JS, Ron E, Sachs RK, Samet JM, Setlow RB, Zaider M. Cancer risks attributable to low doses of ionizing radiation: assessing what we really know. Proc Natl Acad Sci U S A. 2003 Nov 25;100(24):13761-6. Epub 2003 Nov 10. PubMed PMID: 14610281; PubMed Central PMCID: PMC283495.

75. Pawel D, Preston D, Pierce D, Cologne J. Improved estimates of cancer site-specific risks for a bomb survivors. Radiat Res 2008;169:87-98. doi: 10.1667/RR1092.1

76. Pierce DA, Preston DL. Radiation-related cancer risk at low doses among atomic bomb survivors. Radiat Res 2000;154:178-86. PMID: 10931690.

77. National Research Council Committee (NRCC). Health Risks from Exposure to Low Levels of Ionizing Radiation: Biological Effects of Ionizing Radiation BEIR VII Phase 2. Washington: National Academy of Sciences; 2006.

78. Ozasa K, Shimizu Y, Suyama A, Kasagi F, Soda M, Grant EJ, Sakata R, Sugiyama H, Kodama K. Studies of the mortality of atomic bomb survivors, Report 14, 1950-2003: an overview of cancer and noncancer diseases. Radiat Res. 2012 Mar;177(3):229-43. Epub 2011 Dec 15. Erratum in: Radiat Res. 2013 Apr;179(4):e40-1. PubMed PMID: 22171960.

79. Cahoon, E. K., Preston, D. L., Pierce, D. A., Grant, E., Brenner, A. V., Mabuchi, K., Utada, M., & Ozasa, K. (2017). Lung, Laryngeal and Other Respiratory Cancer Incidence among Japanese Atomic Bomb Survivors: An Updated Analysis from 1958 through 2009. Radiation research, 187(5), 538–548. https://doi.org/10.1667/RR14583.1.

80. Preston, D. L., Ron, E., Tokuoka, S., Funamoto, S., Nishi, N., Soda, M., Mabuchi, K., & Kodama, K. (2007). Solid cancer incidence in atomic bomb survivors: 1958-1998. Radiation research, 168(1), 1–64. https://doi.org/10.1667/RR0763.1

81. Muller HJ. ARTIFICIAL TRANSMUTATION OF THE GENE. Science. 1927 Jul 22;66(1699):84-7. PubMed PMID: 17802387.

82. A.R. Olson and G.N. Lewis. Natural reactivity and the origin of species. Nature, 121 (3052) (1928), pp. 673-674.

83. H.H. Dixon. Cosmic radiation and evolution. Nature, 123 (3113) (1929), p. 981.

84. Calabrese EJ, O'Connor MK. Estimating risk of low radiation doses - a critical

review of the BEIR VII report and its use of the linear no-threshold (LNT) hypothesis. Radiat Res. 2014 Nov;182(5):463-74. doi: 10.1667/RR13829.1. Epub 2014 Oct 20. Review. PubMed PMID: 25329961.

85. Tubiana M, Feinendegen LE, Yang C, Kaminski JM. The linear no-threshold relationship is inconsistent with radiation biologic and experimental data. Radiology. 2009 Apr;251(1):13-22. doi: 10.1148/radiol.2511080671. PubMed PMID: 19332842; PubMed Central PMCID: PMC2663584.

86. Baldwin J, Grantham V. Radiation Hormesis: Historical and Current Perspectives. J Nucl Med Technol. 2015 Dec;43(4):242-6. doi: 10.2967/jnmt.115.166074. Epub 2015 Nov 19. PubMed PMID: 26584616.

87. Hoel, D. G., & Li, P. (1998). Threshold models in radiation carcinogenesis. Health physics, 75(3), 241–250. https://doi.org/10.1097/00004032-199809000-00002.

88. Luckey T. D. (1986). Ionizing radiation promotes protozoan reproduction. Radiation research, 108(2), 215–221.

89. Li, W., Wang, G., Cui, J., Xue, L., & Cai, L. (2004). Low-dose radiation (LDR) induces hematopoietic hormesis: LDR-induced mobilization of hematopoietic progenitor cells into peripheral blood circulation. Experimental hematology, 32(11), 1088–1096. https://doi.org/10.1016/j.exphem.2004.07.015.

90. Ogawa Y. (2016). Paradigm Shift in Radiation Biology/Radiation Oncology-Exploitation of the "H_2O_2 Effect" for Radiotherapy Using Low-LET (Linear Energy Transfer) Radiation such as X-rays and High-Energy Electrons. *Cancers*, *8*(3), 28. https://doi.org/10.3390/cancers8030028.

91. Royal H. D. (2008). Effects of low level radiation-what's new? *Seminars in nuclear medicine*, *38*(5), 392–402. https://doi.org/10.1053/j.semnuclmed.2008.05.006

92. Mitsue Nakanishi, Kimio Tanaka, Takahiro Shintani, Tomoko Takahashi, Nanao Kamada, Chromosomal Instability in Acute Myelocytic Leukemia and Myelodysplastic Syndrome Patients among Atomic Bomb Survivors, *Journal of Radiation Research*, Volume 40, Issue 2, June 1999, Pages 159–167, https://doi.org/10.1269/jrr.40.159

93. Chauveinc, L, Gaboriaux, G, Dutrillaux, A M, Dutrillaux, B, Chauveinc, L, Ricoul, M, Sabatier, L, & Dutrillaux, B. Radiation-induced malignant tumours: a specific cytogenetic profile?. 1997, France.

94. Berrington de Gonzalez A, Iulian Apostoaei A, Veiga LH, Rajaraman P, Thomas BA, Owen Hoffman F, Gilbert E, Land C. RadRAT: a radiation risk assessment tool for lifetime cancer risk projection. J Radiol Prot. 2012 Sep;32(3):205-22. doi: 10.1088/0952-4746/32/3/205. Epub 2012 Jul 19. PubMed PMID: 22810503; PubMed Central PMCID: PMC3816370.

95. Analytica 4.1. Lumina Decisions Systems, Inc.; Los Gatos, CA: 2008.

96. https://radiationcalculators.cancer.gov/radrat/about/.

97. Fisher DR, Fahey FH. Appropriate Use of Effective Dose in Radiation Protection and Risk Assessment. Health Phys. 2017 Aug;113(2):102-109. doi: 10.1097/HP.0000000000000674. PubMed PMID: 28658055; PubMed Central PMCID: PMC5878049.

98. International Commission on Radiation Units and Measurements. Report 85: Fundamental quantities and units for ionizing radiation. J ICRU. 2011 Apr;11(1):1-31. doi: 10.1093/jicru/ndr011. PubMed PMID: 24174259.

99. Mettler FA Jr, Huda W, Yoshizumi TT, Mahesh M. Effective doses in radiology and diagnostic nuclear medicine: a catalog. Radiology. 2008 Jul;248(1):254-63. doi: 10.1148/radiol.2481071451. Review. PubMed PMID: 18566177.

100. Hemke R, Yang K, Husseini J, Bredella MA, Simeone FJ. Organ dose and total effective dose of whole-body CT in multiple myeloma patients. Skeletal Radiol. 2019 Oct 15. doi: 10.1007/s00256-019-03292-z. [Epub ahead of print] PubMed PMID: 31612246.

101. Rao R, Browne D, Lunt B, Perry D, Reed P, Kelly P. Radiation doses in diagnostic imaging for suspected physical abuse. Arch Dis Child. 2019 Sep;104(9):863-868. doi: 10.1136/archdischild-2018-316286. Epub 2019 Apr 17. PubMed PMID: 30995983.

102. Hrubec Z, Boice JD Jr, Monson RR, Rosenstein M. Breast cancer after multiple chest fluoroscopies: second follow-up of Massachusetts women with tuberculosis. Cancer Res. 1989 Jan 1;49(1):229-34. PubMed PMID: 2908849.

103. Berrington de González A, Darby S. Risk of cancer from diagnostic X-rays: estimates for the UK and 14 other countries. Lancet. 2004 Jan 31;363(9406):345-51. PubMed PMID: 15070562.

104. Ronckers CM, Land CE, Miller JS, Stovall M, Lonstein JE, Doody MM. Cancer mortality among women frequently exposed to radiographic examinations for spinal disorders. Radiat Res. 2010 Jul;174(1):83-90. doi: 10.1667/RR2022.1. PubMed PMID: 20681802; PubMed Central PMCID: PMC3982592.

105. Pignol JP, Keller BM, Ravi A. Doses to internal organs for various breast radiation techniques--implications on the risk of secondary cancers and

cardiomyopathy. Radiat Oncol. 2011 Jan 14;6:5. doi: 10.1186/1748-717X-6-5. PubMed PMID: 21235766; PubMed Central PMCID: PMC3027128.

106. Brenner DJ, Shuryak I, Einstein AJ. Impact of reduced patient life expectancy on potential cancer risks from radiologic imaging. Radiology. 2011 Oct;261(1):193-8. doi: 10.1148/radiol.11102452. Epub 2011 Jul 19. PubMed PMID: 21771956.

107. Munley MT, Moore JE, Walb MC, Isom SP, Olson JD, Zora JG, Kock ND, Wheeler KT, Miller MS. Cancer-prone mice expressing the Ki-rasG12C gene show increased lung carcinogenesis after CT screening exposures. Radiat Res. 2011 Dec;176(6):842-8. Epub 2011 Sep 30. PubMed PMID: 21962004; PubMed Central PMCID: PMC3244170.

108. National Lung Screening Trial Research Team, Aberle DR, Berg CD, Black WC, Church TR, Fagerstrom RM, Galen B, Gareen IF, Gatsonis C, Goldin J, Gohagan JK, Hillman B, Jaffe C, Kramer BS, Lynch D, Marcus PM, Schnall M, Sullivan DC, Sullivan D, Zylak CJ. The National Lung Screening Trial: overview and study design. Radiology. 2011 Jan;258(1):243-53. doi: 10.1148/radiol.10091808. Epub 2010 Nov 2. PubMed PMID: 21045183; PubMed Central PMCID: PMC3009383.

109. Mascalchi M, Mazzoni LN, Falchini M, Belli G, Picozzi G, Merlini V, Vella A, Diciotti S, Falaschi F, Lopes Pegna A, Paci E. Dose exposure in the ITALUNG trial of lung cancer screening with low-dose CT. Br J Radiol. 2012 Aug;85(1016):1134-9. doi: 10.1259/bjr/20711289. Epub 2011 Oct 5. PubMed PMID: 21976631; PubMed Central PMCID: PMC3587091.

110. Ng J, Shuryak I, Xu Y, Clifford Chao KS, Brenner DJ, Burri RJ. Predicting the

risk of secondary lung malignancies associated with whole-breast radiation therapy. Int J Radiat Oncol Biol Phys. 2012 Jul 15;83(4):1101-6. doi: 10.1016/j.ijrobp.2011.09.052. Epub 2012 Jan 13. PubMed PMID: 22245205; PubMed Central PMCID: PMC4005006.

111. Hung MC, Hwang JJ. Cancer risk from medical radiation procedures for coronary artery disease: a nationwide population-based cohort study. Asian Pac J Cancer Prev. 2013;14(5):2783-7. PubMed PMID: 23803032.

112. Rampinelli C, De Marco P, Origgi D, Maisonneuve P, Casiraghi M, Veronesi G, Spaggiari L, Bellomi M. Exposure to low dose computed tomography for lung cancer screening and risk of cancer: secondary analysis of trial data and risk-benefit analysis. BMJ. 2017 Feb 8;356:j347. doi: 10.1136/bmj.j347. PubMed PMID: 28179230; PubMed Central PMCID: PMC5421449.

113. Mendes BM, Trindade BM, Fonseca TCF, de Campos TPR. Assessment of radiation-induced secondary cancer risk in the Brazilian population from left-sided breast-3D-CRT using MCNPX. Br J Radiol. 2017 Dec;90(1080):20170187. doi: 10.1259/bjr.20170187. Epub 2017 Oct 27. PubMed PMID: 28937271; PubMed Central PMCID: PMC6047661.

114. Berris T, Mazonakis M, Stratakis J, Tzedakis A, Fasoulaki A, Damilakis J. Calculation of organ doses from breast cancer radiotherapy: a Monte Carlo study. J Appl Clin Med Phys. 2013 Jan 7;14(1):4029. doi: 10.1120/jacmp.v14i1.4029. PubMed PMID: 23318389; PubMed Central PMCID: PMC5713920.

115. Yang C, Liu R, Ming X, Liu N, Guan Y, Feng Y. Thoracic Organ Doses and Cancer Risk from Low Pitch Helical 4-Dimensional Computed Tomography Scans.

Biomed Res Int. 2018 Sep 24;2018:8927290. doi: 10.1155/2018/8927290. eCollection 2018.

PubMed PMID: 30345309; PubMed Central PMCID: PMC6174794.

116. Gladdy RA, Qin LX, Moraco N, Edgar MA, Antonescu CR, Alektiar KM, Brennan MF, Singer S. Do radiation-associated soft tissue sarcomas have the same prognosis as sporadic soft tissue sarcomas? J Clin Oncol. 2010 Apr 20;28(12):2064-9. doi:10.1200/JCO.2009.25.1728. Epub 2010 Mar 22. PubMed PMID: 20308666; PubMed Central PMCID: PMC3651600.

117. Cha C, Antonescu CR, Quan ML, Maru S, Brennan MF. Long-term results with resection of radiation-induced soft tissue sarcomas. Ann Surg. 2004 Jun;239(6):903-9; discussion 909-10. PubMed PMID: 15166970; PubMed Central PMCID: PMC1356299.

118. Shibahara D, Furugen M, Kasashima S, Kaneku K, Yamashiro T, Arakaki W, Ariga T, Atsumi E, Aoyama H, Matsumoto H, Maehara H, Fujita J. Radiation-induced sarcoma in a 10-year survivor with stage IV EGFR-mutated lung adenocarcinoma. Respir Med Case Rep. 2019 Jun 18;28:100889. doi: 10.1016/j.rmcr.2019.100889. eCollection 2019. PubMed PMID: 31304084; PubMed Central PMCID: PMC6604042.

119. Haciislamoglu E, Cinar Y, Gurcan F, Canyilmaz E, Gungor G, Yoney A. Secondary cancer risk after whole-breast radiation therapy: field-in-field versus intensity modulated radiation therapy versus volumetric modulated arc therapy. Br J Radiol. 2019 Oct;92(1102):20190317. doi: 10.1259/bjr.20190317. Epub 2019 Jul 22. PubMed PMID: 31295011; PubMed Central PMCID: PMC6774602.

120. Kourinou KM, Mazonakis M, Lyraraki E, Papadaki HA, Damilakis J. Probability of carcinogenesis due to involved field and involved site radiation therapy techniques for supra- and infradiaphragmatic Hodgkin's disease. Phys Med. 2019 Jan;57:100-106. doi: 10.1016/j.ejmp.2018.12.036. Epub 2019 Jan 3. PubMed PMID: 30738513.

121. Specht L, Yahalom J, Illidge T, Berthelsen AK, Constine LS, Eich HT, Girinsky T, Hoppe RT, Mauch P, Mikhaeel NG, Ng A; ILROG. Modern radiation therapy for Hodgkin lymphoma: field and dose guidelines from the international lymphoma radiation oncology group (ILROG). Int J Radiat Oncol Biol Phys. 2014 Jul 15;89(4):854-62. doi: 10.1016/j.ijrobp.2013.05.005. Epub 2013 Jun 18. PubMed PMID: 23790512.

122. Journy N, Dreuil S, Rage E, De Zordo-Banliat F, Bonnet D, Hascoët S, Malekzadeh-Milani S, Petit J, Laurier D, Bernier MO, Baysson H. Projected Future Cancer Risks in Children Treated With Fluoroscopy-Guided Cardiac Catheterization Procedures. Circ Cardiovasc Interv. 2018 Nov;11(11):e006765. doi: 10.1161/CIRCINTERVENTIONS.118.006765. PubMed PMID: 30571202.

123. Marant-Micallef C, Shield KD, Vignat J, Cléro E, Kesminiene A, Hill C, Rogel A, Vacquier B, Bray F, Laurier D, Soerjomataram I. The risk of cancer attributable to diagnostic medical radiation: Estimation for France in 2015. Int J Cancer. 2019 Jun 15;144(12):2954-2963. doi: 10.1002/ijc.32048. Epub 2019 Jan 15. PubMed PMID: 30537057.

124. Simonetto C, Rennau H, Remmele J, Sebb S, Kundrát P, Eidemüller M, Wolf U, Hildebrandt G. Exposure of remote organs and associated cancer risks from

tangential and multi-field breast cancer radiotherapy. Strahlenther Onkol. 2019 Jan;195(1):32-42. doi: 10.1007/s00066-018-1384-1. Epub 2018 Oct 22. PubMed PMID: 30350118.

125. Hoekstra N, Fleury E, Merino Lara TR, van der Baan P, Bahnerth A, Struik G, Hoogeman M, Pignol JP. Long-term risks of secondary cancer for various whole and partial breast irradiation techniques. Radiother Oncol. 2018 Sep;128(3):428-433. doi: 10.1016/j.radonc.2018.05.032. Epub 2018 Jun 18. PubMed PMID: 29914648.

126. Fogliata A, De Rose F, Franceschini D, Stravato A, Seppälä J, Scorsetti M, Cozzi L. Critical Appraisal of the Risk of Secondary Cancer Induction From Breast Radiation Therapy With Volumetric Modulated Arc Therapy Relative to 3D Conformal Therapy. Int J Radiat Oncol Biol Phys. 2018 Mar 1;100(3):785-793. doi: 10.1016/j.ijrobp.2017.10.040. Epub 2017 Oct 31. PubMed PMID: 29249528.

127. Mazonakis M, Lyraraki E, Tzedakis A, Damilakis J. Radiotherapy for non-malignant shoulder syndrome: Is there a risk for radiation-induced carcinogenesis? Phys Med. 2017 Nov;43:73-78. doi: 10.1016/j.ejmp.2017.10.021. Epub 2017 Nov 2. PubMed PMID: 29195566.

128. Perisinakis K, Seimenis I, Tzedakis A, Karantanas A, Damilakis J. Radiation burden and associated cancer risk for a typical population to be screened for lung cancer with low-dose CT: A phantom study. Eur Radiol. 2018 Oct;28(10):4370-4378. doi: 10.1007/s00330-018-5373-7. Epub 2018 Apr 12. PubMed PMID: 29651767.

129. Chao PJ, Lee HF, Lan JH, Guo SS, Ting HM, Huang YJ, Chen HC, Lee TF. Propensity-score-matched evaluation of the incidence of radiation pneumonitis and

secondary cancer risk for breast cancer patients treated with IMRT/VMAT. Sci Rep. 2017 Oct 23;7(1):13771. doi: 10.1038/s41598-017-14145-x. PubMed PMID: 29062118; PubMed Central PMCID: PMC5653804.

130. Corradini S, Ballhausen H, Weingandt H, Freislederer P, Schönecker S, Niyazi M, Simonetto C, Eidemüller M, Ganswindt U, Belka C. Left-sided breast cancer and risks of secondary lung cancer and ischemic heart disease : Effects of modern radiotherapy techniques. Strahlenther Onkol. 2018 Mar;194(3):196-205. doi: 10.1007/s00066-017-1213-y. Epub 2017 Sep 15. Erratum in: Strahlenther Onkol. 2018 Mar;194(3):273-274. PubMed PMID: 28916844.

131. Vogel J, Lin L, Litzky LA, Berman AT, Simone CB 2nd. Predicted Rate of Secondary Malignancies Following Adjuvant Proton Versus Photon Radiation Therapy for Thymoma. Int J Radiat Oncol Biol Phys. 2017 Oct 1;99(2):427-433. doi: 10.1016/j.ijrobp.2017.04.022. Epub 2017 Apr 24. PubMed PMID: 28871993.

132. Mazonakis M, Lyraraki E, Damilakis J. Second cancer risk assessments after involved-site radiotherapy for mediastinal Hodgkin lymphoma. Med Phys. 2017 Jul;44(7):3866-3874. doi: 10.1002/mp.12327. Epub 2017 Jun 9. PubMed PMID: 28493609.

133. Rintoul RC, Atherton R, Tweed K, Yates S, Chilvers ER. Exposure of patients to ionising radiation during lung cancer diagnostic work-up. Thorax. 2017 Sep;72(9):853-855. doi: 10.1136/thoraxjnl-2016-209641. Epub 2017 Apr 25. PubMed PMID: 28442554.

134. Taylor C, Correa C, Duane FK, Aznar MC, Anderson SJ, Bergh J, Dodwell D, Ewertz M, Gray R, Jagsi R, Pierce L, Pritchard KI, Swain S, Wang Z, Wang Y,

Whelan T, Peto R, McGale P; Early Breast Cancer Trialists' Collaborative Group. Estimating the Risks of Breast Cancer Radiotherapy: Evidence From Modern Radiation Doses to the Lungs and Heart and From Previous Randomized Trials. J Clin Oncol. 2017 May 20;35(15):1641-1649. doi: 10.1200/JCO.2016.72.0722. Epub 2017 Mar 20. PubMed PMID: 28319436; PubMed Central PMCID: PMC5548226.

135. Huda W, Schoepf UJ, Abro JA, Mah E, Costello P. Radiation-related cancer risks in a clinical patient population undergoing cardiac CT. AJR Am J Roentgenol. 2011 Feb;196(2):W159-65. doi: 10.2214/AJR.10.4981. PubMed PMID: 21257857.

136. Berrington de Gonzalez A, Gilbert E, Curtis R, Inskip P, Kleinerman R, Morton L, Rajaraman P, Little MP. Second solid cancers after radiation therapy: a systematic review of the epidemiologic studies of the radiation dose-response relationship. Int J Radiat Oncol Biol Phys. 2013 Jun 1;86(2):224-33. doi: 10.1016/j.ijrobp.2012.09.001. Epub 2012 Oct 24. Review. PubMed PMID: 23102695; PubMed Central PMCID: PMC3816386.

137. Okajima K, Ishikawa K, Matsuura T, Tatebe H, Fujiwara K, Hiroi K, Hasegawa H, Nishimura Y. Multiple primary malignancies in patients with prostate cancer: increased risk of secondary malignancies after radiotherapy. Int J Clin Oncol. 2013 Dec;18(6):1078-84. doi: 10.1007/s10147-012-0496-3. Epub 2012 Nov 20. PubMed PMID: 23179638.

138. Stokkevåg CH, Engeseth GM, Ytre-Hauge KS, Röhrich D, Odland OH, Muren LP, Brydøy M, Hysing LB, Szostak A, Palmer MB, Petersen JB. Estimated risk of radiation-induced cancer following paediatric cranio-spinal irradiation with electron, photon and proton therapy. Acta Oncol. 2014 Aug;53(8):1048-57. doi:

10.3109/0284186X.2014.928420. Epub 2014 Jul 14. PubMed PMID: 25017376.

139. Moskowitz CS, Chou JF, Wolden SL, Bernstein JL, Malhotra J, Novetsky Friedman D, Mubdi NZ, Leisenring WM, Stovall M, Hammond S, Smith SA, Henderson TO, Boice JD, Hudson MM, Diller LR, Bhatia S, Kenney LB, Neglia JP, Begg CB, Robison LL, Oeffinger KC. Breast cancer after chest radiation therapy for childhood cancer. J Clin Oncol. 2014 Jul 20;32(21):2217-23. doi: 10.1200/JCO.2013.54.4601. Epub 2014 Apr 21. PubMed PMID: 24752044; PubMed Central PMCID: PMC4100937.

140. Berrington de González A, Kim KP, Berg CD. Low-dose lung computed tomography screening before age 55: estimates of the mortality reduction required to outweigh the radiation-induced cancer risk. J Med Screen. 2008;15(3):153-8. doi: 10.1258/jms.2008.008052. PubMed PMID: 18927099; PubMed Central PMCID: PMC2782431.

141. Kim DW, Chung WK, Shin D, Hong S, Park SH, Park SY, Chung K, Lim YK, Shin D, Lee SB, Lee HH, Yoon M. Risk of second cancer from scattered radiation of intensity-modulated radiotherapies with lung cancer. Radiat Oncol. 2013 Mar 4;8:47. doi: 10.1186/1748-717X-8-47. PubMed PMID: 23452670; PubMed Central PMCID: PMC3599921.

142. Zhou L, Bai S, Zhang Y, Ming X, Zhang Y, Deng J. Imaging Dose, Cancer Risk and Cost Analysis in Image-guided Radiotherapy of Cancers. Sci Rep. 2018 Jul 4;8(1):10076. doi: 10.1038/s41598-018-28431-9. PubMed PMID: 29973695; PubMed Central PMCID: PMC6031630.

143. Almagro-Casado E, Sánchez A, Cantos B, Salas C, Pérez-Callejo D, Provencio M. Lung cancer and other second neoplasms after treatment of Hodgkin lymphoma. Clin

Transl Oncol. 2016 Jan;18(1):99-106. doi: 10.1007/s12094-015-1342-7. Epub 2015 Nov 3. PubMed PMID: 26530956.

144. Grantzau T, Mellemkjær L, Overgaard J. Second primary cancers after adjuvant radiotherapy in early breast cancer patients: a national population based study under the Danish Breast Cancer Cooperative Group (DBCG). Radiother Oncol. 2013 Jan;106(1):42-9. doi: 10.1016/j.radonc.2013.01.002. Epub 2013 Feb 8. PubMed PMID: 23395067.

145. Valuckas KP, Atkocius V, Kuzmickiene I, Aleknavicius E, Liukpetryte S, Ostapenko V. Second malignancies following conventional or combined ²□²Cf neutron brachytherapy with external beam radiotherapy for breast cancer. J Radiat Res. 2013 Sep;54(5):872-9. doi: 10.1093/jrr/rrt009. Epub 2013 Feb 7. PubMed PMID: 23397075; PubMed Central PMCID: PMC3766283.

146. Han C, Schultheiss TE, Wong JYC. Estimation of radiation-induced secondary cancer risks for early-stage non-small cell lung cancer patients after stereotactic body radiation therapy. Pract Radiat Oncol. 2017 May - Jun;7(3):e185-e194. doi: 10.1016/j.prro.2016.10.009. Epub 2016 Oct 19. PubMed PMID: 28089479.

147. Li, J., Wu, D. M., Han, R., Yu, Y., Deng, S. H., Liu, T., Zhang, T., & Xu, Y. (2020). Low-Dose Radiation Promotes Invasion and Migration of A549 Cells by Activating the CXCL1/NF-κB Signaling Pathway. OncoTargets and therapy, 13, 3619– 3629. https://doi.org/10.2147/OTT.S243914

148. Liu, Q., Li, H., You, L., Li, T., Li, L., Zhou, P., Bo, X., Chen, H., Chen, X., & Hu, Y. (2019). Genome-wide identification and analysis of A-to-I RNA editing events in

the malignantly transformed cell lines from bronchial epithelial cell line induced by α-particles radiation. PloS one, 14(6), e0213047. https://doi.org/10.1371/journal.pone.0213047

149. Weaver, D. A., Hei, T. K., Hukku, B., McRaven, J. A., & Willey, J. C. (1997). Cytogenetic and molecular genetic analysis of tumorigenic human bronchial epithelial cells induced by radon alpha particles. Carcinogenesis, 18(6), 1251–1257. https://doi.org/10.1093/carcin/18.6.1251

150. Zhao YL, Piao CQ, Hall EJ, Hei TK. Mechanisms of radiation-induced neoplastic transformation of human bronchial epithelial cells. Radiat Res. 2001;155(1 Pt 2):230‐234. doi:10.1667/0033-7587(2001)155[0230:morint]2.0.co;2

151. Piao, C. Q., & Hei, T. K. (2001). Gene amplification and microsatellite instability induced in tumorigenic human bronchial epithelial cells by alpha particles and heavy ions. Radiation research, 155(1 Pt 2), 263–267. https://doi.org/10.1667/0033-7587(2001)155[0263:gaamii]2.0.co;2

152. Sun, J. F., Sui, J. L., Zhou, P. K., Geng, Y., Hu, Y. C., Cao, Z. S., Ge, S. L., Lou, T. Z., & Wu, D. C. (2002). Decreased efficiency of gamma-ray-induced DNA double-strand break rejoining in malignant transformants of human bronchial epithelial cells generated by alpha-particle exposure. International journal of radiation biology, 78(9), 773–780. https://doi.org/10.1080/09553000210141441

153. Smith-Bindman R, Miglioretti DL, Larson EB. Rising use of diagnostic medical imaging in a large integrated health system. Health Aff (Millwood). 2008 Nov-Dec;27(6):1491-502. doi: 10.1377/hlthaff.27.6.1491. PubMed PMID: 18997204; PubMed Central PMCID: PMC2765780.

154. Korreman SS. Image-guided radiotherapy and motion management in lung cancer. Br J Radiol. 2015 Jul;88(1051):20150100. doi: 10.1259/bjr.20150100. Epub 2015 May 8. Review. PubMed PMID: 25955231; PubMed Central PMCID: PMC4628536.

155. McPartlin AJ, Li XA, Kershaw LE, Heide U, Kerkmeijer L, Lawton C, Mahmood U, Pos F, van As N, van Herk M, Vesprini D, van der Voort van Zyp J, Tree A, Choudhury A;MR-Linac consortium. MRI-guided prostate adaptive radiotherapy – A systematic review. Radiother Oncol. 2016 Jun;119(3):371-80. doi: 10.1016/j.radonc.2016.04.014. Epub 2016 May 6. Review. PubMed PMID: 27162159.

156. Lou Y, Dholaria B, Soyano A, Hodge D, Cochuyt J, Manochakian R, Ko SJ, Thomas M, Johnson MM, Patel NM, Miller RC, Adjei AA, Ailawadhi S. Survival trends among non-small-cell lung cancer patients over a decade: impact of initial therapy at academic centers. Cancer Med. 2018 Oct;7(10):4932-4942. doi: 10.1002/cam4.1749. Epub 2018 Sep 2. PubMed PMID: 30175515; PubMed Central PMCID: PMC6198232.

157. Wrona A. Role of immunotherapy in stage III nonsmall cell lung cancer. Curr Opin Oncol. 2019 Jan;31(1):18-23. doi: 10.1097/CCO.0000000000000493. PubMed PMID: 30489337.

158. Mazonakis M, Damilakis J. Cancer risk after radiotherapy for benign diseases. Phys Med. 2017 Oct;42:285-291. doi: 10.1016/j.ejmp.2017.01.014. Epub 2017 Feb 8. Review. PubMed PMID: 28189418.

159. Trott KR, Kamprad F. Estimation of cancer risks from radiotherapy of benign diseases. Strahlenther Onkol. 2006 Aug;182(8):431-6. Review. PubMed PMID: 16896588.

160. Lee WJ, Choi Y, Ko S, Cha ES, Kim J, Kim YM, Kong KA, Seo S, Bang YJ, Ha YW. Projected lifetime cancer risks from occupational radiation exposure among diagnostic medical radiation workers in South Korea. BMC Cancer. 2018 Dec 4;18(1):1206. doi: 10.1186/s12885-018-5107-x. PubMed PMID: 30514249; PubMed Central PMCID: PMC6278159.

161. Khosroabadi M, Haeri SA, Moghaddam HR, Mirdoraghi M. Data on excessive risk of cancer from gamma radiation in residents of Bojnurd city. Data Brief. 2018 Oct 23;21:790-794. doi: 10.1016/j.dib.2018.10.052. eCollection 2018 Dec. PubMed PMID: 30417041; PubMed Central PMCID: PMC6216078.

162. Bernier MO, Baysson H, Pearce MS, Moissonnier M, Cardis E, Hauptmann M, Struelens L, Dabin J, Johansen C, Journy N, Laurier D, Blettner M, Le Cornet L, Pokora R, Gradowska P, Meulepas JM, Kjaerheim K, Istad T, Olerud H, Sovik A, Bosch de Basea M, Thierry-Chef I, Kaijser M, Nordenskjöld A, Berrington de Gonzalez A, Harbron RW, Kesminiene A. Cohort Profile: the EPI-CT study: A European pooled epidemiological study to quantify the risk of radiation-induced cancer from paediatric CT. Int J Epidemiol. 2018 Nov 2. doi: 10.1093/ije/dyy231. [Epub ahead of print] PubMed PMID: 30388267.

163. Péus D, Newcomb N, Hofer S. Appraisal of the Karnowski Performance Status and proposal of a simple algorithmic system for its evaluation. BMC Med Inform Decis Mak. 2013 Jul 19;13:72. doi: 10.1186/1472-6947-13-72. PubMed PMID: 23870327; PubMed Central PMCID: PMC3722041.

164. Power Analysis and Sample Size Software (2018). NCSS, LLC. Kaysville, Utah, USA, ncss.com/software/pass.

165. Maquilan G, Timmerman R. Stereotactic Body Radiation Therapy for Early- Stage Lung Cancer. Cancer J. 2016 Jul-Aug;22(4):274-9. doi: 10.1097/PPO.0000000000000204. Review. PubMed PMID: 27441747.

166. Zavala, V. A., Bracci, P. M., Carethers, J. M., Carvajal-Carmona, L., Coggins, N. B., Cruz-Correa, M. R., Davis, M., de Smith, A. J., Dutil, J., Figueiredo, J. C., Fox, R., Graves, K. D., Gomez, S. L., Llera, A., Neuhausen, S. L., Newman, L., Nguyen, T., Palmer, J. R., Palmer, N. R., Pérez-Stable, E. J., … Fejerman, L. (2020). Cancer health disparities in racial/ethnic minorities in the United States. *British journal of cancer*, 10.1038/s41416-020-01038-6. Advance online publication. https://doi.org/10.1038/s41416-020-01038-6

167. Steele CB, Li J, Huang B, Weir HK. Prostate cancer survival in the United States by race and stage (2001-2009): Findings from the CONCORD-2 study. Cancer. 2017 Dec 15;123 Suppl 24:5160-5177. doi: 10.1002/cncr.31026. PubMed PMID: 29205313; PubMed Central PMCID: PMC6077841.

168. Thomas A, Rhoads A, Pinkerton E, Schroeder MC, Conway KM, Hundley WG, McNally LR, Oleson J, Lynch CF, Romitti PA. Incidence and Survival Among Young Women With Stage I-III Breast Cancer: SEER 2000-2015. JNCI Cancer Spectr. 2019 Jun 7;3(3):pkz040. doi: 10.1093/jncics/pkz040. eCollection 2019 Sep. PubMed PMID: 31392297; PubMed Central PMCID: PMC6668585.

169. Mayerhoefer ME, Prosch H, Beer L, Tamandl D, Beyer T, Hoeller C, Berzaczy D, Raderer M, Preusser M, Hochmair M, Kiesewetter B, Scheuba C, Ba-Ssalamah A, Karanikas G, Kesselbacher J, Prager G, Dieckmann K, Polterauer S, Weber M, Rausch I, Brauner B, Eidherr H, Wadsak W, Haug AR. PET/MRI versus PET/CT in oncology: a

prospective single-center study of 330 examinations focusing on implications for patient management and cost considerations. Eur J Nucl Med Mol Imaging. 2020 Jan;47(1):51-60. doi: 10.1007/s00259-019-04452-y. Epub 2019 Aug 13. PubMed PMID: 31410538; PubMed Central PMCID: PMC6885019.

170. Rai R, Kumar S, Batumalai V, Elwadia D, Ohanessian L, Juresic E, Cassapi L, Vinod SK, Holloway L, Keall PJ, Liney GP. The integration of MRI in radiation therapy: collaboration of radiographers and radiation therapists. J Med Radiat Sci. 2017 Mar;64(1):61-68. doi: 10.1002/jmrs.225. Epub 2017 Feb 16. PubMed PMID: 28211218; PubMed Central PMCID: PMC5355372.

171. Kirchner J, Sawicki LM, Nensa F, Schaarschmidt BM, Reis H, Ingenwerth M, Bogner S, Aigner C, Buchbender C, Umutlu L, Antoch G, Herrmann K, Heusch P. Prospective comparison of (18)F-FDG PET/MRI and (18)F-FDG PET/CT for thoracic staging of non-small cell lung cancer. Eur J Nucl Med Mol Imaging. 2019 Feb;46(2):437-445. doi: 10.1007/s00259-018-4109-x. Epub 2018 Aug 3. PubMed PMID: 30074073.

172. Fendler WP, Czernin J, Herrmann K, Beyer T. Variations in PET/MRI Operations: Results from an International Survey Among 39 Active Sites. J Nucl Med. 2016 Dec;57(12):2016-2021. Epub 2016 Aug 11. PubMed PMID: 27516448; PubMed Central PMCID: PMC5135589.

Table 5: Select studies of radiation-induced cancers from medical imaging.

Reference	Study	RIC Site	RIC risk	Comments
Hrubec Z et al. 1989	X-rays in TB patients	breast	86% higher risk vs unexposed	Relationship linear up to 4Gy
Berrington de González A et al. 2004	Diagnostic imaging	Multiple sites	Attributable risk 0.6-1.8%	Bladder most common in men and colon most common in women
Ronckers CM et al. 2010	Spine imaging	Breast, lung, liver, cervical	Excess absolute risk (EAR) was 18.8 deaths/10,000 woman-years,	Breast cancer mortality was elevated (significant) while lung, liver, cervix lower (ns)

			-0.6 deaths/10,000 EAR for lung	
Pignol JP et al. 2011	Comparison of 5 radiation techniques for breast cancer	Breast and lung	Overall, risk of breast RIC was 0.2%/Sv and 0.85%/Sv for lung RIC	Breast IMRT good for EBRT and 3D-CRT better than iridium for partial breast techniques.
Huda W et al. 2011	Risks in patients undergoing cardiac CT angiography	Lung and breast	Median cancer risk induction 0.065% in men and 0.17% in women	Lung cancer RIC was the dominant risk in both genders, RIC breast significant in women
Brenner DJ et al. 2011	CT exams in cardiac disease as well as CT exams for surveillance	Lung cancer	Risk reduction if patients scanned later in life	
Mascalchi M et al. 2012	ITALUNG screening trial	Lung cancer	RIC risk was 0.12-0.33/1000 subjects	Low-risk with LDCT screening
Ng J et al. 2012	RT for breast cancer	Lung cancer	Prone patients associated with lower risk of RIC	
Hung MC et al. 2013	Cardiac imaging for CAD	Lung, breast and other cancers	Increased risk of breast cancer with imaging for CAD	Multiple procedures increase risk
Rampinelli C et al. 2017	Screening trial (COSMOS study)	Lung cancer	RIC risk is 0.05%	Lifetime attributable Risk in women 4 times higher than men
Mendes BM et al. 2017	MCPNx based RIC risk assessment in breast RT	Multiple cancers	RIC risk 2.2% and risk was highest in contralateral breast	Risk highest in young patients and lower in older patients.

Yang C et al. 2018	4D versus 3D scan RIC risk	Lung/thoracic cancers	Relative risk higher in 4D-CT scans versus 3D scans	
Kourinou KM et al. 2019	HD, IFRT versus ISRT	Multiple cancers	IFRT risk 0.5-8.2% vs ISRT 0.5-5.19%	ISRT resulted in reduced RIC risk
Journy N et al. 2018	CCP in children for heart conditions	Lung and breast	RIC 0.4% in boys and 2.2% in girls	Lung cancer is the dominant RIC in boys and breast cancer in girls.
Marant-Micallef C et al. 2019	French study to estimate RIC risk from all imaging	Multiple cancers	RIC risk is 0.7% of all new cancer cases	Risk small compared to benefit
Simonetto C et al. 2019	RIC risk with various RT techniques in breast cancer RT treatment	Multiple cancers	For 3D-CRT, Relative risk 1.4, Higher RR with IMRT for c/l breast	Risk of liver, uterus, pancreas RIC comparable and low in the two techniques
Hoekstra N et al. 2018	RIC risk with various RT techniques to treat breast cancer such as APBI, 3D.	Multiple cancers	Whole breast technique and VMAT technique increased RIC lung cancer	Risk of RIC of thyroid, c/l breast, ovaries, uterus close to baseline
Fogliata A et al. 2018	RIC risk with various RT techniques in treatment of breast cancer	Breast cancer	VMAT_full technique has the highest risk of RIC	
Mazonakis M et al. 2017	Modeling study to assess RIC risk in non-malignant clinical situation, shoulder syndrome undergoing radiation	Multiple cancers	Lifetime risk of RIC in a 50y male 0.00024-0.00027% and in a female is 0.00014-0.00028%	Risk of RIC lung cancer using a non-linear model 0.11-0.16% and risk of 0.12-0.18% using a linear model.
Perisinakis K et al. 2018	RIC risk from LDCT use in lung cancer screening	Lung cancer as well as other cancers	Cumulative LAR risk increases	For females, the cumulative risk increases from

			from baseline 0.11% to 0.27%	0.13% baseline to 0.30%.
Vogel J et al. 2017	RIC risk comparison between photons and protons in treatment of thymic tumors	Multiple cancers	Significantly higher risk with photons versus protons. 17.3 excess RIC/10,000 per year with photons versus 2.8 excess/10,000 per year with protons	5 excess second cancers could be avoided per 100 patients treated with protons
Mazonakis M et al. 2017	RIC risk in treatment for HL with ISRT versus IFRT	Lung, breast and esophagus cancer	ISRT resulted in lower risk of Lung and Breast cancer versus IFRT	No difference between ISRT and IFRT for esophagus cancer risk.
Rintoul RC et al. 2017	RIC risk from diagnostic imaging during management of lung cancer receiving curative treatment	Lung cancer and other secondary cancers.	LAR from diagnostic imaging was 0.059%	Lung specific risk was 0.019%
Okajima K et al. 2013	RIC risk in patients undergoing curative radiation for prostate cancer	Multiple cancers	Higher risk of RIC of ureter cancer, malignant lymphoma	Higher risk in bladder cancer not statistically significant.
Stokkevåg CH et al. 2014	RIC risk in children undergoing cranio-spinal radiation for	Multiple cancers	Protons had the best RIC risk profile although IMPT had a slightly higher	Electron treatment had the highest RIC risk in lung.

	CNS malignancies with photons or protons, electrons		risk of the two proton techniques	
Han C et al. 2017	RIC risk from SBRT treatment for lung cancer	Lung and breast cancer	EAR estimate for lung RIC 15.7±5.3 to 16.0±6.5/10,000 patients per year	RIC risk for breast cancer 18.0 ± 14.0 to 21.0 ± 15.0 / 10,000 patients per year.

Ns: non-significant, Sv: sievert, IMRT: intensity-modulated radiation therapy, RIC: radiation-induced cancer, 3D-CRT: 3-dimensional conformal radiation therapy, EAR: excess absolute risk, Gy: gray, LDCT: low-dose CT scan, CAD: coronary artery disease, 4D-CT: 4-dimensional CT scan, 3D-CT: 3-dimensional CT scan, HD: Hodgkin's disease, IFRT: Involved field radiation therapy, ISRT: Involved site radiation therapy, CCP: Cardiac catheterization procedures, c/l: contralateral, LDCT: low-dose CT, HL: Hodgkin's lymphoma, ISRT: involved site radiation therapy, IFRT: involved-field radiation therapy, LAR: Lifetime attributable risk, CNS: central nervous system, IMPT: Intensity-modulated proton therapy,